ANALYSIS OF PUMPING TEST DATA FOR THE IDENTIFICATION OF THE SPATIAL DISTRIBUTION OF HYDROLOGICAL PARAMETERS

by

Çağrı Gökdemir

BS. in Env E., Yildiz Technical University, 2006

Submitted to the Institute of Environmental Sciences in partial fulfillment of

the requirements for the degree of

Master of Science

in

Environmental Technology

Boğaziçi University

2011

ANALYSIS OF PUMPING TEST DATA FOR THE IDENTIFICATION OF THE SPATIAL DISTRIBUTION OF HYDROLOGICAL PARAMETERS

APPROVED BY:

Prof. Dr. Nadim Copty . . . .
(Thesis Supervisor)

Assist. Prof. Dr. Başak Güven . . . .

Prof. Dr. Beyza Üstün . . . .

DATE OF APPROVAL 17/08/2011

ACKNOWLEDGEMENTS

I would like to express my sincere gratitude to my thesis advisor, Prof Dr. Nadim Copty for his scientific guidance, valuable advices, precious support and endless patience during this study.

I am also thankful to my jury members: Assist. Prof. Dr. Başak Güven and Prof Dr. Beyza Üstün, for their critical and supportive comments.

I would also like to thank Research Assistant Savaş Sarıoğlu for his valuable help throughout this study.

I would like to express my gratitude to my friends from institute, Serkan Kaptan, Emre Kalkan and Begüm Karakoçak for their valuable support.

The Research Fund of Boğaziçi University (B.A.P. 5577) is acknowledged for the financial support.

I appreciate my dear family and friends; Dora Mengüç, Keremcan Karabatak, Hüseyin Uğur and Güneş Çıgay for their endless encouragement, patience, support and understanding.

ABSTRACT

The evaluation of groundwater resources holds an important role for the development of sustainable reservoir management plans. An important step in that direction is the detailed characterization of subsurface systems. The use of pumping tests is standard technique for the estimation of subsurface hydraulic properties. The analysis of drawdown data from pumping tests is normally performed using graphical techniques based on the assumption of aquifer homogeneity. However, natural subsurface formations are heterogeneous with complex patterns of spatial variability. This heterogeneity plays an important role in subsurface flow and contaminant transport processes. Therefore, estimating the spatial variability of subsurface flow parameters is essential for the development of models that can accurately predict groundwater flow and contaminant transport.

This thesis examines the use of different interpretation methods for the analysis of time-drawdown data derived from pumping tests The main goal of the research was to estimate the flow parameters of the subsurface system, namely: transmissivity, storativity, conductance and leakance, and to infer some information about the spatial variability of these parameters. Both leaky and non-leaky confined aquifer systems were considered. The pumping test interpretation methods evaluated include conventional methods such as the Theis method, the Cooper-Jacob method for confined aquifers, and the Walton and Hantush inflection point method for leaky aquifers. In addition two recently developed methods, the Continuous Derivation method and the double inflection point method were tested. In order to demonstrate the effect of heterogeneity on pumping test interpretations, heterogeneous transmissivity fields were first generated and used to simulate transient drawdown data which was then used to estimate the flow parameters using the different interpolation methods. The interpretation methods were also applied to real field data. The resulting estimated parameters are shown to be space dependent and vary with the interpretation method since each method gives different emphasis to different parts of the time-drawdown data. Also, the heterogeneity in the pumped aquifer influences the estimates and they show different behaviors according to interpretation method. It was also shown that more information about the flow parameters can be obtained when the results of different interpretation methods are combined together.

ÖZET

Yeraltı suyu kaynaklarının değerlendirilmesi, sürdürülebilir havza yönetimi planlamasında önemli bir rol oynamaktadır. Bu yöndeki önemli adımlardan biri de yer altı sistemlerinin detaylı karakterizayonudur. Yeraltındaki suların özelliklerini hesaplamada standart yöntem olarak pompaj testleri kullanılır. Pompaj testlerinden çıkan su seviyesi düşme verileri, yaygın olarak akiferlerin homojenlik tahminlerine dayanan grafik yöntemleri ile analiz edilmektedir. Ancak, doğal yeraltı oluşumları heterojen bir yapıya sahiptir. Bu heterojen yapı, yeraltı akıntıları ve kirleticilerin taşınma süreçlerine önemli derecede etki etmektedir. Bu nedenle, yeraltındaki uzamsal değişkenlik parametrelerini hesaplamak, yeraltı sularının akışlarını ve kirleticilerin taşınmasını gerçeğe yakın şekilde öngören modellerin geliştirilmesinde temel unsur olarak karşımıza çıkmaktadır.

Araştırmanın temel hedefi, geçirimlilik, sutaşıma kapasitesi, iletkenlik ve geçirimlilik olarak sıralayabileceğimiz yeraltı sisteminin akış parametrelerinin tahmini ve bu parametrelerin uzamsal değişkenliğini gösterebilmektir. Çalışmada, hem sızdıran hem de sızdırmayan kapalı akifer sistemler incelemeye dâhil edilmiştir. Pompalama testi verileri, kapalı akiferler için Theis metodu, Cooper-Jacob metodu, sızdıran akiferler için eğri örtüştürme prensibine dayana Walton metodu ve Hantush bükülme noktası metodu gibi geleneksel yöntemler ile değerlendirilmiştir. Ayrıca, son dönemlerde geliştirilen iki yeni yöntem olan Devamlı Derivasyon yöntemi ve Çifte Bükülme noktası yöntemi de test edilmiştir. Pompalama testi yorumlarında heterojenliğin etkilerini gösterebilmek adına, sentetik heterojen geçirimlilik alanları oluşturulmuş ve geçici su seviyesi düşme verileri simüle edilerek, farklı analiz yöntemleri ile akış parametrelerinin hesaplamasında kullanılmıştır. Yorumlama yöntemleri aynı zamanda gerçek arazi verileri üzerinde de uygulanmıştır.

Sonuç olarak karşımıza çıkan parametrelerin, uygulanan alan ve kullanılan yorumlama yöntemlerine göre çeşitlilik gösterdiği ortaya çıkmıştır; çünkü her metot hesaplamasını, zaman-su seviyesi düşme verilerinin farklı bölümlerine, farklı şekilde eğilerek gerçekleştirmektedir. Aynı zamanda, pompalanan akiferin homojenlik derecesi tahminleri etkilemekte ve her analiz yöntemine göre farklı davranışlar sergilemektedir. Ayrıca, farklı analiz metotlarının sonuçları bir arada değerlendirildiğinde, akış parametreleri hakkında daha fazla bilgi elde edilebildiği görülmüştür.

TABLE OF CONTENTS

ABSTRACT iv

ÖZET........ v

TABLE OF CONTENTS........ vi

LIST OF TABLES........ x

LIST OF FIGURES........ xii

LIST OF SYMBOLS/ABBREVIATIONS xvi

1. INTRODUCTION........ 1

2. RESEARCH OBJECTIVES 6

3. THEORETICAL BACKGROUND........ 10

3.1. Literature Review 10

3.1.1. Leaky Aquifer Hydraulics 10

3.1.2. Pumping Tests in Heterogeneous Media 13

3.1.3. Stochastic Approach to Heterogeneity 14

4. METHODOLOGY........ 16

4.1. Analytical Methods for the Analysis of Pumping Tests........ 16

4.1.1. Conventional Methods Used for Non-leaky Confined Aquifer........ 17

4.1.1.1. Theis's Method. 18

4.1.1.2. Cooper-Jacob Method........ 19

4.1.2. Conventional Methods Used for Leaky Confined Aquifer........ 21

4.1.2.1. Walton's Curve-Fitting Method........ 23

4.1.2.2. Hantush Inflection Point Method........ 25

4.1.3. The Double Inflection Point Method........ 27

4.2. Data Smoothing and Differentiation Techniques 31

4.2.1. Smoothing Techniques 35

4.2.1.1. Moving Average Method 36

4.2.1.2. Exponential Smoothing Methods 36

4.2.1.3. LOESS Smoothing 37

4.2.2. Fitting Methods 38

4.2.2.1. Polynomial Fitting 38

4.2.2.2. Rational Fitting 38

4.2.2.3. Smoothing Spline 38

4.3. Numerical Simulation 39

5. CONTINUOUS DERIVATION METHOD 42

5.1. Continuous Derivation for Confined Aquifer 43

5.2. Effect of Leakage on CD Method 45

6. FIELD PROPERTIES AND PUMPING TESTS 49

6.1. Pumping Tests 49

6.1.1. Constant Rate Pumping Tests 49

6.2. Correction of the Data 51

6.2.1. Barometric Pressure and Trend Corrections 52

6.3. Structure of Drawdown Data 55

7. RESULTS AND DISCUSSION 57

7.1. Calculation of the first and second derivative of drawdown 58

7.1.1. Homogeneous Case 58

7.1.1.1. Non-leaky Confined Aquifer 58

7.1.1.2. Leaky Confined (Semiconfined) Aquifer 60

7.1.2. Heterogeneous Case 67

7.1.2.1. Non-leaky Confined Aquifer 67

7.1.2.2. Leaky Confined Aquifer figures. 70

7.2. Estimation of Flow Parameters-Synthetic Data from Confined Aquifers 73

7.2.1. Conventional Methods 74

7.2.2. CD – Confined Method........76
7.3. Estimation of Flow Parameters- Synthetic Data from Leaky Aquifers........78
7.3.1. Conventional Methods........79
7.3.2. DIP Method........81
7.4. Estimation of Flow Parameters-Field Data from Confined Aquifer Approach........83
7.4.1. Fitting and Derivation on Field Data........84
7.4.1.1. Smoothing of the Field Drawdown Data........86
7.4.1.2. Derivation of Smoothed Curves........87
7.4.1.3. Fitting Procedure and Derivations of Fitting curves........90
7.4.2. Conventional Methods........93
7.4.3. CD Method........95
7.4.3.1.Identification of Aquifer type........95
7.4.3.2.Estimation of Flow Parameters........98
7.5. Estimation of Flow Parameters- Field Data from Leaky Aquifers........103
7.5.1. Conventional Method........103
7.5.2. DIP Method........106
8. CONCLUSIONS AND RECOMMENDATIONS........110
REFERENCES........115
APPENDIX A: SECOND DERIVATIVES OF SYNTHETIC HETEROGENEOUS DATA........124
APPENDIX B: CD-CONFINED METHOD ESTIMATIONS FOR SYNTHETIC HETEROGENEOUS DATA........126
APPENDIX C: CD-CONFINED METHOD ESTIMATIONS FOR FIELD DATA........129
APPENDIX D: PROGRAM FOR SIMULATED DATA READING........135
APPENDIX E: PROGRAM FOR THE APPLICATION OF CONVENTIONAL AND DIP METHOD ANALYSIS TO THE SYNTHETIC DATA........137

APPENDIX F: PROGRAM FOR THE APPLICATION OF CD-CONFINED METHOD ANALYSIS TO THE SYNTHETIC DATA 147

APPENDIX G: PROGRAM FOR THE APPLICATION OF CD-CONFINED METHOD AND COOPER-JACOB METHOD ANALYSIS TO THE FIELD DATA 153

APPENDIX H: PROGRAM FOR THE APPLICATION OF DIP METHOD ANALYSIS TO THE FIELD DATA... 156

LIST OF TABLES

Table 7.1. MSE estimates for comparison of derivation methods 63

Table 7.2. MSE values of the second derivates estimated using the Bourdet method......65

Table 7.3. MSE values of the second derivates estimated using the Spane method.........67

Table 7.4. MSD statistics for the degree of difference from homogeneus case in realizations for first derivatives 70

Table 7.5. MSD statistics for the degree of difference from homogeneous case in realizations for second derivatives..71

Table 7.6. Estimates of Hydrological Parameters using Theis Method 75

Table 7.7. Estimates of Hydrological Parameters using the Cooper-Jacob Method.........75

Table 7.8. Estimates of hydrological parameters using the Walton's Type Curve method with synthetic heterogeneous data 79

Table 7.9. Estimates of hydrological parameters using the Hantush's Inflection Point Method 80

Table 7.10. Estimates of hydrological parameters using DIP method for early data for synthetic heterogeneous data 81

Table 7.11. Estimates of hydrological parameters using DIP method for late data for synthetic heterogeneous data 82

Table 7.12. Goodness of Fit Statistics...91

Table 7.12. Estimated Parameters using the Walton and Theis methods for real data 93

Table 7.13. Paremeter Estimations of Cooper-Jacob method for real data 94

Table 7.14. Parameters estiamted with the Hantush's Inflection Point method with extrapolation 105

Table 7.15. Parameters estiamted with theHantush's Inflection Point method using last point 106

Table 7.16. Paramters estimated using the DIP the field data based on the first inflection point and second inflection point of the second derivatives 108

LIST OF FIGURES

Figure 1.1. An example for generalized configuration of ground-water-flow model layers used along model and active cells in the ground-water-flow model grid 5
Figure 2.1. Demonstration of aquifer systems and cross section of reservoir..................... 7
Figure 2.2. Schematic diagrams of aquifers and respective drawdown 9
Figure 4.1. Homogeneous and Heterogeneous Confined aquifers, both isotropic and anisotropic 17
Figure 4.2. Theis graphical method 19
Figure 4.3. Time Drawdown data analyzed with the Cooper-Jacob method 20
Figure 4.4. Vertical leaky aquifers (A,B) and Multi-layered Aquifer System 21
Figure 4.5. Conceptual model of cross section of a pumped leaky aquifer....................... 22
Figure 4.6. Interpretation of the synthetic pumping test using the type-curve method..... 24
Figure 4.7. Walton's Type Curves numerical application.. 25
Figure 4.8. Hantush's Infliction point method for, a) Heterogeneous realization A, b) Theoretical Realization 26
Figure 4.9. Drawdown versus time variation at an observation well of semiconfined aquifer due to constant rate water extraction 27
Figure 4.10. Drawdown and its first and second derivatives as a function of log time based on homogeneous assumption 28
Figure 4.11. First and second derivative of the drawdown from the synthetic pumping test in the heterogeneous aquifer and in the equivalent homogeneous aquifer 29
Figure 4.12. First and second derivatives of heterogeneous synthetic drawdown by using the central difference method.. 33
Figure 4.13. Comparison of Central Difference and Bourdet Derivation 34
Figure 4.14. Comparison between the Bourdet and Spane & Wurstner differentiation methods 35
Figure 4.15. Randomly-generated transmissivity fields 40
Figure 4.16. Boundary conditions and location of observation scheme for synthetically simulated pumping test 41
Figure 5.1. Plot of γ_c, ratio of drawdown to drawdown rate, as a function of *1/u* 44

Figure 5.2. Plot of γ_L, ratio of drawdown to drawdown rate, as a function of *1/u* for leaky aquifer 47
Figure 6.1. Research A showing the location of test wells, monitoring wells, boreholes and piezometers 50
Figure 6.2. Research B showing the location of test wells, monitoring wells, boreholes and piezometers 51
Figure 6.3. Two examples of monitoring well water elevation data, and background trend was specified 53
Figure 6.4. Elevation data from a monitoring well for different BE values to correction 55
Figure 6.5. Corrected drawdown measurements of monitoring wells in area A 56
Figure 7.1. First derivatives for the case of non-leaky confined aquifer and observation points 59
Figure 7.2. First derivatives of the drawdown from a leaky confined aquifer using the Bourdet method and for different smoothing intervals 61
Figure 7.3. First derivatives of the drawdown from a leaky confined aquifer using the Spane & Wurstner method and for different smoothing intervals 62
Figure 7.4.Comparison of second derivations calculated with the Bourdet method 64
Figure 7.5. Comparison of second derivations calculated with the Spane & Wurstner method 66
Figure 7.6. Estimates of the first derivative of the drawdown for the case of heterogeneous aquifer using the Spane & Wurstner method and for different L values 69
Figure 7.7. First derivatives of the drawdown data for 5 randomly generated heterogeneous field realizations 72
Figure 7.8. Second derivatives of the drawdown data for realization A, using different intervals by Spane and CDD methods 73
Figure 7.9. Estimated transmissivity and Storativity data as a function of time 76
Figure 7.10. Transmissivity and Storativity data as a function of distance for the realization A, estimated from different observation points 77
Figure 7.11. First derivatives of drawdown at four different monitoring points as a function of time due to pumping from TW2A for real field data. 85

Figure 7.12. Application of different smoothing techniques to the second derivative of the synthetic heterogeneous drawdown at observation point in 1 m radius due to pumping 86

Figure 7.13. First derivatives of smoothed real drawdown data for monitoring wells 2A and 2B 88

Figure 7.14. First derivatives of smoothed real drawdown data for monitoring wells 2C and 2D 89

Figure 7.15. Drawdown fitted polynomials/Splines and residuals 90

Figure 7.16. Derivatives of fitting curves for the field data from test well 2A and monitoring wells 2A, 2B, 2C and 2D 92

Figure 7.17. $\gamma_L = \frac{2.3s}{s'}$ estimated from the drawdown data and its time derivative........ 97

Figure 7.18. Estimation of flow parameters using the CD–Confined method for test wells 2A and 2B and for different drawdown fitting methods 99

Figure 7.19. Estimation of flow parameters using the CD-Confined method for test wells 2C and 2D and for different drawdown fitting methods 100

Figure 7.20. Different extrapolation of the drawdown data for the determination for the maximum drawdown points 104

Figure 7.21. First and second derivatives of drawdown using LOESS smoothing and Spline fitting method 107

Figure A. 1. Second derivatives of synthetic pumping test data for each realizations for 1m radius 124

Figure A. 2. Second derivatives of synthetic pumping test data for each realizations for 1m radius 125

Figure B. 1. Estimations of CD-confined method from synthetic data for realizations A and B 126

Figure B. 2. Estimations of CD-confined method from synthetic data for realizations C and D 127

Figure B. 3. Estimations of CD-confined method from synthetic data for realization E 128

Figure C. 1. Estimations of CD-confined method from real data for MW2B and MW2C 129

Figure C. 2. Estimations of CD-confined method from real data for MW2E and MW2F 130

Figure C. 3. Estimations of CD-confined method from real data for MW2H and MW5B 131

Figure C. 4. Estimations of CD-confined method from real data for NW5 and ST7 132

Figure C. 5. Estimations of CD-confined method from real data for MW1 and BH68 133

Figure C. 6. Estimations of CD-confined method from real data for ST8 134

LIST OF SYMBOLS/ABBREVIATIONS

Symbol	**Explanation**	**Units used**
B	Leakage Factor	(m)
BE	Barometric Efficiency	(%)
BP	Barometric Pressure	(psi)
b	Aquifer Thickness	(m)
b’	Aquitard Thickness	(m)
C	Conductance	(m/sec)
K	Hydraulic Conductivity	(m/sec)
L	Differentiation Interval	(Number/Number)
p	Smoothing Parameter for Spline	(unitless)
S	Storativity	(unitless)
$S_{est.}$	Estimated Storativity	(unitless)
s	Drawdown	(m)
s’	First Derivative of Drawdown	(m/s)
s’’	Second Derivative of Drawdown	(m/s^2)
T	Transmissivity	(m^2/s)
T_{est}	Estimated Transmissivity	(m^2/s)
$T_{geometric}$	Geometric Means of Transmissivity Values	(m^2/s)
u	Characteristic time	(unitless)

ASTM	American Society for Testing and Materials
BH	Borehole
CD	Continuous Derivation Method
DIP	Double Inflection Point
HW	Holt-Winter’s Smoothing Method
LOESS	Locally Weighted Regression
MSD	Mean Square Difference
MSE	Mean Square Error
MW	Monitoring Well

MWL	Monitoring Well Water Level	
PDE	Partial Differential Equations	
PZ	Piezometer	
RMSE	Root Mean Squared Error	
SSE	Sum of Squared Errors	
ST	Slug Test	
TW	Test Well	
USGS	United States Geological Survey	
α	Smoothing Factor	(Unitless)
γ_c	Drawdown-first derivative ratio (confined aquifer)	(s)
γ_L	Drawdown-first derivative ratio (semiconfined aquifer)	(s)

1. INTRODUCTION

Groundwater has become an indispensable natural resource for domestic use, agriculture and industry. The importance of groundwater resulted naturally from its global abundance and accessibility. Current estimates suggest that groundwater constitutes about two-thirds of world's fresh-water. Additionally if one ignores polar ice because of its inaccessibility, about 96% of all the global freshwater is in the form of groundwater. (UNESCO, 1978). However, due to the excessive and unabated exploitation and mismanagement of this resource, regional groundwater budget is coming to its limits and large amounts of pollutants have found their way into groundwater systems.

One of the critical aspects of a reservoir is the sustainable amount of water that the reservoir can transmit. The amount of water dependents on characteristic parameters those affect water flow and storage in the reservoir. The effects of human activities on water level, groundwater storage, and discharge to streams and other surface–water bodies also influence the quantity and quality of groundwater discharge. The volume of water that can be removed from any aquifer is dependent on the subsurface material's ability to store water, and so the expansion and reduction of groundwater dominated reservoir are normally dictated by governing hydrogeological variables (Singha, 2008). The definition of hydrogeological variables, such as inflow, stage, and outflow may naturally have various sources of uncertainties (Yanmaz et al., 2008).

The hydrogeologic parameters of subsurface systems are normally characterized as heterogeneous, whereby the values of these parameters vary with space. It is widely recognized that heterogeneity, or the spatial variability of physical and chemical parameters, plays a critical role in the spread of contaminants (e.g., Dagan, 1989). Foremost among these parameters is the hydraulic conductivity. In order to be able to develop models that can accurately predict the spread of pollutants in the subsurface and for groundwater remediation activities, it is essential to be able to estimate the spatial variability of the flow parameters.

Reservoir models have attracted a lot of attention particularly in the last twenty years. The first solutions were presented in the 60's (Warren, Root, 1963; Kazemi, 1969), but these only became commonly used much more recently. The publication of the paper of Freeze (1975) pointing out the spatial variability of hydraulic conductivity on groundwater flow across a column, brought to the attention of most hydrogeologists that aquifers are extremely heterogeneous. According to Ogilvy et al. (1969) hydraulic conductivity (K) is arguably the most heterogeneous parameter in nature. Laboratory measurements of K span more than 12 orders of magnitude. Even in seemingly homogeneous aquifers, measured values of transmissivity (T), which is the hydraulic conductivity integrated over the depth of the aquifer, may range over some orders of magnitude.

This realization spurred a large amount of work on the problem of finding the effect of heterogeneity on flow and transport such as Bear (1972), Mualem (1976), Gilham et al. (1976), and Dagan (1989). Since groundwater flow and contaminant transport is largely dependent on the value of the hydraulic conductivity and transmissivity, an immediate question is whether the heterogeneous distribution can be substituted by a representative value. As an example, Copty et al. (2006) developed analytic relation that expresses the equivalent transmissivity for leaky aquifers which can be defined as a representative value of heterogeneous field.

Reservoir heterogeneities are identified by variations in the pressure response. Sometimes the pressure data deviates from the homogeneous behavior only during the first minutes of the test period under investigation, in other cases it takes from several hours to several days before the heterogeneity becomes evident. The introduction of high accuracy pressure measurements and computerized log-log analysis technique explains today's recent use of heterogeneous interpretation models. In addition, the derivative of pressure exaggerates the characteristic features of the response.

In reality characterization of field applications are being conducted by limited field measurements which make the pattern of spatial variability hard to estimate. Recent works about spatial variability has overcome the limitation of field measurements with formulation of the groundwater problem in a stochastic formulation. From this point of view, practice of stochastic approach referred to as geostatistics (Sanches-Vila, 1999b; Yeh et al., 1995, 1996; and Zhang and Yeh, 1997), the common methodology in related works is to define the hydraulic conductivity as a random spatial variable. The practice in this approach relies on to the statistical parameters such as the mean, variance and integral scale, by these statistical parameters definition of hydraulic conductivity field can be made. One advantage of the stochastic formulation is to make the quantification of the uncertainty determinable.

The most common method of determining in the field the hydraulic parameters of an aquifer is the performance of pumping tests (Batu, 1998). In a pumping test water is extracted from the ground, and the response of the system (consisting of hydraulic head data as a function of time) is used to estimate the local hydraulic conductivity. Typically, several of these tests are conducted at different locations, leading to several hydraulic conductivity estimates at various locations.

One of the main goals of the analysis of pumping test is to estimate representative hydraulic parameters of the specified aquifer volume by using time-drawdown data. Even findings of representative parameters give information about aquifer hydrology because of the assumption of homogeneity of existing pumping test analysis methods this information would be limited. On the other hand, under such assumptions of homogeneity graphical or analytical methods can provide representative parameters of subsurface system sue to the quality of the drawdown data. As a few example related with pumping test practices was provided in the works of Theis (1935) for confined, Hantush and Jacob (1955) for leaky aquifers. As a comment to the limited character of the assumption of homogeneity in conventional analytical methods that interpreted flow parameters cannot represent the field heterogeneity, they only can provide a general averaged value of the whole system. In reality observations made from numerous fields demonstrate that hydraulic parameters are characterized by complex patterns of spatial variability (Dagan, 1989).

The accurate determination of hydraulic conductivity is an important element of successful groundwater flow modeling. However, the exhaustive measurement of this hydrogeological parameter is quite costly and, as a result, unrealistic. Alternatively, relationships between hydraulic conductivity and other hydrogeological variables, such as soil properties, rock types from borehole log analyses, (Chapellier, 1992; Temples and Waddell, 1996) less costly to measure have been used to estimate this crucial parameter.

Simulations using groundwater models are also useful tools for the visualization of behaviors of different special conditions and the responses of the subsurface water system to changes in the ambient conditions. Analog models to simulate the flow and transport in an aquifer are sometimes used such as the cross sectional Hele- Shaw model of coastal sea-water intrusion (Bear, 1971; Collins et al., 1972), or electrical analog methods (Gupta et al., 2006). Experimental methods such as two-dimensional or three-dimensional sand boxes have been also developed and tested to observe contaminant transport paths and concentration distribution in porous media [for example, Beach et al. (2005); McCray et al.(2004, 2005); Kechavarzi (2005)] .

Analog models (especially sand box models) have several advantages such as good visualization of flow dynamics, easy to execute and the actual use of flow through porous media. On the other hand, they also have some disadvantages such as expensiveness of construction, hardness to represent field situations and scaling all processes (e.g., permeability and capillarity rise), non-flexibility of applications of field models (eg., applied to only one situation) (Illman et al., 2008). During the past several decades, computer models for simulating ground-water and surface-water systems have played an increasing role in the evaluation of ground-water development and management alternatives. The use of these models has provided an opportunity for water managers to quantitatively understand how ground water moves and to estimate the effects of human use of the water (Konikow and Reilly, 1999). Development of computer based models for simulations of the groundwater, reservoir systems helped to cope with the setbacks of analog models.

In the most general terms, a model is a simplified representation of the appearance or operation of a real object or system (Apostel, 1961; Rollan et al., 1998). Groundwater flow models attempt to reproduce, or simulate, the operation of a real groundwater system with a mathematical counterpart (a mathematical model). Mathematical models may use different methods to simulate ground-water-flow systems (Konikow and Reilly, 1999).

One such method is called the finite-difference method (for example, McDonald and Harbaugh, 1988), which is the method employed in MODFLOW, the computer program used to simulate the pumping tests in this study. As a further approach multi-layer reservoir systems have been using which mainly initiated for modeling oil fields but then became commonplace in using for ground-water-flow models (Kernodle and Scott, 1986; Kernodle, Miller, and Scott, 1987; and Kernodle, McAda, and Thorn, 1995; Sanford and others, 2001). (For a schematic look see Figure 1.1)

The main purpose of this study is to develop a novel pumping test interpretation method that can give information about the spatial variability of the flow parameters. The specific objectives of this study are described in the next chapter.

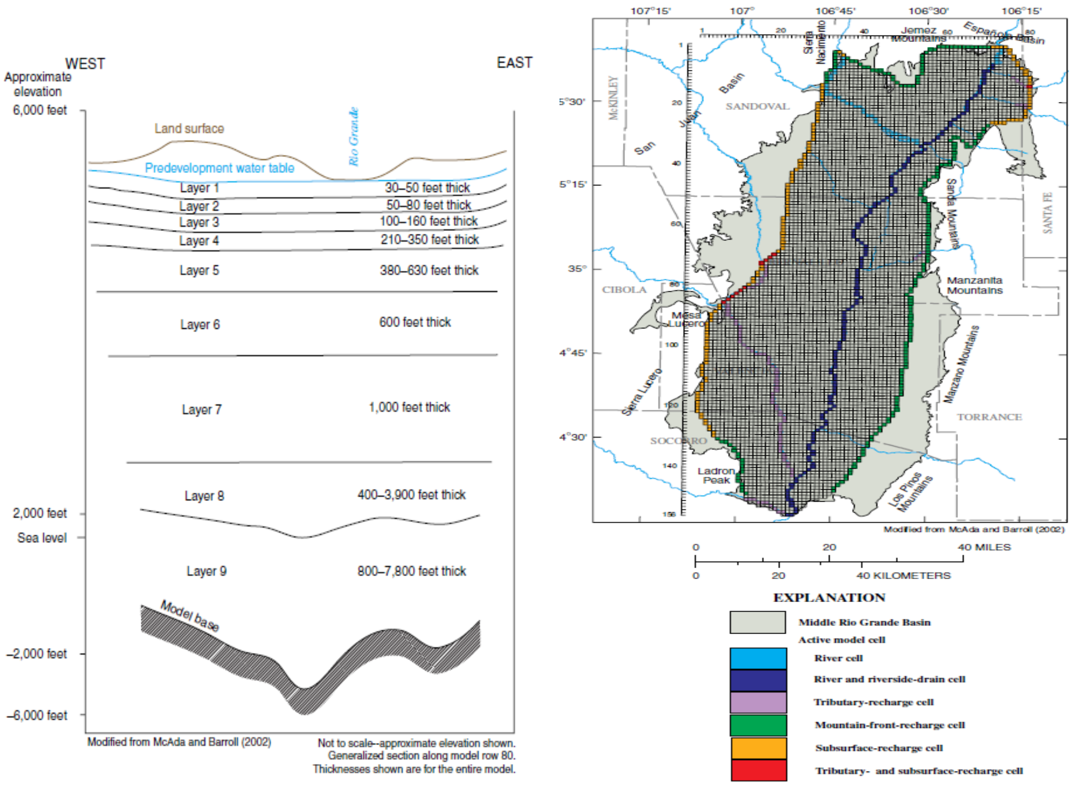

Figure 1.1. An example for generalized configuration of ground-water-flow model layers used along model and active cells in the ground-water-flow model grid (layer 1) of McAda and Barroll (2002). Different types of recharge and drain cells are shown.

2. RESEARCH OBJECTIVES

The general objective of this study is to develop a novel pumping test interpretation method that can give information about the spatial variability of the flow parameters. The study will consider both confined aquifers (whereby the top and bottom boundaries of the aquifer allow no flow) and leaky aquifers defined as an aquifer that allows some flow through its top or bottom boundary. A theoretical vertical section of a leaky aquifer is shown in Figure 2.1. A leaky aquifer, also known as a semi-confined aquifer, is a completely saturated aquifer that is bounded below by an aquiclude (a layer that completely prevents flow across it) and above by an aquitard (a layer that allows some flow across it). If the overlying aquitard extends to the land surface, it may be partly saturated, but if it is overlain by an unconfined aquifer that is bounded above by the water table it will be fully saturated. If there is hydrological equilibrium, the piezometric level in a well tapping a leaky aquifer may coincide with the water table. In areas with upward or downward flow, in other words, in discharge or recharge areas, the piezometric level may rise above or fall below the water table.

A multi-layered aquifer is a succession of leaky aquifers sandwiched between aquitards (Figure 2.1). Systems of interbedded permeable and less permeable layers like this are very common in deep sedimentary basins.

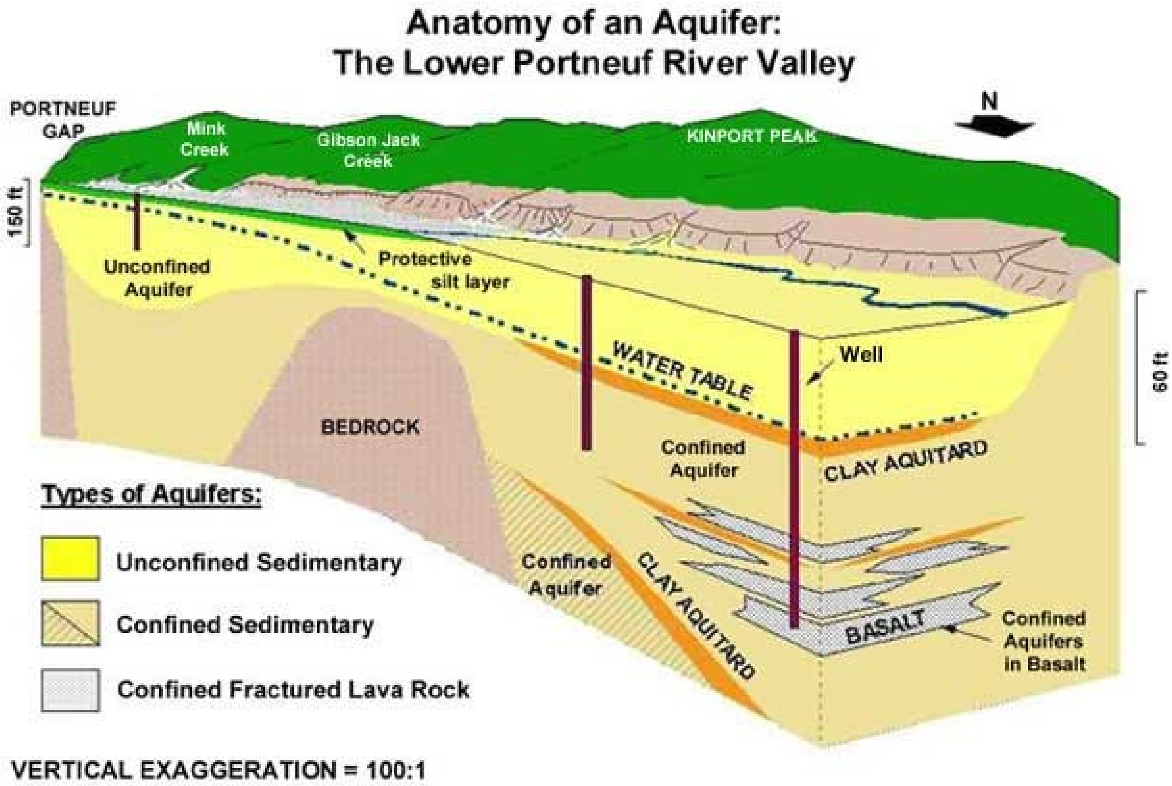

Figure 2.1. Demonstration of aquifer systems and cross section of reservoir. The Lower Portneuf River Valley (Provided by Idaho Geological Survey).

Figure 2.1 shows three different types of aquifers: confined, unconfined, and perched. Recharge zones are typically at higher altitudes but can occur wherever water enters an aquifer, such as from rain, snowmelt, and river and reservoir leakage. Discharge zones can occur anywhere; in the diagram, discharge occurs not only in springs near the stream and in wetlands at low altitude, and also from wells and high-altitude springs.

The Specific questions that this study will address include:

- Can we use the drawdown data and its derivatives at one particular point in time to estimate the parameters? The method will particularly focus on the incorporation of the drawdown derivative in the estimation procedure because the derivative is more sensitive to variations in the flow parameters around the pumping test in comparison with the cumulative drawdown
- Can we use the entire time drawdown data to estimate the representative flow parameters as a function of time? This would give use some information about the

heterogeneity as a function of distance from the well and needs more accurate method to differentiate the early data and late data.

How do the parameters estimated from these novel methods compare with single "representative" estimates of the flow parameters obtained from conventional pumpingtest interpretation methods.

The developed method will be tested with synthetically generated pumping tests data and applied to real data collected from a series of pumping tests conducted in California, United States. As noted above, the identification of the aquifer heterogeneity is an essential step in the accurate modeling and prediction of contaminant transport. The specific practices in this study are (1) to develop a conceptual model representing the hydrogeological condition of the well-field based on ground observations and data analysis. (2) Simulating pumping tests using MODFLOW and acquisition of data from the simulation from different distances from the test well. (3) Using conventional and novel analytic methods, including derivative methods, (4) and the interpretation of the field data analysis to define if the aquifer system is Leaky/Confined, Non-leaky/Confined, Leaky/Unconfined and Non-leaky/Unconfined with the specific behavior of the drawdown data and its derivative (e.g. Figure 2.2)

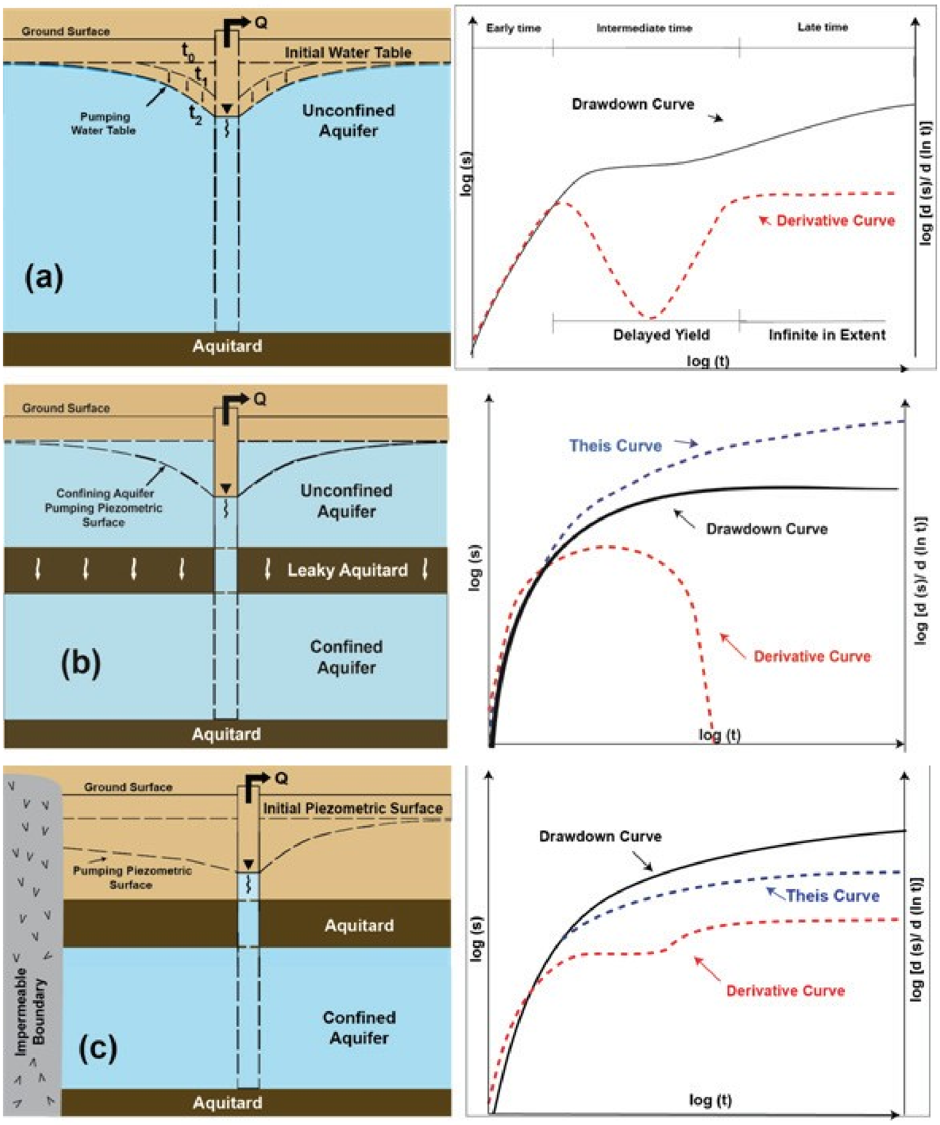

Figure 2.2. Schematic diagrams of aquifers and respective drawdown (black) and derivative (red) curves: (a) unconfined with instantaneous delayed gravity drainage, (b) leaky confined, (c) confined with impermeable boundary. Variables used are s, drawdown; t, time; and, d, derivative. (Goetz, 2010)

3. THEORETICAL BACKGROUND

3.1. Literature Review

Many complex geologic systems exist in which vertical fluxes through confining overlying and/or underlying layers are not negligible. These formations are commonly known as leaky or semiconfined aquifers. A classical example is that of alluvial multilayered aquifer-aquitard systems, which are present worldwide. The analysis of the drawdown due to pumping in a leaky aquifer allows the estimation of representative hydraulic parameters of both the aquifer being tested and the aquitard. Evaluations of the hydrological parameter estimations are essential for the proper management of the aquifer, the accurate prediction of contaminant migration, assessing vulnerability, and risk assessment in general.

3.1.1. Leaky Aquifer Hydraulics

The first mathematical analysis of well hydraulics in leaky aquifers was developed by Hantush and Jacob (1955). The authors presented the analytical solution for the transient drawdown due to constant pumping rate in leaky aquifers based on a series of simplifying assumptions: vertical flow in the aquitard, horizontal flow in the aquifer, negligible storage in the aquitard, constant hydraulic head in the unpumped (recharging) aquifer, and a pumping well of infinitesimal radius that fully penetrates the pumped aquifer. Under such conditions, the drawdown becomes a function of the hydraulic parameters of the aquifer (transmissivity, T and storage, S [dimensionless]) and the conductance of the aquitard, C, defined as the ratio of the vertical hydraulic conductivity over the thickness of the aquitard, C (K'/b'). Alternatively, the drawdown can be expressed as a function of the leakage factor, B, which combines two of the previous hydraulic parameters, given by:

$$B = \sqrt{\frac{Tb'}{K'}} \tag{3.1}$$

The solution of Hantush and Jacob formed the starting point in the development of other pumping test interpretation techniques such as the inflection point method (Hantush 1956) and the type-curves method defined by Walton (1962).

Some of the assumptions made by Hantush and Jacob (1955) were relaxed in subsequent studies. Hantush (1960) accounted for the storage capacity of the aquitard. He obtained a series of type curves as a function of the leakage factor, B, and of a new parameter that depends on the storage of both the aquifer and the aquitard. Neuman and Witherspoon (1969a, 1969b) provided a more generic solution, taking into account the aquitard storage as well as the drawdown in the unpumped aquifer. The assumption of zero well radiuses was relaxed by incorporating the large-diameter well theory and accounting for wellbore skin (Moench 1985). All these solutions are based on the assumption that the hydraulic parameters of individual layers are homogeneous.

As an intrinsic characteristic, natural geologic formations are heterogeneous with their spatial variability. From this approach the problem of radially convergent flow has been investigated in heterogeneous aquifers for last decades and a number of publications has been made on this topic (e.g., Renard and de Marsily, 1997; Rubin, 2003; Raghavan, 2004; Sanchez-Vila et al., 2006). Some papers focused on to the determination of effective hydraulic conductivity flow-parameter which can be accepted as the negative ratio between the expected values of the flow and the any local hydraulic gradient in Darcy's theorem approach (e.g., Dagan, 1982, 1989; Sanchez-Vila, 1997; Riva et al., 2001). To consider the effective hydraulic conductivity as constant in investigated field within specified boundary, it was considered as intrinsic property of the said medium. However, in case of convergent flow such a constant value cannot be accepted as intrinsic property of any medium (Shvidler, 1962). The works of Indelman and Abramovich (1994) and Sanchez-Vila (1997) proved inaccuracy of the constant hydraulic conductivity approach. In general terms, effective hydraulic conductivity increases from the harmonic mean near the pumping well to the geometric mean at some distance from the well, and this distance depends on the correlation length of the hydraulic conductivity field (Copty et al., 2008). The paper of Dagan (1982) demonstrated that the effective flow parameters are functions of the flow spatial dimension and time.

After building up the heterogeneity approach, some papers investigated the assessment of the effect of the heterogeneity of flow-parameters on the interpretation of pumping tests. Barker and Herbert (1982), Butler (1988), and Butler and Liu (1993) investigated the effect of heterogeneity as variability of T field on homogeneous plane specified high or low transmissivity values with deterministic approach. Also some analytical solutions have been developed relies on to the mean and variance transmissivity of confined aquifers correlated with the explorative statistics of drawdown data (Serrano, 1997). Implementation of Cooper-Jacob method (Cooper and Jacob, 1946) also have been evaluated and tested in aquifers with heterogeneous transmissivity (Meier et al., 1998; Sanchez-Vila et al., 1999). They showed that the transmissivity estimated using the Cooper-Jacob method does not depend on the observation point location; differently storativity could significantly vary with the location of this point. Then as an advance approach Copty and Findikakis (2004) used Monte Carlo method to investigate the effect of spatial heterogeneity in confined aquifers and they proved that Cooper-jacob assumptions would be valid. Wu et al. (2005) also tried the Theis method to estimate hydrological parameters from a single observation well in a synthetically generated heterogeneous field for confined aquifer. According to study, Theis method estimates the transmissivity and storativity values from the early time-drawdown data.

Several researchers such as Bourdet et al. (1983), Horne (1995), and Bourdet (2002) proposed the interpretation of pumping tests using the time-derivative of the drawdown curve (diagnostic plot), which is more sensitive to changes caused by boundary conditions (impermeable or leaky limit, wellbore storage, skin effect). Amin (2005) proposed a methodology for the estimation of the rate of leakage based on the analysis of the slope of the drawdown vs. time curve. Another method for the interpretation of pumping tests in leaky aquifers was developed, referred to as the double inflection-point (DIP) method. The method is based on the analysis of the first and second derivatives of the drawdown with respect to log time for the estimation of the flow parameters. In particular, the combination of the DIP method and Hantush method is shown to lead to the identification of contrasts between the local transmissivity in the vicinity of the well and the equivalent transmissivity of the perturbed aquifer volume Trinchero et al. (2008).

3.1.2. Pumping Tests in Heterogeneous Media

Most of the early pumping test analysis methods are based on the assumption of homogeneous field variables such as transmissivity and storativity. In reality heterogeneity of porous media has been a troublesome topic from the very beginning of groundwater hydrology as a quantitative science. Darcy (1856) recognized the necessity to quantify flow through porous media using a macroscopic, rather than a microscopic, viewpoint; he defined a flux based on average linear flow path through a representative volume of porous media. From this viewpoint, characterization of geological formations attempts to estimate representative values of the parameters rather than local small scale variability. In another early work, Meinzer (1932) also emphasized the importance as well as difficulty of quantifying aquifer parameters in the presence of heterogeneity. Shortly after this, Theis (1935) addressed the problem of heterogeneity by developing a way of calculating effective aquifer parameters. He demonstrated that by measuring the drawdown of water levels in response to pumping, it is possible to use an analytical solution to calculate effective aquifer parameters for average transmission and storage characteristics. Theis' method, as the first analytical method to use pumping test values, replaces the heterogeneous aquifer with an equivalent homogeneous porous medium. However, as Theis criticized himself in his work in 1967, the equivalent homogeneous porous medium concept is not adequate for dealing with transport phenomena because the method cannot simulate accurately the transport of contaminants nor can it quantify the effect of uncertainty in hydraulic conductivity on the head distribution (Freeze, 1975).

The above developments show that the importance of the analysis of pumping test head, elevation and/or drawdown variables. In the last two decades several studies have focused on the interpretation of pumping tests in heterogeneous confined aquifers. Examples of earlier studies which take into account the heterogeneity of the medium were those of Barker and Herbert (1982), Butler (1988), Butler and Liu (1993). Their works however considered idealized system consisting of a uniform aquifer with an inclusion of different hydraulic properties embedded in the otherwise uniform aquifer. For very large times the slope of the drawdown versus log time was shown to be unaffected by the transmissivity of the inclusion.

More recently, Meier et al. (1998) analyzed numerically the meaning of the parameters obtained using the Cooper-Jacob method (1946) to interpret pumping tests in heterogeneous confined aquifers. They found that for low to moderate levels of heterogeneity, the estimated transmissivity is very close to the geometric mean of the transmissivity field, while the estimated storage can vary by orders of magnitude depending on the location of the observation point. They also showed that the effective transmissivity estimated from the late drawdown data and the Cooper-Jacob method are practically independent of the location of the observation point. These results were confirmed analytically by Sanchez-Vila et al. (1993). Several researchers such as Bourdet et al. (1983), Horne (1995), Bourdet (2002) proposed the interpretation of pumping tests using the time-derivative of the drawdown curve which is more sensitive to changes caused by boundary conditions such as impermeable or leaky limit, well-bore storage, and skin effects and heterogeneity.

By comparison relatively few papers have focused on the analysis of pumping tests in heterogeneous leaky aquifers. Some of these methods have emphasized the importance of incorporating the drawdown derivative, also called the diagnostic plot, in the parameter estimation procedure. Copty & Findikakis (2004) examined the impact of the local-scale heterogeneity of the transmissivity on the transient drawdown due to pumping. Amin (2005) proposed a methodology for the estimation of the rate of leakage based on the analysis of the slope of the drawdown versus time curve. Trinchero et al. (2008) specified that the estimated representative parameters are also dependent on the interpretation method used and developed a novel diagnostic method usable for the heterogeneous media.

3.1.3. Stochastic Approach to Heterogeneity

Geo statistics is the application of statistical techniques to the field of earth sciences including groundwater flow and contaminant transport. Geostatistics is used routinely to interpolate values of parameters at unsampled locations from nearby measurements. In some cases, geostatistics is combined with deterministic approaches to forecast uncertainty. At a more academic level, geostatistics is used extensively to study physical processes in heterogeneous aquifers. However, the practical use of the stochastic methods to the real applications is primarily to define the heterogeneity of the parameters (e.g., Transmissivity, Storativity) and state variables (e.g., groundwater levels, concentrations, Temperature) (Renard, 2007).

From a practical point of view, the main advantage of stochastic techniques is their ability to quantify the uncertainty inherent to any underground study (Winter 2004). It allows evaluating risks resulting from heterogeneity and lack of information on design and management. Stochastic hydrogeology is used to understand the impact of heterogeneity on processes and models. For example, it allows for the derivation of expressions to estimate effective governing laws for composite media and effective properties (Sanchez-Vila et al., 2006). The scientific and engineering sides of stochastic hydrogeology are tightly linked. For instance, improvements in the understanding of effective behaviors had a large impact on simulation techniques such as the multiscale approach (Lunati and Jenny 2006) later used by practitioners.

In 1975, Freeze published the first paper that analyzed one-dimensional (1D) flow in porous medium in a stochastic manner (Freeze 1975). In the model constant values are taken randomly in a lognormal distribution and independently in each grid cell. Freeze applied the Monte Carlo method to analyze the first moments of heads. In a Monte Carlo approach, a large number of plausible parameter values are randomly generated using the available data and the problem is solved for each set of parameters. The resultant output is then analyzed statistically. The variation in the outputs is attributed to uncertainty in the definition of the input parameters. Subsequent studies (e.g., Dagan 1976; Freeze 1977; Gellar et al., 1977), contributed to the generalization of the stochastic concepts to flow in more than one dimension (Bark et al., 1978), stochastic analysis of the random coefficients of partial differential equations that frequently used (Sager 1978), One of the first papers that addressed the issue of conditional simulation was by Delhomme (1979).

Practical application of this works included the identification of potential locations for new water supply, estimation of water resources, design of water supply wells, aquifer protection, identification of contamination sources, design of remediation systems, aquifer management, design of dewatering schemes, etc. In all these application information is collected that allows characterizing the geometry and the physical and biogeochemical properties of the subsurface. The main purpose of using geostatistical methods is the identification of the spatial distribution of hydrological parameters.

4. METHODOLOGY

This chapter describes the existing methods used to estimate the hydrological parameters of leaky and non-leaky aquifers. To test and evaluate these methods, synthetic pumping tests were simulated using the computer program MODFLOW (Harbaugh et al., 2000). These synthetic pumping tests require the generation of hypothetical transmissivity distributions to be used as input in the groundwater flow model. Hence this section also includes the data generation procedure used for this purpose.

In addition to the conventional methods recently developed methods that have attempted to characterize the heterogeneity of parameters will be described in this section and evaluated, along with the conventional methods, in the following chapter.

4.1. Analytical Methods for the Analysis of Pumping Tests

Accurate definition of subsurface flow parameters is an essential step in any hydrogeological study. A common approach for the estimation of flow parameters is through the interpretation of pumping tests. As conventional and still widely used pumping test interpretation techniques Theis method (Theis, 1935) and Cooper –Jacob method (Cooper and Jacob, 1946) for confined aquifers, and the Hantush inflection point method (Hantush, 1956) and the graphical Walton method (Walton, 1962) for leaky aquifers has been used in this work. All these methods assume that the subsurface system can be represented by one or at most a few homogeneous units. However, in reality natural subsurface systems are heterogeneous and, hence, hydraulic parameters are spatially variable and support-dependent. Hence it is expected that these conventional methods will be only provide limited information about the aquifer properties because of the homogeneous assumptions embedded in these assumptions. Difference from the homogeneity was estimated with simple statistical methods such as sum of difference squared estimator (Trinchero, 2009).

4.1.1. Conventional Methods Used for Non-leaky Confined Aquifer

A confined aquifer is bounded above and below by an aquiclude. In a confined aquifer, the pressure of the water is usually higher than that of the atmosphere, so that if a well taps the aquifer, the water in it stands above the top of the aquifer, or even above the ground surface (Figure 4.1). In confined aquifer, the loss of hydraulic head propagates rapidly because the release of water from storage is entirely due to the compressibility of the aquifer material and that of the water (Batu, 1998). The drawdown will be measurable at great distances from the well, and if it is non-leaky and unbounded the drawdown never reaches steady–state. For such non-steady or transient flow to the well in a confined aquifer, the two most used pumping test interpretation techniques are the Theis type curve method (1935), Cooper-Jacob (1946) time drawdown and distance drawdown methods.

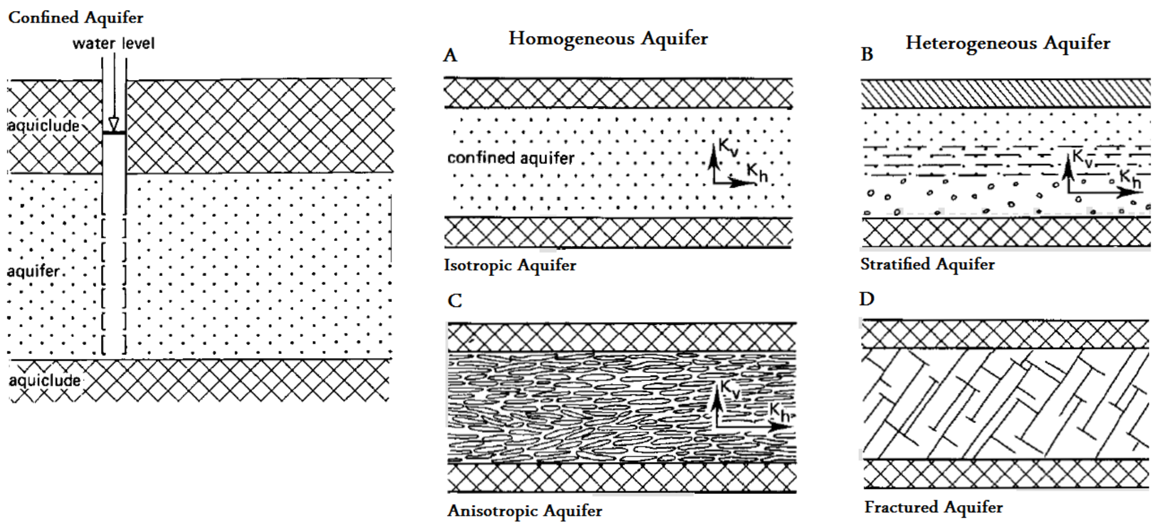

Figure 4.1. Homogeneous and Heterogeneous Confined aquifers, both isotropic and anisotropic (from Analysis and Evaluation of Pumping Test Data, G.P Kruseman, N.A de Ridder)

The general assumptions of conventional methods for confined non-leaky aquifers are;

- The aquifer has infinite areal extend;
- The aquifer is homogeneous, isotropic, and of uniform thickness over the area influenced by the test;
- Prior to pumping, the water table and/or the piezometric level is over the area that will be influenced by the test;

- The aquifer is pumped at a constant–discharge rate;
- The water removed from storage is discharged instantaneously with decline of head.

4.1.1.1. Theis's Method. Theis (1935) was the first to develop a formula for unsteady-state flow that introduces the time factor and the storativity. He noted that when a well penetrating an extensive confined aquifer is pumped at a constant rate, the influence of the discharge extends outward with time. The rate of decline of head, multiplied by the storativity and summed over the area of influence, equals the discharge. The unsteady-state (or Theis) equation, which was derived from the analogy between the flow of groundwater and the conduction of heat, is written as;

$$s(r,t) = \frac{Q}{4\pi T}\int_{u}^{\infty}\frac{e^{-y}dy}{y} = \frac{Q}{4\pi T}W(u) \tag{4.1}$$

where

s: drawdown measured in a piezometer at a distance r from the pumping well.

Q; constant well discharge.

T: transmissivity.

u: characteristic time, $\frac{r^2 S}{4Tt}$

S: storativity of the aquifer.

W(u): well function

Figure 4.2 shows the Theis well function W(u) plotted against l/u on log-log plot. To use the Theis method to interpret a pumping test, the observed drawdown data as a function of time are plotted on a log-log scale and matched to the theoretical well function, W(u) by moving the two curves sideways or upwards/downwards. Once an acceptable match is obtained, a match point is selected as Shown in Figure 4.2 and the flow parameters are calculated from the coordinates of the match point and Equation(4.1) above.

In applying the Theis curve-fitting method, and consequently all curve-fitting methods, one should, in general, give less weight to the early data because they may not closely represent the theoretical drawdown equation on which the type curve is based. Among other things, the theoretical equations are based on the assumptions that the well discharge remains constant and that the release of the water stored in the aquifer is immediate and directly proportional to the rate of decline of the pressure head. In fact, there may be a time lag between the pressure decline and the release of stored water, and initially also the well discharge may vary as the pump is adjusting itself to the changing head. This probably causes initial disagreement between theory and actual flow. As the time of pumping extends, these effects are minimized and closer agreement may be attained; if the observed data on the logarithmic plot exhibit a flat curvature, several apparently good matching positions, depending on personal judgment, may be obtained. In such cases, the graphical solution becomes practically indeterminate and one must resort to other methods.

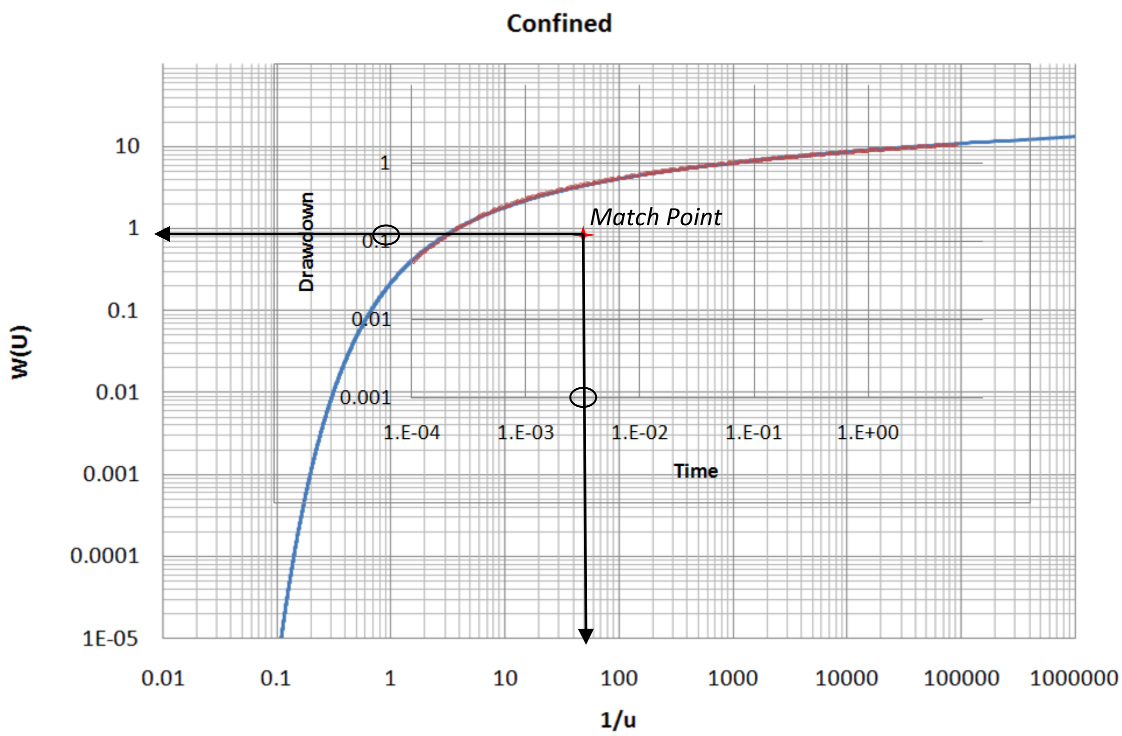

Figure 4.2. Theis graphical method, drawdown stated in red line

4.1.1.2. Cooper-Jacob Method. Another commonly used pumping test analysis method valid for constant-rate pumping tests in confined aquifers is the Jacob's method (Cooper and Jacob, 1946). It consists of plotting drawdown versus log time and fitting a straight line to late time data points. Estimates of the transmissivity (T) and storage coefficient (S) are obtained from the slope and intercept of this line (Figure 4.3). It is generally accepted that the estimated values (Test and Sest) derived from Jacob's method are representative values for the test area (some area surrounding the pumping and observation wells). This method again uses infinite series from the Theis solution. At later times, the Theis well function exhibits a straight-line segment. The Theis-Jacob method is based on this phenomenon. This method showed that for the straight-line segment, Equation (4.1) can be approximated by

$$s = \frac{2.3Q}{4\pi T} \log \frac{2{,}25Tt}{r^2 S} \qquad (4.2)$$

The properties of a confined aquifer can be found by developing the time-drawdown relationship based on Equation(4.2). If the pumping time is sufficiently long, a plot of the drawdown s(r,t) observed in a particular piezometer at a distance r from the pumped well versus the logarithm of time t, will appear as a straight line.

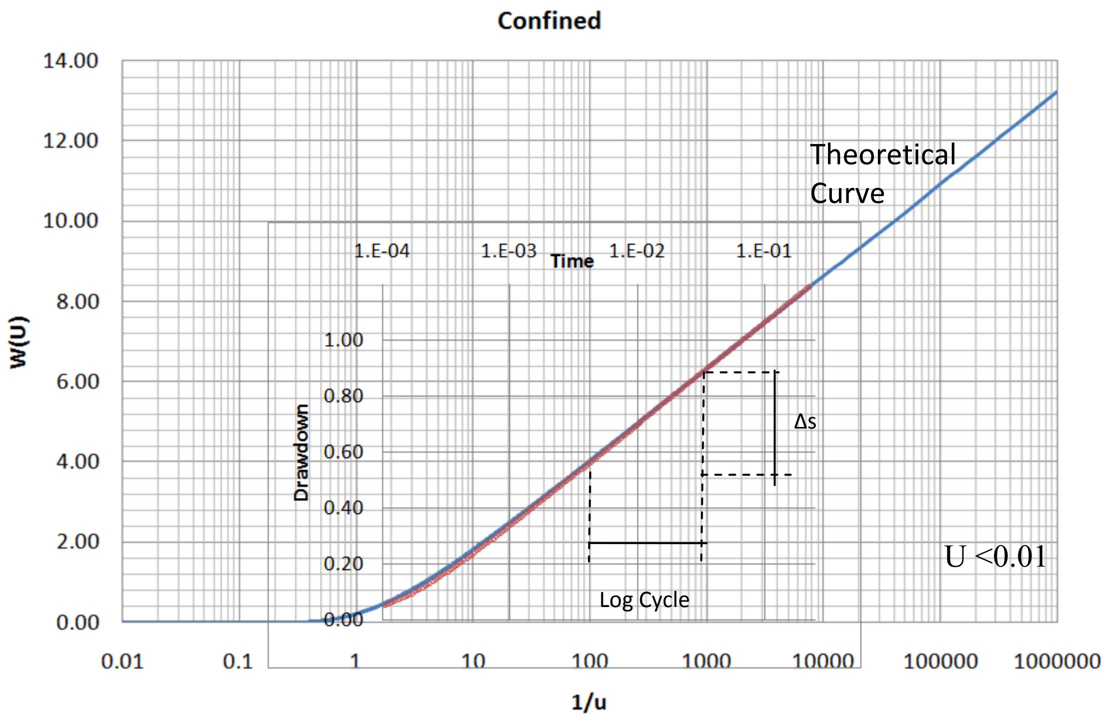

Figure 4.3. Time Drawdown data analyzed with the Cooper-Jacob method, drawdown stated in red line

Test values calculated from a single pumping test using drawdown measured at different observation wells tend to be fairly constant. However, the corresponding S_{est}

values display large variability (Meier et al., 1998). Actually, Meier et al. (1998) and others have shown that these effects in T_{est} and S_{est} are a consequence of the homogeneity assumption used in the interpretation. Thus, in pumping tests performed in heterogeneous media, the variability in the transmissivity field is apparent as variability in the S estimates, while the estimated T values remain almost constant.

4.1.2. Conventional Methods Used for Leaky Confined Aquifer

A leaky aquifer (Figure 4.4, A and B), also known as a semi-confined aquifer, is an aquifer whose upper and lower boundaries are aquitards, or one boundary is an aquitard and the other is an aquiclude. Water is free to move through the aquitards, either upward or downward. If a leaky aquifer is in hydrological equilibrium, the water level in a well tapping it may coincide with the watertable. The water level may also stand above or below the watertable, depending on the recharge and discharge conditions. In deep sedimentary basins, an interbedded system of permeable and less permeable layers that form a multi-layered aquifer system (Figure 4.4) is very common. But such an aquifer system is more a succession of leaky aquifers, separated by aquitards, rather than a main aquifer type.

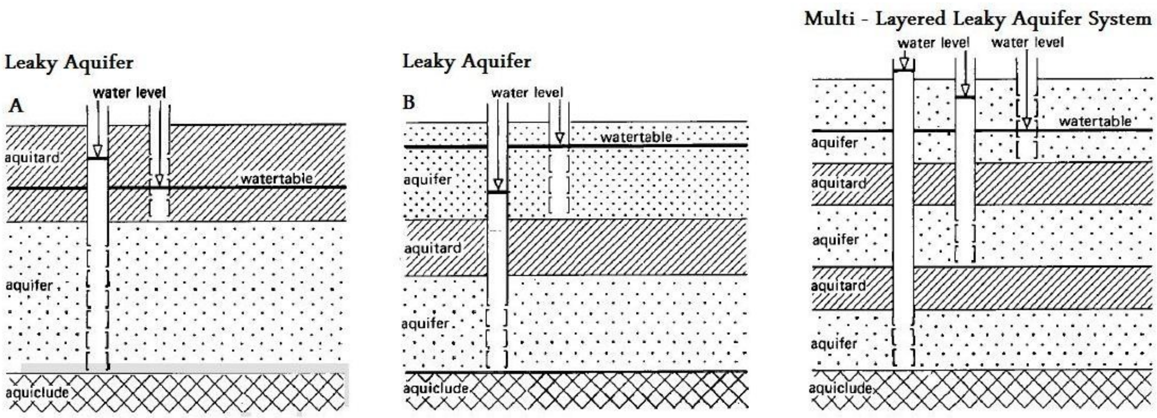

Figure 4.4. Vertical leaky aquifers (A,B) and Multi-layered Aquifer System (from Analysis and Evaluation of Pumping Test Data, G.P Kruseman, N.A de Ridder)

With regard to the analysis of pumping tests in leaky aquifers, the solution of Hantush and Jacob (1955) formed the starting point in the development of pumping test interpretation techniques such as the inflection point method (Hantush, 1956) and the type curves method defined by Walton (1962). The vertical cross-section of the leaky aquifer system considered in this study is similar to that analyzed by Hantush and Jacob (1955). The system consists of two horizontally unbounded aquifers, separated by an aquitard. A fully penetrating pumping well of infinitesimal radius is placed in one aquifer and is fully isolated from the other (Figure 4.5). Before pumping, the system is assumed to be at equilibrium, with both aquifers and the aquitard having the same hydraulic head. The aquitard is assumed to have no storage capacity. Because of the large contrast in hydraulic conductivity values, the flow induced by the pumping is approximately vertical in the aquitard and horizontal in the aquifer.

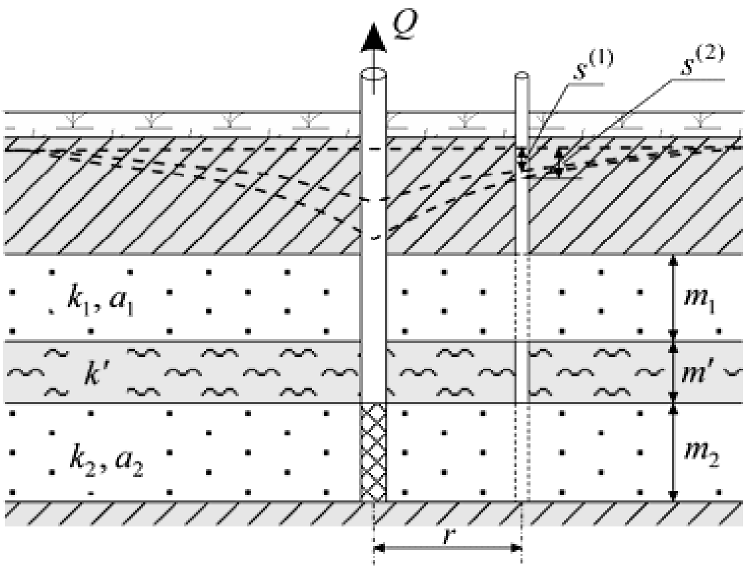

Figure 4.5. Conceptual model of cross section of a pumped leaky aquifer **(**http://www.ansdimat.com/schemes.shtml)

The general assumptions of conventional methods for semiconfined aquifers are summarized below:

- All assumptions specified in section 4.1.1 before;
- Aquifer is leaky;
- Flow in aquitard is vertical and the aquitard is incompressible;
- Drawdown in unpumped aquifer is negligible.

When the well is pumped, water is released from storage, leaks through the aquitard from the unpumped aquifer. Over time, more and more of the water pumped comes from storage in the unpumped aquifer until a steady state is reached.

4.1.2.1. Walton's Curve-Fitting Method. Walton's curve fitting method is similar with Theis's curve fitting method explained before, but with one important difference: Walton's method does not just rely on one curve but a family of curves as a function of leakance. With the effects of aquitard storage considered negligible, the transient drawdown for a homogeneous aquifer–aquitard system due to pumping in a leaky aquifer is described by the following formula which is the modification of Equation (4.1) (Hantush and Jacob 1955).

$$s(r,t) = \frac{Q}{4\pi T}\int_u^{\infty}\frac{1}{y}\exp\left(-y-\frac{r^2}{4B^2y}\right)dy = \frac{Q}{4\pi T}W\left(u, r/B\right) \tag{4.3}$$

where r is the radial coordinate, with origin at the pumping well, $s(r, t)$ is the drawdown; Q is the constant pumping rate, T is the spatially uniform transmissivity, and $W(u, r/B)$ is the leaky well function. The curve-fitting method (Walton, 1962) finds the representative hydraulic parameters by comparing the observed time-drawdown data on a log-log plot to a family of type curves developed based on the analytical solution given in equation(4.3).

One important comment is during unsteady-state flow, storage capacity of the aquifer needs to be accounted for. If it is not, conductivity (K) in leaky aquifer can be overestimated or underestimated in aquitard; there would be also false impression of heterogeneity in aquifer.

Parameters may be estimated by two different procedures via Walton's Curve Fitting Method. The first is simple manual fitting by visually matching the appropriate theoretical curve and determining approximate aquifer parameters (Figure 4.6). The other practice is with the trial and error approach that minimizes sum of squared differences between simulated drawdown and the theoretical drawdown (e.g., Copty et. al., 2008) which has the similar logic with the residual statistics used for curve fitting practices. The sum of squares differences is given by:

$$\sum_i [\bar{s}(r,t_i) - s(r,t_i)]^2 \tag{4.4}$$

where, $s(r, t_i)$ is the observed drawdown at distance r from the pumping well and time t_i and $\bar{s}(r, t_i)$ is the trial drawdown derived from the type curves.

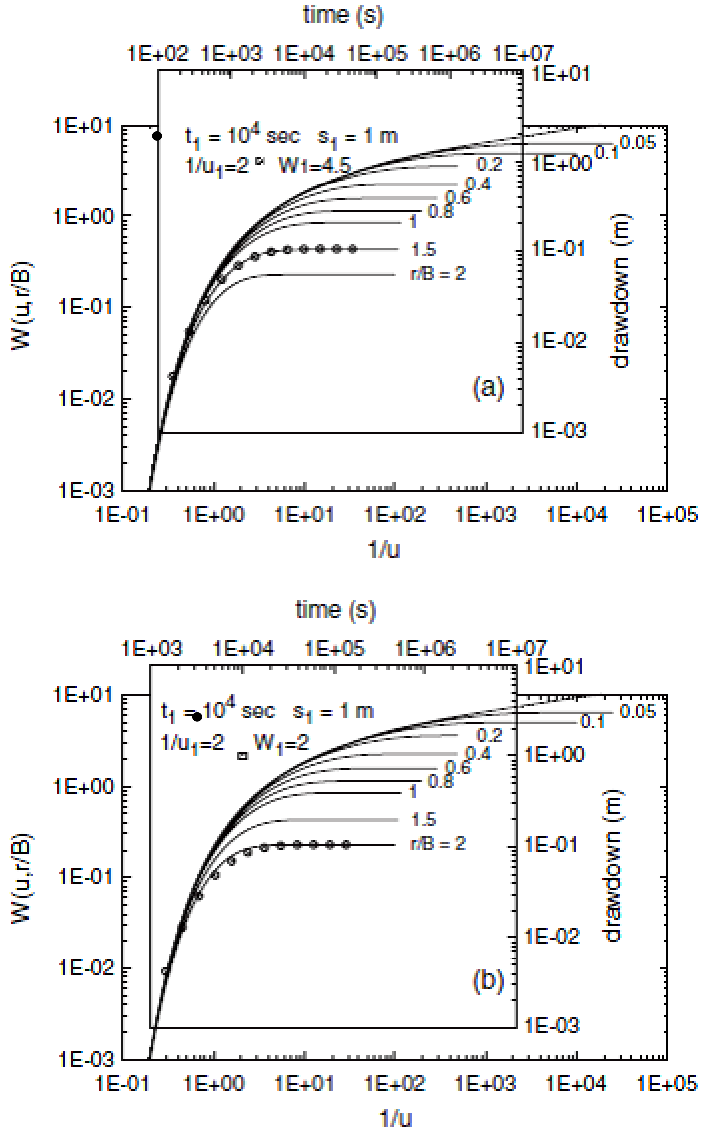

Figure 4.6. Interpretation of the synthetic pumping test using the type-curve method of Walton. Fit curves are a) *r/B* = 1.5 and b) *r/B* = 2.0.(Trinchero et al., 2008)

In this study both procedures were used with the Walton's method. For the procedure involving the minimization of the sum of square differences method, a FORTRAN code was prepared. An example of this code is shown in Figure 4.7.

To obtain the unique fitting position of the data plot with one of the type curves, a sufficient number of the observed drawdown data should fall within the early period when leakage effects are negligible, or r/B should be rather large.

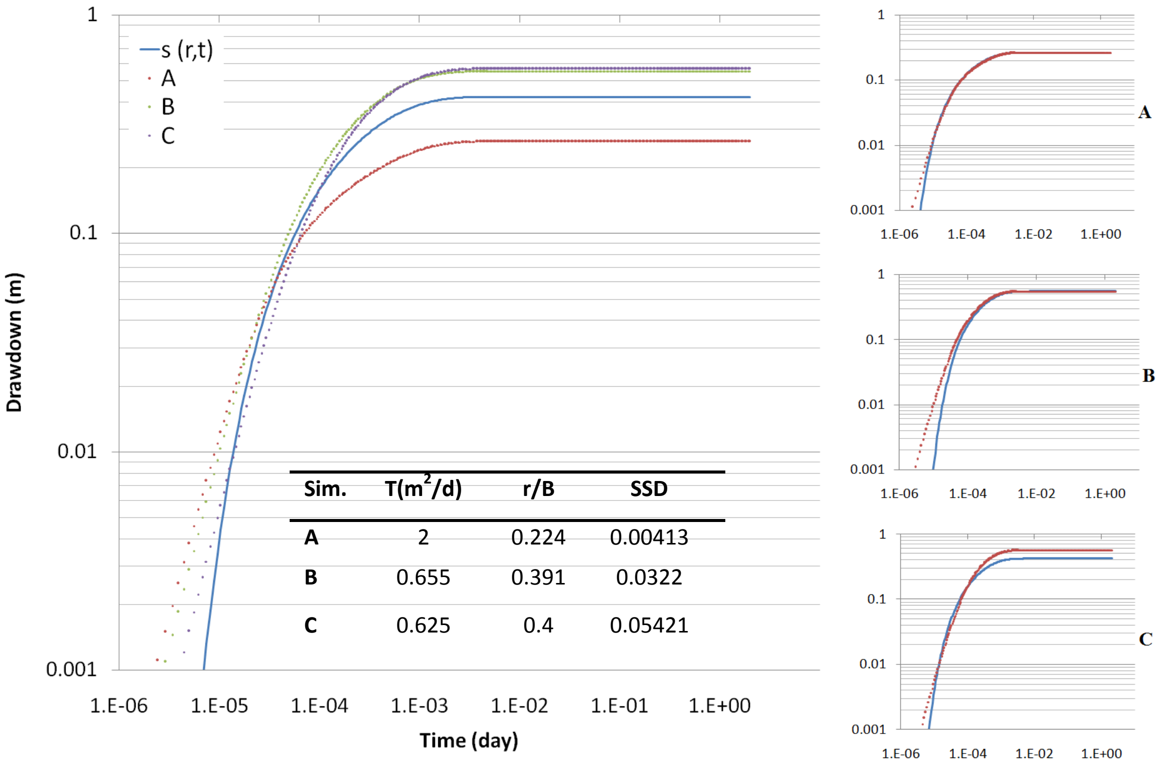

Figure 4.7. Walton's Type Curves numerical application**,** **(**A, B, C; different heterogeneous simulations. Blue lines are theoretical curves)

<u>4.1.2.2. Hantush Inflection Point Method.</u> The inflection point method developed by Hantush (1956) is based on the drawdown equation for leaky confined aquifers originally developed by Hantush and Jacob (1955), Eq. (4.3). The inflection-point method uses analytically derived relationships of the drawdown versus log-time curve to estimate the flow parameters. In particular, it uses the ratio between the drawdown, sp, and its derivative at the inflection-point location, Δsp, is function of the ratio *r/B* only [Hantush, 1956],

$$2{,}3\frac{s_p}{\Delta s_p} = \exp(r/B)K_0(r/B) \tag{4.5}$$

The time corresponding to the inflection point, t_p, can be written in terms of the different system parameters.

$$t_p = \frac{rSB}{2T} \quad (4.6)$$

Once the leakage factor, *B*, is estimated from Equation (4.5), the transmissivity, *T*, and storativity, *S*, of the perturbed aquifer can be determined sequentially from equations (4.6) and the steady drawdown equation, s_m as given by de Glee (1930), Equation(4.7).

$$s_m = \frac{Q}{2\pi T_0} K_0(r/B) \quad (4.7)$$

It is possible to demonstrate analytically that the steady-state drawdown, s_m, is twice the drawdown at the inflection point $s_m = 2s_p$. Hence, in real applications, there are two different ways of applying the Hantush inflection point method. First, from the steady-state drawdown, one can estimate $s_p = 0.5s_m$. Then from the drawdown curve, we estimate T_p and Δs_p. As another application of inflection - point method, which is more sensitive, is that one can locate the inflection-point as the point where the derivative of the drawdown vs. log-time is maximum, and from that determine s_p and Δs_p. While in homogeneous media both methods would render the same parameter values, in real (heterogeneous) media this is not necessarily true (Figure 4.8). The two variants of the method will be compared and evaluated as part of the present study.

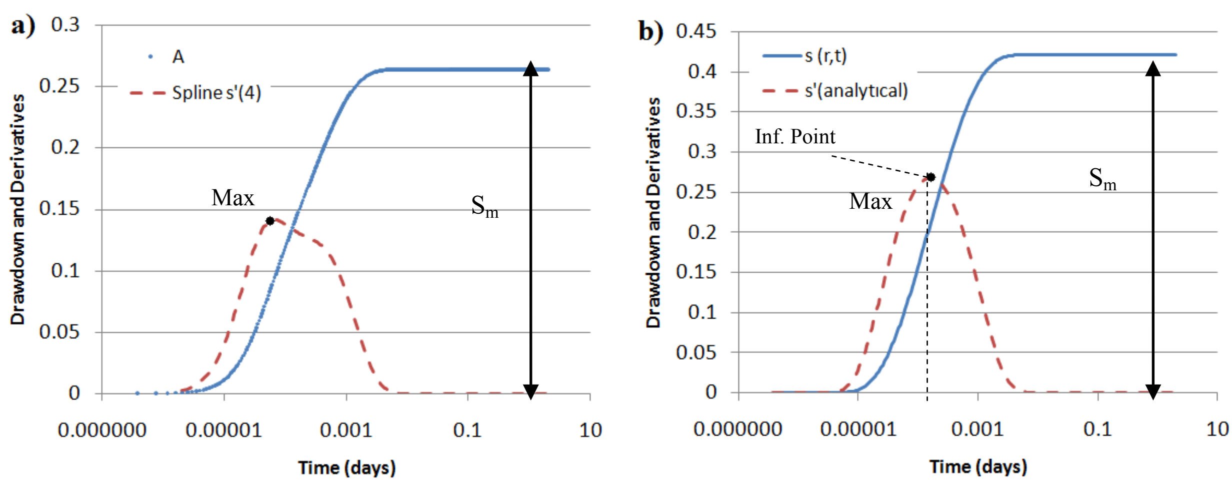

Figure 4.8. Hantush's Infliction point method for, a) Heterogeneous realization A, b) Theoretical Realization

It is hard to specify the exact maximum point for the inflection point in heterogeneous case, which is normally encountered in real world applications. So it is decided that to find the slope or the trend of the drawdown curve, and use the equation (4.8) to estimate aquifer parameters, (Figure 4.9).

$$m = \frac{\Delta s}{[\Delta Log(t)]} = \frac{2.3Q}{4\pi T} \exp\left(-u - \frac{r^2}{4B^2 u}\right) \tag{4.8}$$

where; m is the drawdown slope. For practical solutions of the Hantush Infliction-Point method a script based on the slope approach was written in FORTRAN to estimate aquifer parameters of simulated well tests.

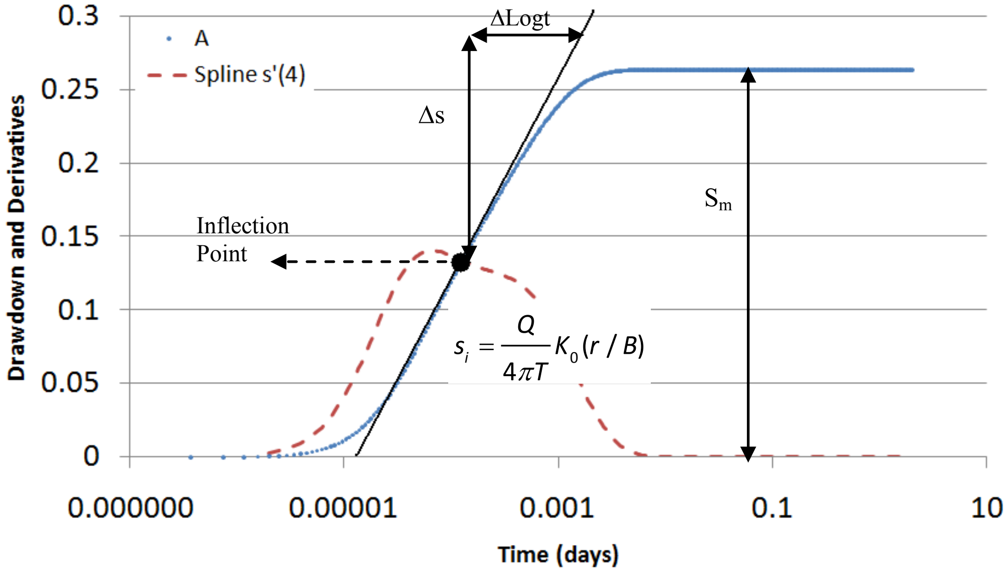

Figure 4.9. Drawdown versus time variation at an observation well of semiconfined aquifer due to constant rate water extraction

4.1.3. The Double Inflection Point Method

Recently, a new method for the interpretation of pumping tests in leaky aquifers was developed, referred to as the double inflection-point (DIP) method (Trinchero et al., 2008). The system considered in the development of this methodology is the same as that defined by Hantush and Jacob (1955) and described in the section 4.1.2. The analytical solution is based on the same principle described in Hantush (1956) including well function, shown in Equation(4.3).

The DIP method requires the estimation of the ratio $\tau = t_p/2t_{s1}$ or $\tau = t_p/2t_{s2}$ where t_p is the time corresponding to the inflection point [Equation(4.6)] and t_{s1} and t_{s2} are the times corresponding to the two inflection points of the first derivative of the drawdown with respect to the logarithm of time (Figure 4.10). Once τ is estimated, the leakage factor is computed directly from (Trinchero et al., 2008):

$$B = \frac{\left(\tau^2 - 1/4\right)^2 r}{\tau\left(\tau^2 + 1/4\right)} \quad (4.9)$$

After the leakage factor, B, is estimated, the other flow parameters (T, S, and C) are calculated from equations(4.7), (4.6) and(3.1), respectively. Because t can be based either on t_{s1} or t_{s2}, two sets of parameters are estimated with the DIP method.

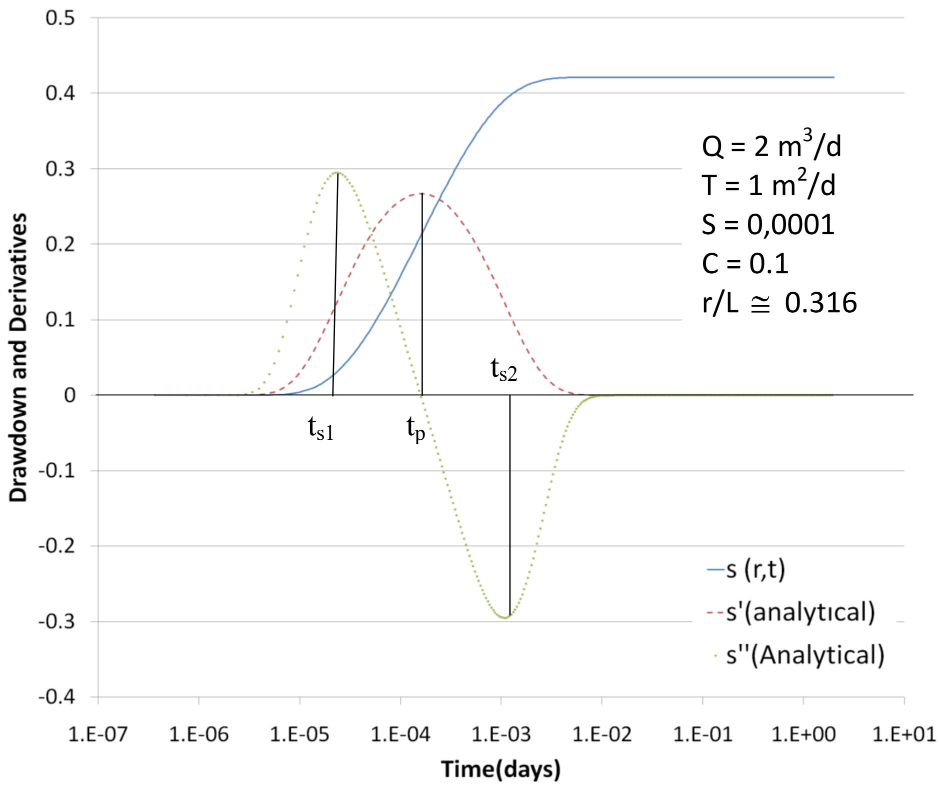

Figure 4.10. Drawdown and its first and second derivatives as a function of log time based on homogeneous assumption (from Trinchero et al., 2008)

The derivative of the drawdown with respect to the base-10 logarithm of time can be written as follows:

$$s' = \frac{\partial s}{\partial \log t} = 2.3t\frac{\partial s}{\partial t} = \frac{2.3Q}{4\pi T}\exp\left(-\frac{r^2 S}{4Tt} - \frac{Tt}{B^2 S}\right) \tag{4.10}$$

Equation (4.10) also allows us to find the inflection point without slope approach specified in previous section. Specification of the time values those; t_{s1} that corresponds to maximum derivative value and t_{s2} which corresponds to minimum derivative value can be calculated by the second derivation equation(4.11) with the same approach in equation(4.9) (Figure 4.10):

$$s'' = \frac{\partial^2 s}{\partial \log t^2} = \left[\frac{2.3Q}{4\pi T}\exp\left(-\frac{r^2 S}{4Tt} - \frac{Tt}{B^2 S}\right)\right]\left(\frac{r^2 S}{4Tt}\frac{Tt}{B^2 S}\right) \tag{4.11}$$

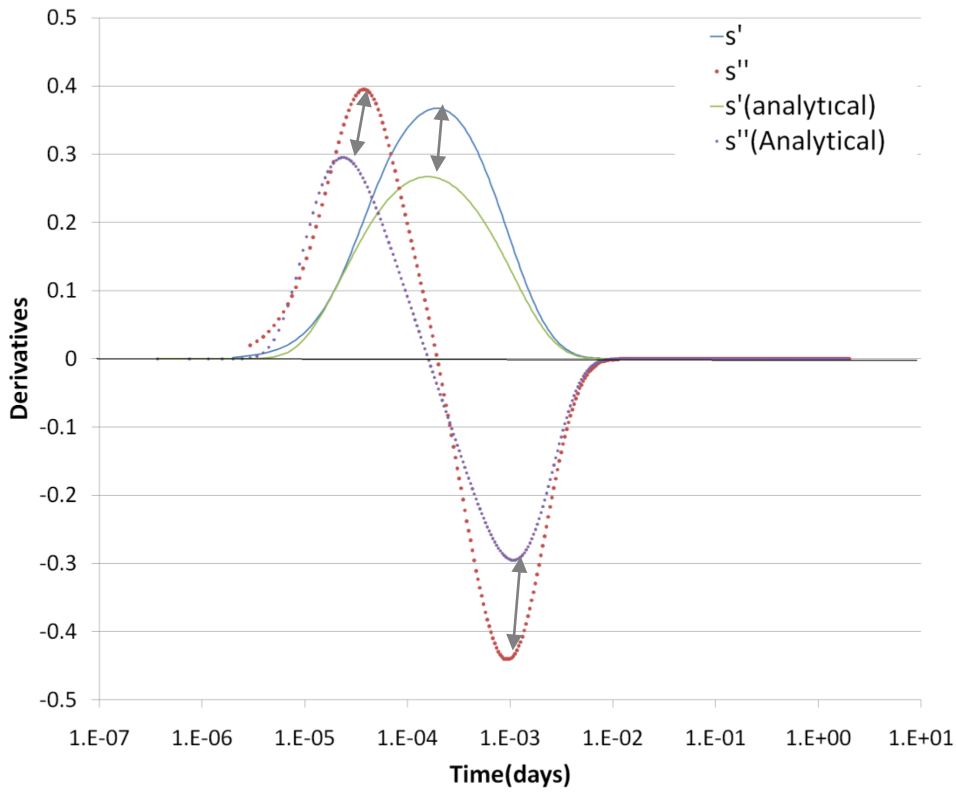

Figure 4.11. First and second derivative of the drawdown from the synthetic pumping test in the heterogeneous aquifer and in the equivalent homogeneous aquifer (defined in terms

of the geometric mean of the transmissivity field). The double arrows show the shift of the singular points.

Pumping test interpretation techniques both conventional (e.g. Theis, Cooper-Jacob, Hantush, Walton), and novel methods [e.g. Double Inflection Point (Trinchero, 2008a), Hydraulic Tomography (Yeh & Liu, 2000) methods] use drawdown data collected at different times to estimate representative values of the flow parameters. For example, the graphical curve fitting approach attempt to fit drawdown data observed at different times to normalized drawdown curves. The Cooper-Jacob method is based on a straight line fit to the late drawdown data. The DIP method uses the location of the inflection point t_{inf} and t_{si1} (or t_{inf} and t_{si2}), while the Hantush inflection method combines the steady state drawdown with the drawdown and drawdown slope at the inflection point. Hydraulic tomography method compares the data sets adopted from different vertical portions or intervals of the aquifer different than other novel methods.

However, we know that for heterogeneous formations, the representative parameters changes as the drawdown cone expands with time. Desbarats & Srivastava (1991) found moderately good agreement between the transmissivity predicting using Gelhar & Axness's (1983) theory for an infinite, two-dimensional, statistically anisotropic field, but found excellent agreement with the theoretical value of effective transmissivity predicted for an infinite, two-dimensional (2D), statistically isotropic field, which is the geometric mean. In addition to this, at early time the transmissivity influencing the pumping test is close to the transmissivity at the well T_w, while at late times, the transmissivity influencing the test is equal to some spatial mean that may or may not be equal to the geometric mean of the transmissivity. The magnitude of this spatial mean would depend on the local transmissivity at the well, the characteristic length scales of the problem, namely: the integral scale and the leakage factor for leaky aquifers, and the transmissivity variance especially fields have high heterogeneity.

Using drawdown data observed at different times may yield some "representative" value of the transmissivity but this value is dependent on the method used because each method gives different emphasis to different portions of the drawdown time series. This may complicate the efforts to characterize the spatial variability of the flow parameters. It is also seen that in the case leaky aquifers where the transmissivity has a monotonic trend (Copty et al., 2008) the estimated transmissivity may not actually match the actual transmissivity used in the simulations. To open the comment up, for decreasing trend with distance from the well, the estimated transmissivity was exceeding the largest value, Tw; for an increasing trend with distance, the estimated transmissivity was smaller than the smaller value.

Another limitation of the Cooper-Jacob for confined aquifers and the DIP and Hantush methods for leaky aquifers is that although they are all straight forward and simple to apply, they use only part of the available information. In the case of the Cooper-Jacob method we use drawdown date for $u<0.1$, while the Hantush and DIP method use information only at the inflection points and ignore the remaining portions of the time-drawdown.

4.2. Data Smoothing and Differentiation Techniques

As discussed above, well testing is one of the most commonly applied methods used to characterize the hydraulic properties of aquifers. It involves imposing a perturbation such as pumping in a well and measuring the response of the aquifer, in terms of head variations or pressure measurements. Those data are then interpreted with the help of analytical or numerical models in order to infer the hydraulic properties of the aquifer.

Chow (1952) who was the first to use the drawdown derivative in the interpretation of pumping tests demonstrated that the transmissivity of an ideal confined aquifer is proportional to the ratio of the pumping rate by the logarithmic derivative of the drawdown at late time. Chow (1952) developed also a graphical technique to apply this principle, but this proposition had some limitations such as it is only relying on the late data until the work of Bourdet and his colleagues (Bourdet et al., 1989; Bourdet et al., 1983). They generalized the idea and analyzed the behavior of the log-derivative for a large number of classical models of flow around a pumping well.

Those developments opened a new approach in pumping test well analysis by which we focus on diagnostic plots for the analysis of the test well data. In particular the drawdown derivative is considered more sensitive to subtle variations in the shape of the drawdown curve. It allows detecting behaviors that are difficult to observe on the drawdown curve alone (Renard et al., 2009). The analysis of the diagnostic plot of a data set facilitates the selection of a conceptual model. For both Hantush Inflection point and DIP methods the values of the derivative have been analyzed and used to estimate rapidly the parameters of the model.

When data collected from the field are used, the logarithmic derivative has to be evaluated numerically from a discrete series of n drawdown s_i and time t_i values. These n couples of values are the circles represented in Figures 2.2, 4.8, 4.9, 4.10, 4.11.There are many ways to compute the log derivative. The simplest derivation is demonstrated in equation(4.12).

$$\left.\frac{\partial s}{\partial \ln t}\right|_{t_m} = \frac{s_i - s_{i-1}}{\ln(t_i) - \ln(t_{i-1})} \tag{4.12}$$

This approximation is associated with the time t_m corresponding to the centre of the time interval ($t_m = (t_i + t_{i-1})/2$) and hence it is called Central Difference Method. To get an accurate result using such simple differentiation approximation, frequent measurements should be made and the noise in the data (both simulated and field) should be minimal, or some noise reduction techniques would be needed. Figure 4.13 shows the second derivative of a specific time-drawdown data differentiated by the central difference method with the lowest differential interval.

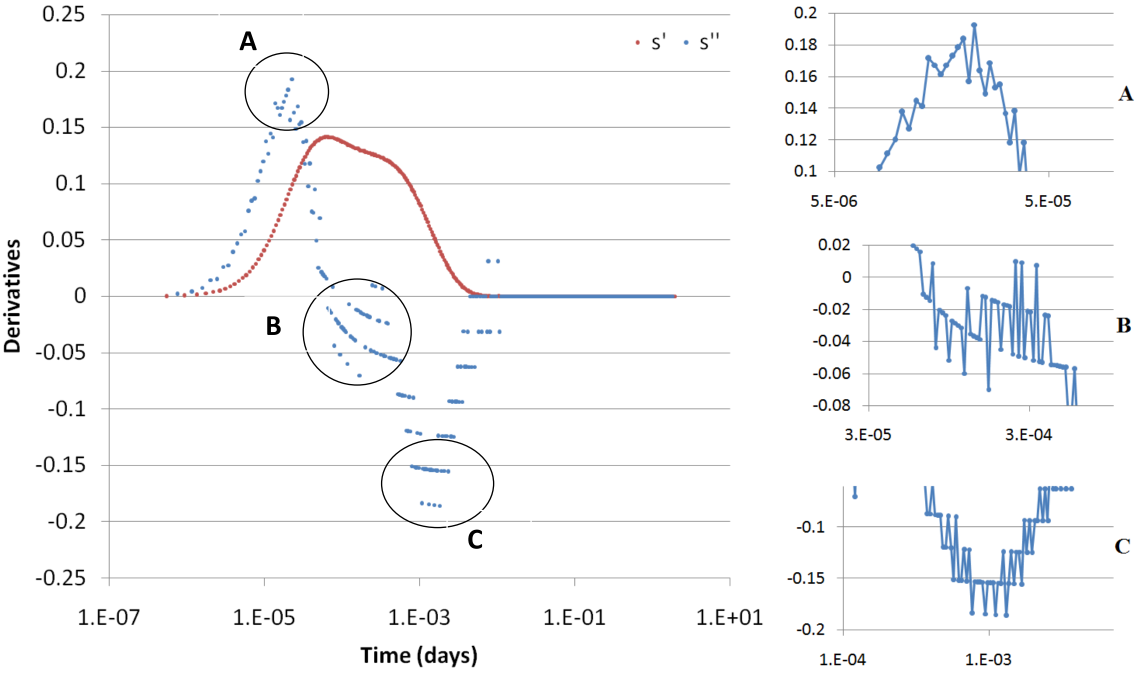

Figure 4.12. First and second derivatives of heterogeneous synthetic drawdown by using the central difference method, A and C shows in turn the maximum and minimum peak points, B shows the middle point of the second derivative which corresponds to peak point of the first derivative.

In order to minimize the artifacts exemplified in Figure 4.12, more robust numerical differentiation schemes have been proposed. Bourdet et al. (1989), Spane and Wurstner (1993), Horne (1995), and Veneruso and Spath (2006) discuss and present different techniques such as smoothing the data prior to the computation of the derivative, or smoothing the derivative. The differentiation algorithm used in this study was proposed by Bourdet et al. (1989). The algorithm is based on the slopes of the drawdown change versus the change in time. Instead of using the arithmetic average of corresponding time, the drawdown derivatives for the points of interest are calculated using the modified relationship of the equation as presented Bourdet et al. (1989):

$$\left(\frac{\partial s}{\partial Logt}\right)=\frac{\left(\Delta s_{i-1}/\Delta Logt_{i-1}\right)\Delta Logt_{i+1}+\left(\Delta s_{i+1}/\Delta Logt_{i+1}\right)\Delta Logt_{i-1}}{\Delta Logt_{i+1}+\Delta Logt_{i-1}} \tag{4.13}$$

where t is calculated using the equivalent time function, Δt_e, presented by Agarwal (1980), also demonstrated in equation(4.14).

$$\Delta t_e = \frac{(t_p \times \Delta t)}{(t_p + \Delta t)} \tag{4.14}$$

In the above equation, t_p is the duration of discharge test and Δt is the time since discharge terminated. Essentially, equation (4.13) is a weighted average of slopes computed from data points on either side of data point i. In the above formula, the two slopes are the left derivative; $\Delta s_{i-1} / \Delta t_{i-1}$ and the right derivative; $\Delta s_{i+1} / \Delta t_{i+1}$.

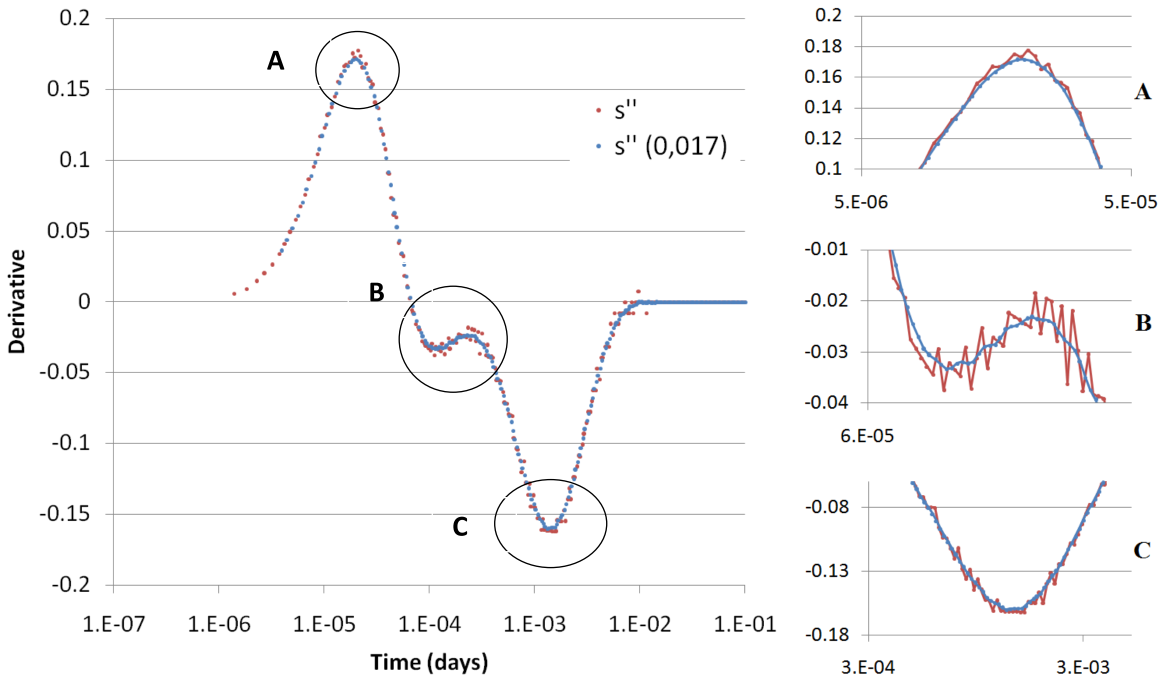

Figure 4.13. Comparison of Central Difference and Bourdet Derivation. (L: 0.017)

In addition to Bourdet differentiation approximation method, Spane and Wurstner (1993) presented an alternative method for computing derivatives. Like the Bourdet method, the Spane method uses a logarithmic differentiation interval; however, instead of using three points in the derivative computation, the Spane method computes the left and right derivatives by applying linear regression to all of the points falling within the differentiation interval. In many cases, according to Figure 4.14 the Spane method produces slightly smoother derivative than the Bourdet method, particularly if the data is noisy.

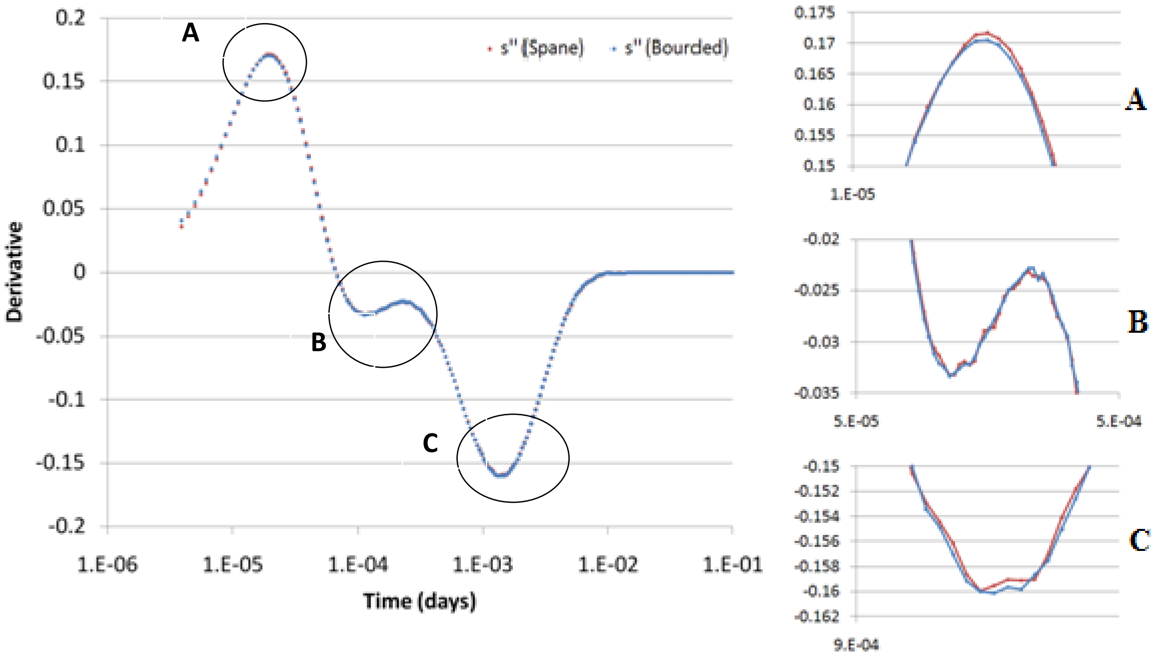

Figure 4.14. Comparison between the Bourdet and Spane & Wurstner differentiation methods

There are two options specified by Spane & Wurstner (1993) for calculating of the mean slopes before and after the point of interest: fixed end-point and least squares regression. The fixed end–point is recommended for calculating pressure derivatives for type–curve values (Cooper et al., 1967) or test data that are relatively free of noise. Because of the noisy data mainly been encountered in the field data, the least–square regression option is preferred.

4.2.1. Smoothing Techniques

Inherent in the collection of test well data taken over time is some form of random noise. Several methods exist for reducing of canceling the effect due to random variation. An often-used technique in statistics is "smoothing". This technique in general, when properly applied, reveals more clearly the underlying trend, seasonal and cyclic components. Even the practice mainly done in some other data types, smoothing techniques can be used for the trend estimation of drawdown data sets. Smoothing methods were not used as differentiation methods; those are used to smooth the estimated derivatives of the data.

The purpose of smoothing data sets is to create an approximating function that attempts to capture important patterns in the data, while leaving out noise. There are mainly accepted as two distinct group of smoothing methods; Averaging Methods and Exponential Smoothing Methods. In this study we different averaging and exponential smoothing methods those were evaluated. Statistical measures were used to find the best method to diagnostic analysis. Six smoothing methods were applied on the data: Moving Average, Single Exponential Smoothing, Linear Exponential Smoothing, Holt-Winter's method and LOESS (Locally Weighted Regression).

4.2.1.1. Moving Average Method. The general expression for the moving average is as a simple arithmetic average;

$$M_t = \left[s_t + s_{t-1} + \cdots + s_{t-N}\right] / N \tag{4.15}$$

the practice is made with placing the average in the middle of the time interval of arranged periods. It is decided to use odd time periods.

4.2.1.2. Exponential Smoothing Methods. Exponential Smoothing assigns exponentially decreasing weights as the observation get older. In exponential smoothing, however, there are one or more smoothing parameters to be determined (or estimated) and these choices determine the weights assigned to the observations. There are three exponential smoothing methods named as single, double and triple exponential smoothing methods. The names are given according to constants the methods have.

The basic equation of single exponential smoothing as in equation (4.16) and the constant or parameter *α* is called the smoothing constant. (Hunter, 1986);

$$s_{t+1} = \alpha y_t + (1-\alpha) s_t \quad 0 < \alpha \le 1 \quad t > 0 \tag{4.16}$$

After adding one more parameter, γ, there should be two equations associated with Double Exponential Smoothing:

$$\begin{aligned} s_t &= \alpha y_t + (1-\alpha)(s_{t-1} + b_{t-1}) \qquad 0 \le \alpha \le 1 \\ b_t &= \gamma(s_t - s_{t-1}) + (1-\gamma) b_{t-1} \qquad 0 \le \gamma \le 1 \end{aligned} \tag{4.17}$$

where α and γ are smoothing parameters, and b denotes the trend of the drawdown. The resulting set of equations is called the "Holt-Winters" (HW) method also named as Triple Exponential Smoothing, with the sum of all previous equations and their representatives are;

$$\begin{aligned} s_t &= \alpha \frac{y_t}{I_{t-L}} + (1-\alpha)(s_{t-1} + b_{t-1}) \\ b_t &= \gamma(s_t - s_{t-1}) + (1-\gamma) b_{t-1} \\ I_t &= \beta \frac{y_t}{s_t} + \left(1-\beta\right) I_{t-L} \end{aligned} \tag{4.18}$$

y is the observation value, s is the smoothed observation, b is the trend factor, I is the seasonality.

4.2.1.3. LOESS Smoothing. Loess smoothing is considered as one of the modern regression methods; however, it does not require the user to specify a single type of function to fit the entire data set. LOESS, originally proposed by Cleveland (1979) and further developed by Cleveland and Devlin (1988), specifically denotes a method that is more descriptively known as locally weighted polynomial regression.

At each point in the data set a low-degree polynomial is fit to a subset of the data, with explanatory variable values near the point whose response is being estimated. The polynomial is fit using weighted least squares, giving more weight to points near the point whose response is being estimated and less weight to points further away. Useful values of the smoothing parameter typically lie in the range 0.25 to 0.5 for most LOESS applications.

4.2.2. Fitting Methods

Another method of estimating the derivatives of data series is to fit the data to some easily differentiable function. The derivatives can then be estimated by taking the derivatives of the fitted functions. Three different fitting functions were considered in this study: Polynomial Fitting, Rational Fitting and Smoothing Spline. Each method is described in the following sections.

4.2.2.1. Polynomial Fitting. Polynomial fitting is a simple to observe the pattern of drawdown data. Polynomial fitting has been considered by several authors (e.g., Illman and Neuman, 2001, Sudicky et al., 2010). Mathematically, a polynomial of degree n can be written as:

$$f(x) = c_1 + c_2 x + c_3 x^2 + \cdots + c_{n+1} x^n \tag{4.19}$$

Higher degree polynomials (4^{th} degree polynomial or higher) were considered because they better fitted the drawdown data.

4.2.2.2. Rational Fitting. The rational fitting method can also be considered as a pseudo-polynomial method because it is evaluates the ratio of different polynomial functions as shown in equation (4.20)

$$y = \frac{\sum_{i=1}^{n+1} p_i x^{n+1-i}}{x^m + \sum_{i=1}^{n+1} q_i x^{m-i}} \tag{4.20}$$

where n is the degree of the numerator polynomial and $0 \le n \le 5$, while m is the degree of the denominator polynomial and $1 \le m \le 5$. Note that the coefficient associated with x_m is always 1. This makes the numerator and denominator unique when the polynomial degrees are the same.

4.2.2.3. Smoothing Spline. The logic of the smoothing spline is similar to the derivative method of Spane, except that smoothing splines are piecewise polynomials and is considered a nonparametric fit type which is defined to be a function on a sample that has no dependency on a statistical parameter.

The smoothing spline *s,* which represents the spline function, is constructed for the specified smoothing parameter p and the specified weights w_i. The smoothing spline minimizes (Green and Silverman, 1994)

$$p\sum_i w_i\left(y_i - s(x_i)\right)^2 + (1-p)\int\left(\frac{d^2 s}{dx^2}\right)^2 dx \tag{4.21}$$

If the weights are not specified, they are assumed to be 1 for all data points. Where p is defined between 0 and 1; x_i is the actual y_i is the predicted value

4.3. Numerical Simulation

In the thesis, we primarily focus on to the spatial variability of the transmissivity field and utilized existing conventional methods and novel relatively untested pumping test interpretation methods, on heterogeneous media. Two sets of pumping tests were considered in this study; synthetically simulated pumping tests and actual pumping tests. This section describes how the synthetic pumping test data in heterogeneous aquifers were generated.

The steps for the simulation in order are i) heterogeneous transmissivity fields were generated using the turning bands method (Mantoglou and Wilson, 1982), ii) using the generated transmissivity data, a pumping test under a constant pumping rate is simulated using MODFLOW (Harbaugh et al., 2000) a commonly used finite-difference code that simulated flow through porous media. iii) The time-drawdown data at selected points were analyzed to estimate the flow parameters T_{est} and S_{est}.

For the generation of heterogeneous transmissivity field, we assumed that the log transform of the transmissivity is a multivariate Gaussian random spatial function with exponential semivariogram, zero mean ($T_{Geometric}$ = 1) as stationary mean, variance of σ^2 =

1 and integral scale equal to 8 length units. The realizations of log transmissivity field (Figure 4.16) as spatially variable parameters were generated using the turning bands method (Mantoglou and Wilson, 1982). Five different realizations were generated in order to test semiconfined and confined pumping test interpretation methodologies that were presented in the previous sections.

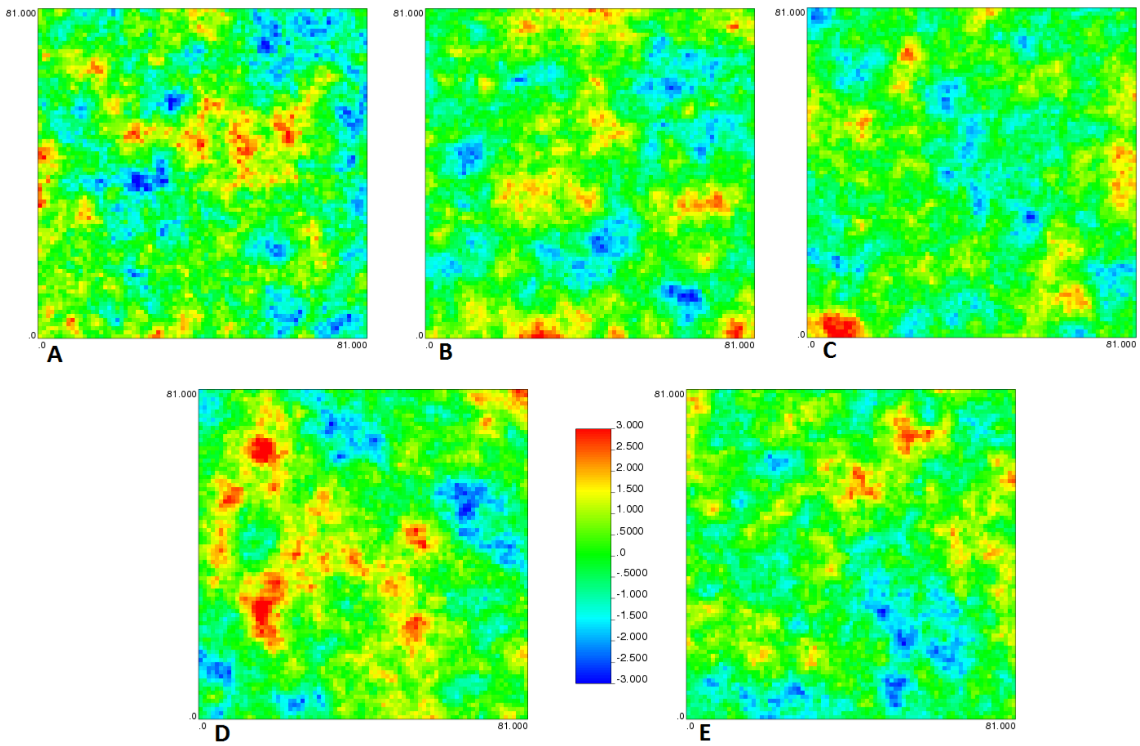

Figure 4.15. Randomly-generated transmissivity fields

The leaky aquifer system is composed of two layers with the confining aquifer assumed to have no storage, as defined by Hantush and Jacob (1955). The leaky aquifer system can be altered to a confined aquifer system by assuming the vertical conductivity of the aquitard equal to zero. The pumping test simulated on the field that consists of 481×481 uniform grid cells each 1×1 m, with constant flow rate of 2 m^3/d. The pumping well is assumed to be a fully penetrating well. It is also assumed to be located at the center of the domain and pumping from the semiconfined aquifer. Parameters of conductance of the aquitard and the storage coefficient of the aquifer are considered uniform, with values of 0.1 1/d and 0.0001, respectively. The upper unpumped aquifer is assumed to be unaffected by the pumping.

The simulations were performed with using the finite difference model MODFLOW (Harbaugh et al., 2000) which solves the governing partial differential equations (PDEs) describing groundwater flow in porous media. For the simulation the initial water level was prescribed as 20 m and drawdown are estimated from the maximum head condition. The test duration was 2 days so it can be also considered as stress period, and a variable time step was used in the simulations, starting with 1 s, and gradually increasing it as the test progressed. Drawdown data were simulated at the cell were the pumping well is placed (corresponds to a distance of about 0.2 m) and at 1 m intervals until 20 m distance from the test well. After that observation points continued with 2 m intervals. The preparation of the data was done using a FORTRAN script shown in Appendix D.

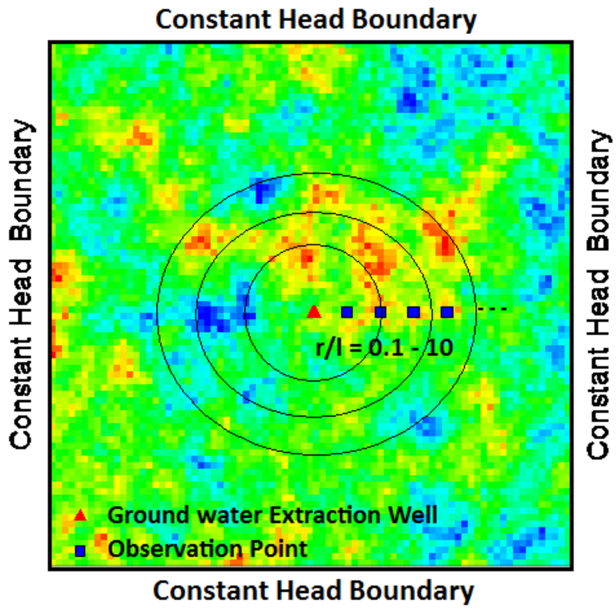

Figure 4.16. Boundary conditions and location of observation scheme for synthetically simulated pumping test

5. CONTINUOUS DERIVATION METHOD

In this chapter a novel procedure for the analysis of pumping tests in heterogeneous confined and semiconfined aquifers is presented. The Continuous Derivation (CD) method is developed to address the limitation of conventional methods which attempt to estimate a single estimate of the flow parameters even if the aquifer is heterogeneous. For instance, as explained in the methodology part, the methods based on graphical curve fitting approach attempt to fit drawdown data observed at different times to normalized drawdown curves. The Cooper-Jacob method is based on a straight line fit to the late drawdown data. The DIP method uses the location of the inflection points t_{inf} and t_{si1} (or t_{inf} and t_{si2}), while the Hantush inflection method combines the steady state drawdown with the drawdown and drawdown slope at the inflection point. All methods explained above rely on the homogeneous field assumption.

However, we know that for heterogeneous formations, the representative parameters changes as the drawdown cone expands with time. For example, at early time the transmissivity influencing the pumping test is close to the transmissivity at the well *Tw*, while at late times, the transmissivity influencing the test is equal to some spatial mean that may or may not be equal to the geometric mean of the transmissivity. The magnitude of this spatial mean is would depend on the local transmissivity at the well, the characteristic length scales of the problem, namely: the integral scale and the leakage factor, and the transmissivity variance.

Using drawdown data observed at different times may yield some "representative" value of the transmissivity but this value is dependent on the method used because each method gives different emphasis to different portions of the drawdown time series, another words it cannot be estimated how the formation so the parameters of the field varies by conventional and DIP methods. This may complicate the efforts to characterize the spatial variability of the flow parameters. We foresee that in the case leaky aquifers where the transmissivity has a monotonic trend, the estimated transmissivity may not actually match the actual transmissivity used in the simulations.

CD method has a simple procedure for the analysis of pumping tests in heterogeneous media as firstly explained in the work of Copty et al. (2011). The main novelty of the proposed method is that it uses the drawdown data and its derivatives at one particular point in time to estimate the flow parameters. The method is repetitively applied to all times in order to develop an estimate of transmissivity and storativity as the cone of depression expands in time along to particular distance. The derived estimates are then compared to the spatial average of the transmissivity around the well for synthetic data derivations; however, this comparison cannot be applied for the real pumping test results on a real field.

Through the application of CD methods we attempt to address the following questions:

- Can we use the drawdown data and its derivatives at one particular point in time to estimate the parameters?
- Can we use the entire time drawdown data to estimate the representative flow parameters as a function of time? This would give use some information about the heterogeneity as a function of distance from the well.
- Can these methods be used to help identify the type of the aquifer (non-leaky confined, unconfined, etc…?

5.1. Continuous Derivation for Confined Aquifer

For radially convergent flow in a confined aquifer, the parameters those controlling the transient drawdown are transmissivity and storativity. CD-Confined method can be included into the derivative methods family; in this method we only need the first derivative of the drawdown. We would need 2 equations at one particular time to estimate these 2 parameters. Assuming homogeneous flow conditions the drawdown in a confined aquifer is given by equation (4.1) and its first derivative is calculated by;

$$s' = \frac{ds}{d\log t} = \frac{2.3Q}{4\pi T}\exp\left(-\frac{r^2 S}{4\pi t T}\right) \tag{5.1}$$

At any point in time, using the ratio of the drawdown and its derivative observed at that particular time, the interpreted flow parameters are estimated (Copty et al., 2011). The ratio of equations (4.1) to (5.1) gives:

$$\gamma_c = \frac{2.3s}{s'} = W(u)\exp(u) \tag{5.2}$$

The characteristic behavior of γ_c is given in Figure 5.1.

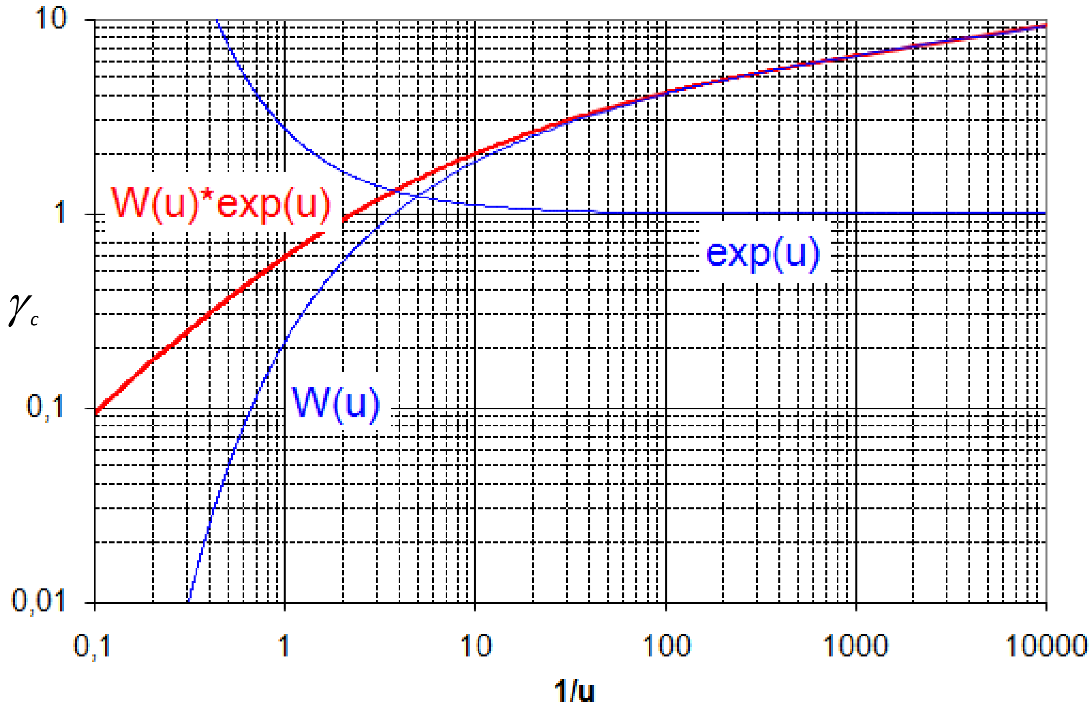

Figure 5.1. Plot of γ_c, ratio of drawdown to drawdown rate, as a function of *1/u* (from Copty et al., 2011)

According to figure 5.1, γ_c increases as the dimensionless time *1/u* increases. For any particular value of γ_c at some time *t*, the corresponding *u* and the well function can be estimated directly. The transmissivity is then estimated from.

$$T_i = \frac{Q}{4\pi s} W(u) \tag{5.3}$$

while the storativity is estimated from:

$$S_i = \frac{4tTu}{r^2} \tag{5.4}$$

so the procedure of the CD confined method as follows

i. From the ratio s/s' at any point in time, we can calculate u
ii. From Equation (5.3), we calculate T_i
iii. From the definition of u, so the Equation (5.4) we calculate S_i

Previous steps direct us to the estimation of flow parameters as a function of time. To convert the time relationship into a radial relationship, we use following relationship:

$$r^* = \sqrt{\frac{4tT}{1.65S}} \tag{5.5}$$

where r^* denotes calculated distance, T, transmissivity, S, storativity and t, corresponding time. The conversion equation has been derived in the work of Copty et al. (2011).

5.2. Effect of Leakage on CD Method

This section describes the effect of the leakage to CD method for non-leaky aquifer. For the field data it cannot be exactly known what is the type of the aquifer so using CD-Confined method for a leaky aquifer can give inaccurate results. For radially convergent flow towards a well in a leaky aquifer (with constant head in the unpumped aquifer and no storage capacity in the aquitard), there are three parameters controlling the transient drawdown: transmissivity, storativity and leakage factor. We would need 3 equations at one particular time to visualize the effect of leakage as a function of *1/u* with repetitive calculation s for every point. These equations can be obtained by making use of the first and second derivatives of the drawdown. Note that in principle this is not very different from the DIP, except that we try to avoid combining data from different times.

Based on the homogeneity assumption the drawdown in a leaky aquifer is given in Equation(4.3). We modified the equations explained in DIP method are first and second derivatives of drawdown nonlinear function, and used the value $\rho = r/B$ in the equations. The derivation below can be seen as an extension or a generalization of the DIP equation because we start from the same equations, however, the method do not be limited only to the inflection points.

$$s' = \frac{\partial s}{\partial \log t} = 2.3t\frac{\partial s}{\partial t} = \frac{2.3Q}{4\pi T}\exp\left(-\frac{r^2 S}{4tT} - \frac{tT}{B^2 S}\right) = \frac{2.3Q}{4\pi T}\exp\left(-u - \frac{\rho^2}{4u}\right) \qquad (5.6)$$

Equations(4.3), (5.6) are the two algebraic nonlinear equations to calculate unknowns: u, T, ρ. Equation (5.6) is the drawdown derivative as a function of logarithm (bas 10) of time.

Taking the ratio of Equations (4.3) and (5.6) yields an expression that is function of the drawdown and its derivatives and u:

$$\gamma_L = \frac{2.3s}{s'} = W(u,\rho)\exp\left(u + \frac{\rho^2}{4u}\right) \qquad (5.7)$$

Equation (5.7) is the equivalent of Equation(5.2) but for leaky aquifers. It allows us to compare the difference between the behavior of confined and semiconfined aquifer in case of using CD method. To see the characteristic behavior of leaky γ_L is given in Figure 5.2.

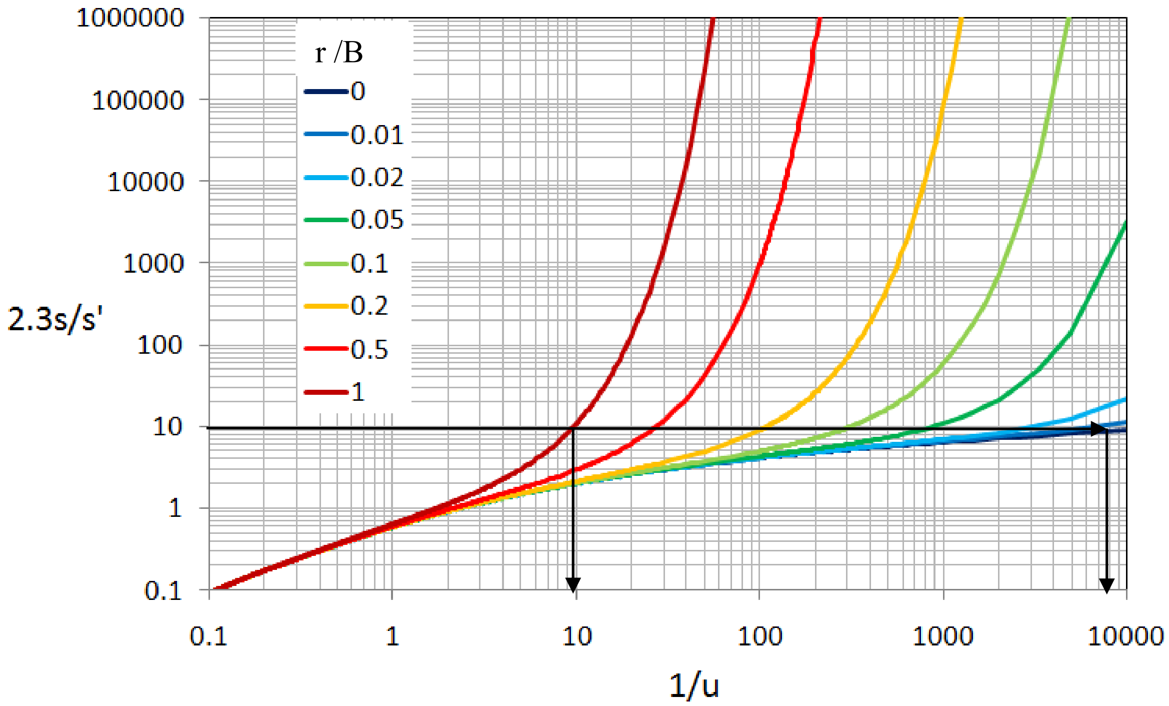

Figure 5.2. Plot of γ_L, ratio of drawdown to drawdown rate, as a function of *1/u* for leaky aquifer

To see effect of the estimation of hydrological parameters using CD-Confined method on a leaky aquifer drawdown data, we consider the following example Using CD–Confined method on highly leaky aquifer in this case *r/B* = 1, if we calculate $\gamma_{sc} = 10$ as seen from the Figure 5.2, characteristic time for non-Leaky aquifer becomes approximately 8000, and for Leaky aquifer it becomes 10. To see the ratio of storativity over transmissivity, we use the equation $u = r^2 S / 4Tt$ explained in Equation(4.1). If we assume that the *r = 1 m* and *t = 100 seconds* the calculations will be;

$$u_{confined} = \frac{r^2 S}{4Tt} = \frac{1}{8000} \cong 1.25 \times 10^{-4} \Rightarrow \frac{S}{T} = 0.05$$

$$u_{Semiconfined} = \frac{r^2 S}{4Tt} = \frac{1}{10} \cong 0.1 \Rightarrow \frac{S}{T} = 40$$

It can be concluded from the calculations that if *T* value accepted as constant, the confined aquifer assumption underestimates the *S* values. In case of constant *S* value, *T* values are overestimated. On the other hand, from the Figure 5.2, for early data (*1/u* < 1) or in case of slightly leaky aquifer (*r/B* < 0.01), CD-Confined method gives close estimations with respect to actual ones.

In the case of the leaky aquifer an estimate of the leakance or aquitard vertical conductance is available (such as for example from other interpretation methods like the Walton method), then the procedure that was explained for the confined aquifer can be applied to drawdown data from leaky aquifers using however the appropriate *r/B* curve in Figure 5.2.

6. FIELD PROPERTIES AND PUMPING TESTS

This chapter describes the field pumping test data used in this study. The data utilized consists of 3 constant rate pumping tests. The correcting made to the data before using them in the interpretation is also discussed below.

6.1. Pumping Tests

6.1.1. Constant Rate Pumping Tests

The different interpretation methods were used to analyze synthetic as well as real pumping test data. This section describes the field pumping test data.

Constant-rate pumping tests were conducted at each test well for typically 72 hours. Background water levels and recovery water levels were measured for periods at least as long as the pumping period at each well. The pumping tests were performed in accordance with ASTM D 4050 (ASTM International, 2002c). Pumping rates ranged from 31 gpm (gallon per minute) to 256 gpm. In the first pumping field two test wells were performed: Test of TW 2A has a constant pumping rate of 194 gpm, and TW -2B has 256 gpm. In the second pumping test field as procedure 72 hours constant pumping test was performed at TW-5A at a constant pumping rate 199 gpm. During the pumping tests, data loggers recording the data in a certain time interval.

Figure 6.1 shows, local area A where test wells 2A and 2B are located. The monitoring wells include 2A, 2B, 2C and 2D to TW-2A, and piezometers PZ-2A, PZ-2B. Test well 2B is located in the southern part of the local area and the monitoring wells in the vicinity of the test well are 2E, 2F and 2G, and piezometers PZ-2C and PZ-2D. In the field area B, there is one test well named TW-5A. The monitoring wells placed in the vicinity of test well 5A (Figure 6.2) are MW-5A, which is adjacent to test well, MW-5B, 5C. The monitoring wells placed more distant than MW-5 group are 4A and 4B; those have approximately 1000 ft (302 m) distance. Piozemeters PZ-5A, and PZ-5B which are located between the points ST-7 and 8, was also used. In addition to the monitoring wells, and piezometers borehole BH-68 data was used for the evaluation.

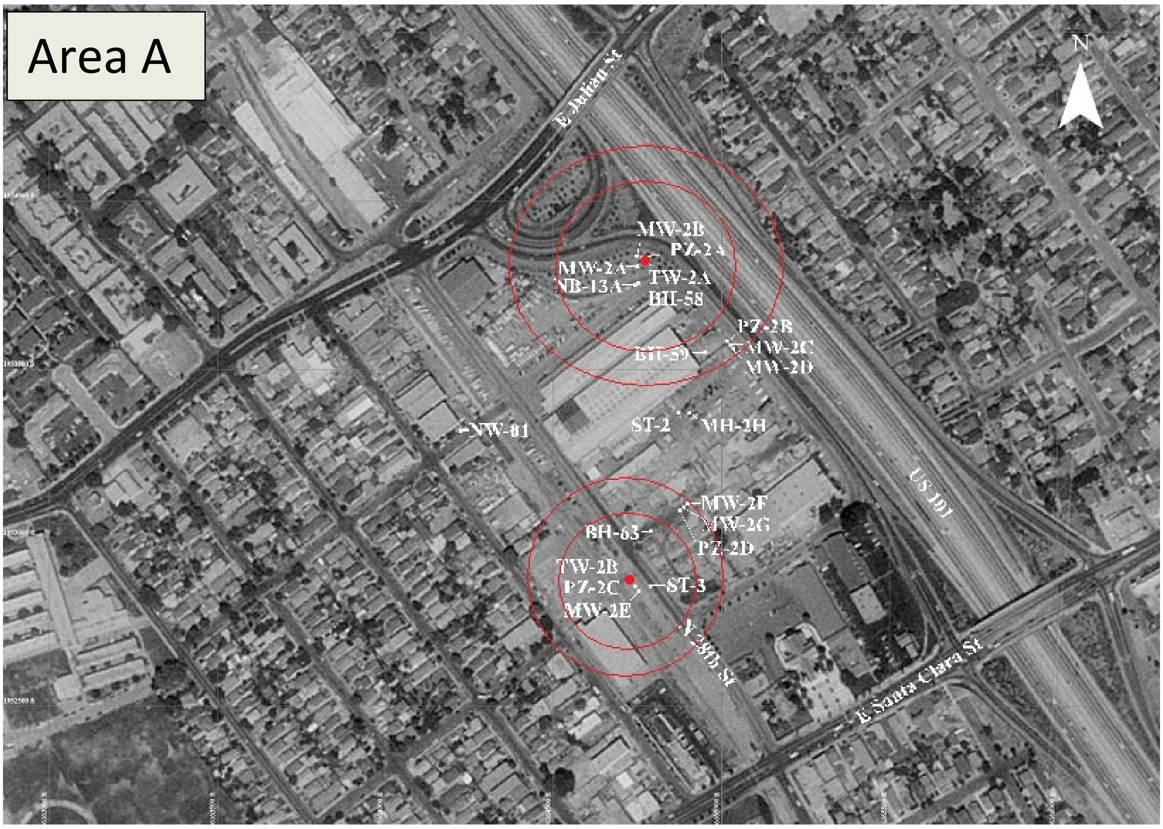

Figure 6.1. Research A showing the location of test wells, monitoring wells, boreholes and piezometers. (Source of USGS Aerial Digital Orthophoto Quadrangles: Terraserver-USA.com)

In the field data evaluations both in Area A and B, data points in the vicinity of test wells were generally selected. However, to also evaluate the interconnectivity between aquifers, points far from the test wells were also considered. For instance, a comparison should be made between the data measured from MW-2A and MW-2B during the pumping test that was performed at testing well 2B, or for the area B, between the measures of MW-5A and ST-7.

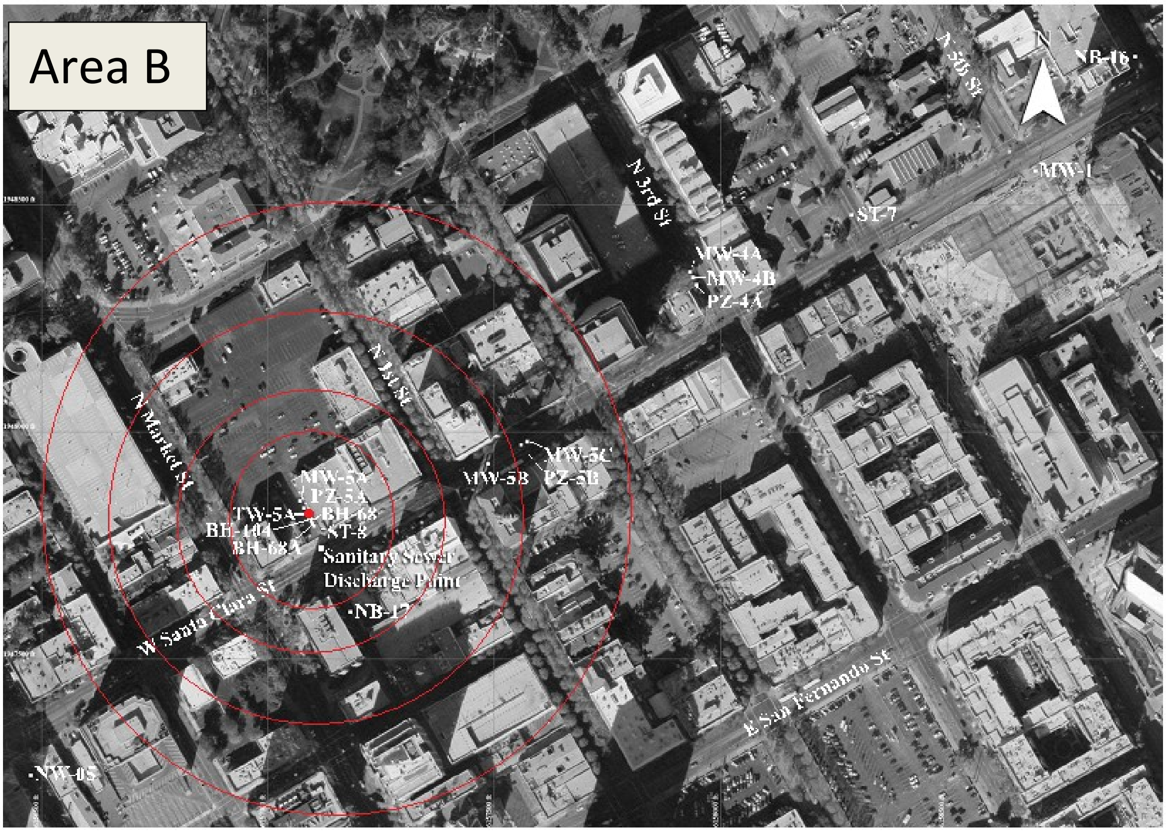

Figure 6.2. Research B showing the location of test wells, monitoring wells, boreholes and piezometers. (Source of USGS Aerial Digital Orthophoto Quadrangles: Terraserver-USA.com)

6.2. Correction of the Data

Normally data adopted from the pumping tests performed in the field exhibit fluctuations that stem from the external influences Thus, prior to using the data for analysis, the data must to be corrected to the extent possible for any influences not related to pumping. The purpose of this is to minimize errors in determining the actual drawdown in response to discharge from the test well. Three influences were identified that required correction. The first influence is water level changes caused by fluctuations in barometric pressure, which can cause instantaneous changes in the water level recorded by a well or vibrating-wire piezometer. The second influence is apparent visual trends in the water level not related to pumping the test well. The third influence is occasional disturbance of the transducer cable during the period of monitoring.

A regional water level trend that is rising (or declining) will cause the magnitude of drawdown to be underestimated (or estimated) if the reference water level is simply the value at the beginning of the test. To eliminate this potential bias, the pre-pumping hydrographs were visually examined for trends and if one was observed, a linear regression was fitted to that portion of the hydrograph and then extrapolated through the period of pumping and recovery. The actual drawdown or recovery was then calculated as the difference between the extrapolated water level trend and the measured water level.

Disturbances to the transducer cable were evident from an instantaneous rise or fall of water level. The timing of the incidents tended to correlate with manual measurements of water level, intended to verify the electronic measurements. These shifts were corrected by adding or subtracting the magnitude of the shift to all water level measurements following observance of the shift.

In the field data considered in this study, the dominant effect to the drawdown data was deemed to be caused by barometric pressure. Therefore, the barometric pressure provides primary external effect on water levels. The correction for fluctuations caused by barometric pressure and tide effect are described in the following subsection.

6.2.1. Barometric Pressure and Trend Corrections

Toll and Rasmussen (2007) describe a method for the removal of barometric or earth tide effects which is titled as regression deconvolution. This is a standard procedure (Dawson and Istok 1991) that needs to be applied whether one uses diagnostic plots or not. This method is based on the general principle of the establishment of a linear set of equations to estimate the unknown barometric response function (Box and Jenkins, 1976);

$$\Delta W(t) = \sum_{i=0}^{m} \alpha(i)\Delta B(t-i) \tag{6.1}$$

where $\Delta W(t)$ and $\Delta B(t)$ are the changes in water level and barometric pressure at time *t*, so $\Delta B(t-i)$ is the change in the barometric pressure *i* time steps before time *t*, $\alpha(i)$ is the unit response function for the correction at lag *i*, and *m* is the maximum time lag of the pressure data.

To determine out whether the barometric correction is necessary, one has to analyze the local trend in the hydraulic head or water table and whether unidirectional or rhythmic changes on to the water level exist. Water level measurements are taken from piezometers that are sufficiently far such that the water level is not affected by pumping. These measurements represent the water level that would have occurred if presumably only barometric pressure is present. The trend correction is based on the calculation of the difference between the interpolated water level at the well using the far away piezometers and the water level corrected for barometric effect that occurs during the pumping.

It is observed that after the recovery period when the discharge has stopped, in some cases, especially in area B, the constant water level is different than the observed level of the pretesting period (Observations before pumping test). Therefore, this suggests that in some cases there are external events influencing the hydraulic head during the test. The estimated trend lines are shown on the hydrographs (Figure 6.3).

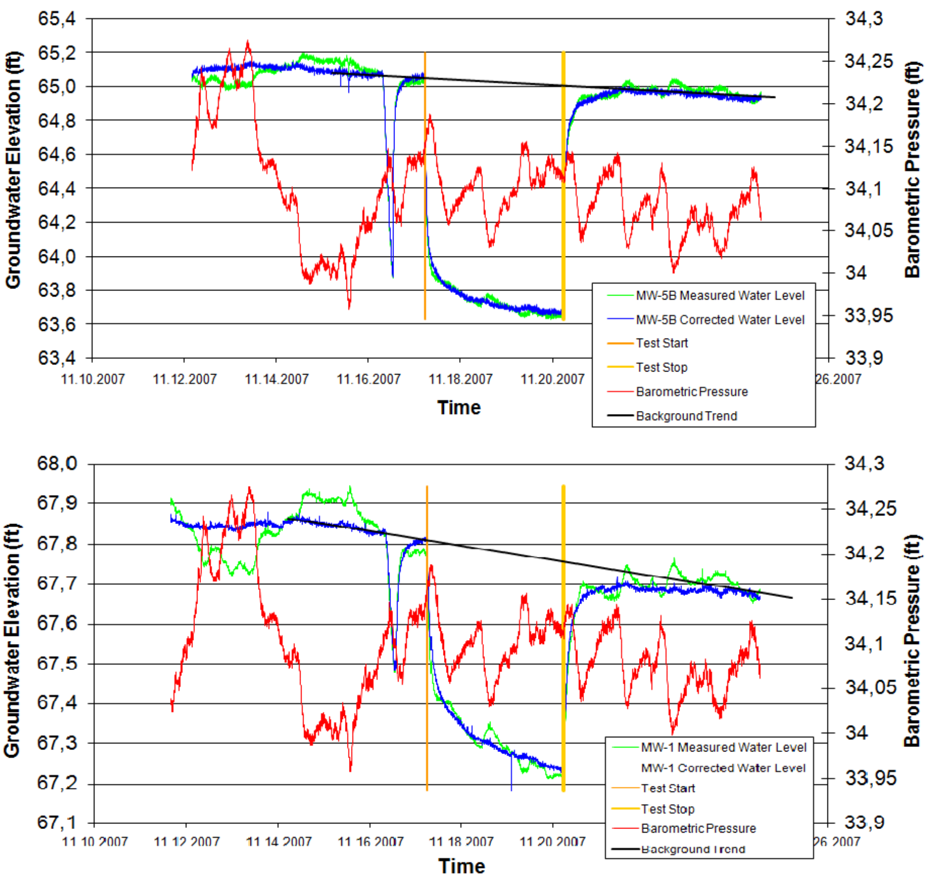

Figure 6.3. Two examples of monitoring well water elevation data, and background trend was specified (from Pumping test data report).

The practice of measuring high resolution barometric records has became common place with the use of electronic down-well pressure transducers with data logging capabilities, and that are not vented to the atmosphere which is also implemented in field measurements. In order for a non-vented logger record to represent changes in water levels the barometric pressure must be subtracted. Barometric pressure effect causes non-rhythmic regular fluctuations, for instance, to changes in atmospheric pressure. In wells or piezometers tapping confined and leaky aquifers, the water levels are continuously changing as the atmospheric pressure changes. When the atmospheric pressure decreases, the water levels rise in compensation, and vice versa.

Under these conditions, for correcting the field data for barometric pressure influences (Figure 6.3, red lines) which causes non-rhythmic regular fluctuations as described by Kruseman and de Ridder (1994). The correction is based on the calculation of mean level of barometric pressure for the period of water level in each well and piezometer. As a second step, the deviation of the barometric pressure from the mean was calculated, for the time of that water level measurement. This deviation from the mean was multiplied by an estimated constant, the barometric efficiency (BE) which is the sensitivity of water level response and the resulting value added to the water level measurement for that time. The BE was found by overlying the raw field data curve with those obtained by the method specified in equation(6.2). The barometric corrections have been made according to observation of noise reduction in field data (Figure 6.3).

$$WL_{i_{Corrected}} = WL_i + BE\left[BP_i - \left(\sum_{i=1}^{N}\frac{BP_i}{N}\right)\right] \tag{6.2}$$

where $WL_{iCorrected}$, is corrected water level at a specific time, WL_i measured water level at the same time, BE; barometric efficiency (%), BP_i barometric pressure at a time i, N is number of pressure readings.

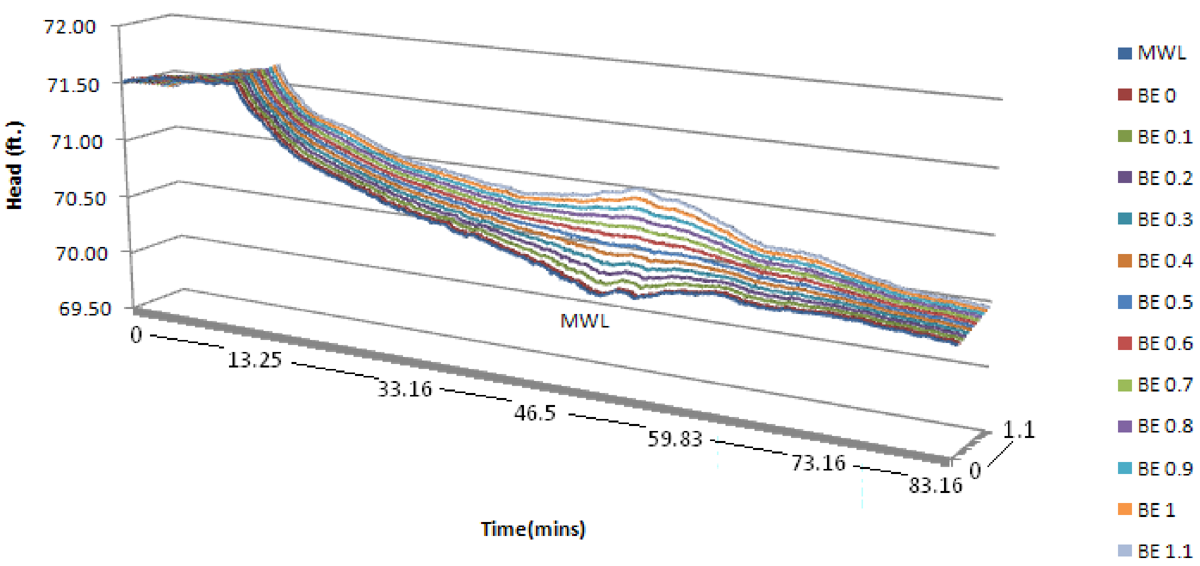

Figure 6.4. Elevation data from a monitoring well for different BE values to correction [The first line is MWL (Monitoring well level) also equal to BE = 0 curve, the best fit for this elevation data is BE = 0.6]

6.3. Structure of Drawdown Data

After barometric and tidal corrections, reduction of the noisy elevation data, drawdown data profiles has been developed for every observation point including the observations at the test wells. Pumping tests conducted at test wells 2A, 2B and 5A with a constant flowrate for a 72-hour period, and measurements have been made from the observation points those were placed at different locations from the test wells. Although the duration of the constant pumping tests were 72 hours, the water levels at the test wells and piezometers were monitored over a 144-hour period (includes 72 hours of recovery). However in this test only the drawdown during the pumping tests were considered, while the recovery data were excluded.

Distance-drawdown analyses are performed to obtain independent estimates of the aquifer properties in addition to the estimates obtained from the time drawdown analyses of each piezometer and monitoring well separately. This allows the consistency of the resulting aquifer properties to be checked. As can be seen from Figure 6.5, rates of the drawdown curves are nearly same however the values of the drawdown are decreasing with distance from the test wells. Other than classical single well tests, it would be sound strategy to use several different monitoring points for distance-drawdown analysis related with point-to-point connectivity between test wells. Thus, comparison of the estimated flow parameters can be done.

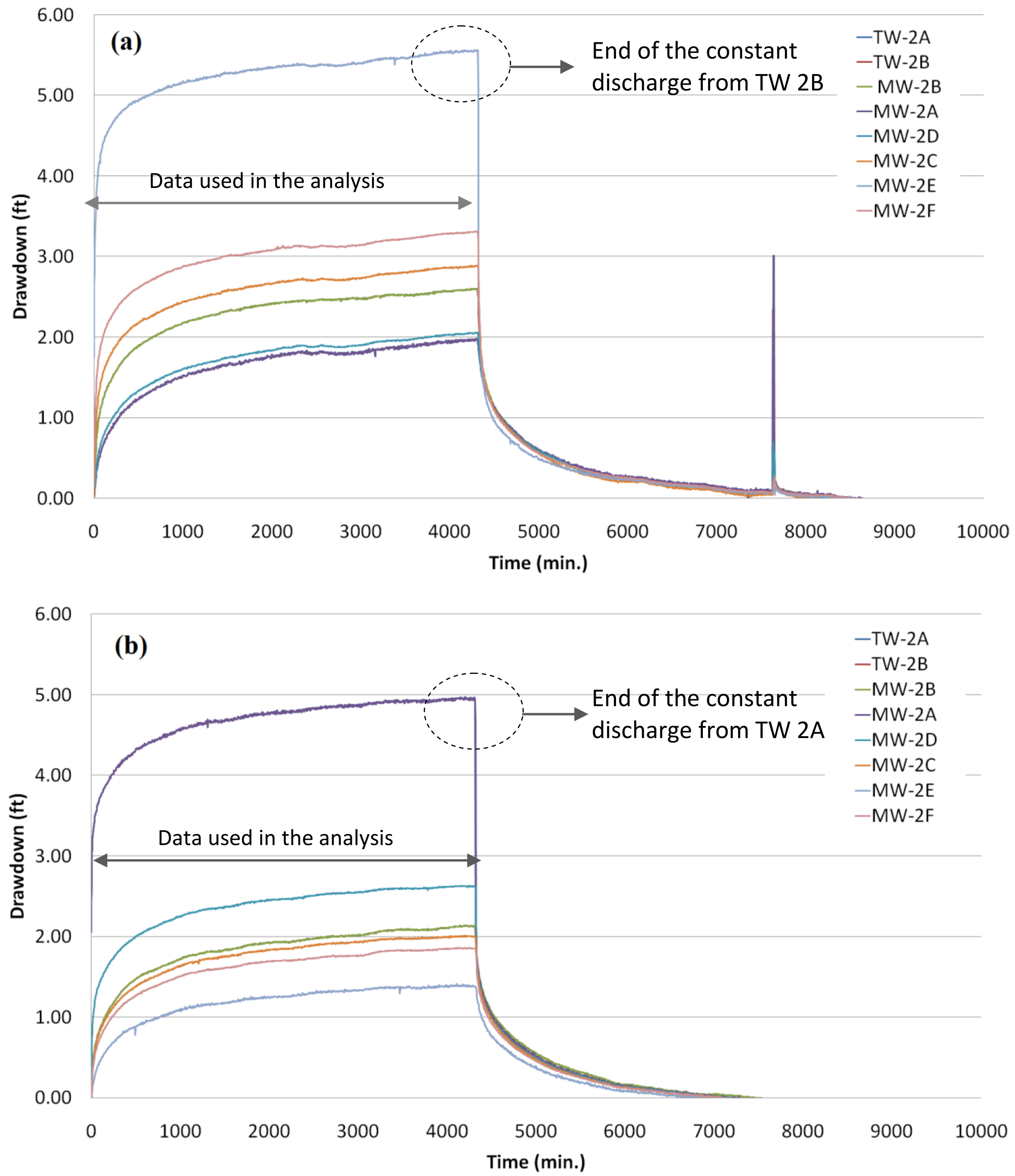

Figure 6.5. Corrected drawdown measurements of monitoring wells in area A. (a) Constant rate test application of test well 2B, (b) Constant rate test application of test well 2A,

7. RESULTS AND DISCUSSION

This section presents the results of the pumping tests analysis methods. The section includes the results obtained with synthetically generated data and with field data. The benefit of using synthetic data is that the underlying parameters that were used in the simulation of the drawdown data are know. Hence, the results obtained from the different pumping test interpretation methods can be compared to the original data used in the drawdown simulation.

The conventional analysis methods considered in this section are the Theis and Cooper-Jacob methods, described in section 4.1.1, for non-leaky confined aquifer and the Walton and Hantush inflection point methods, described in section 4.1.2 leaky confined aquifer. Two novel methods were also considered: the DIP method for leaky aquifers which was described in section 4.1.3, and the Continuous Derivation (CD) method which is presented in chapter 5. As noted in Chapter 5, the CD method has two different variations; one is for non-leaky confined aquifer (CD-Confined) and the other for leaky confined aquifer (CD-semiconfined).

Because some of the methods described above require the estimation of first and second derivatives of the drawdown, this chapter will first present the results obtained with the different smoothing and differentiation techniques described in Section 4.2. This is followed by a presentation of the results obtained with the different pumping test interpretation methods.

7.1. Calculation of the first and second derivative of drawdown

Estimations of derivatives are needed for the Hantush's inflection point, Double Inflection Point and Continuous Derivation Methods. Derivative analysis is considered a powerful diagnostic tool for determining the type of aquifer (leaky vs. non-leaky, confined vs. unconfined) and for detecting the presence of boundaries and for identifying variation in the spatial distribution of the hydrological parameters.

The derivation method considered is the Bourdet derivation method with Spane and Wurstner modification, (see Section 4.2). To take derivations and at the same time to get smoothed derivatives, the derivations were computed for differentiation intervals 0.001 to 0.5 (Number/Number). The impact of the differentiation interval, denoted as L space which is the ratio of the chosen distance between the abscissa of the points and that of point *i* with the whole data (Bourdet et al., 1989), is also discussed.

The derivation method was firstly used on the synthetic data before applying it to the real field data. The application to synthetic data was first applied to homogeneous aquifer cases were an analytic expression of the derivative is available and can be used for comparison.

7.1.1. Homogeneous Case

7.1.1.1. Non-leaky Confined Aquifer. The homogeneous case is for a discharge rate of 2 m3/d, from a confined homogeneous aquifer with 1 m^2/d transmissivity and with 0.0001 storativity.

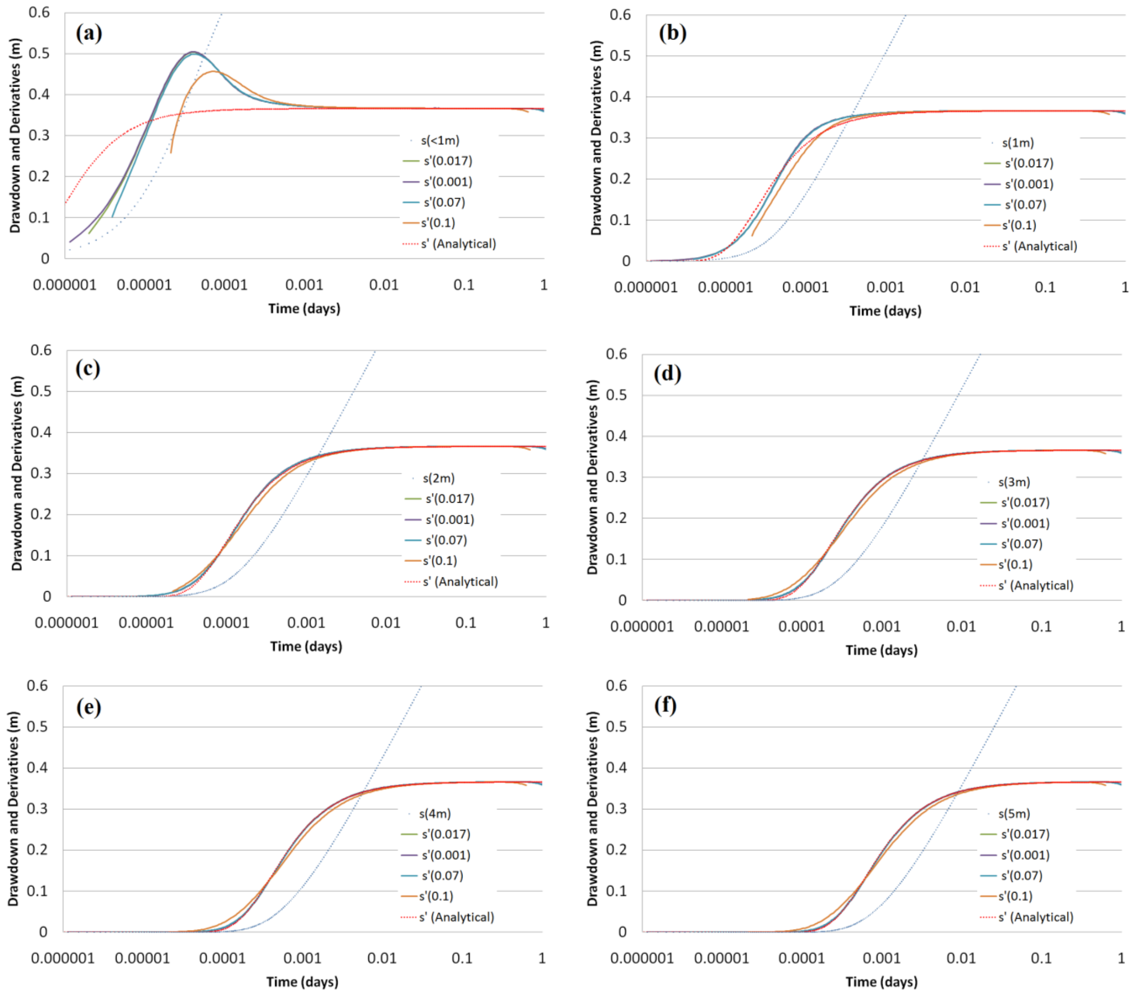

Figure 7.1. First derivatives for the case of non-leaky confined aquifer and observation points located at (a) 0.2 m radius, (b) 1 m radius, (c) 2 m radius, (d) 3 m radius, (e) 4 m radius, (f) 5 m radius from the pumping well for different L values.

Figure 7.1 shows the first derivative of the drawdown with respect to time at different distances from the well and using different interval values. Higher differential interval causes more data loss but on the other hand data becomes smoother. Smoothing with higher differential interval shows a shift in the early data, especially in drawdown measured in the vicinity of the wells, (see Figure 7.1 A). At late times and for observations made further from the test well, less differences between the different curves are observed. On the other hand, it can be observed that after a specific time all derivation curves become similar, and the derivative becomes independent of the differential interval and radius

7.1.1.2. Leaky Confined (Semiconfined) Aquifer. For the case of a leaky confined aquifer, numerical methods will be used to estimate the first and second derivatives of the drawdown because the second derivative in particular can be very noisy (Figure 4.13, section 4.2.) Additional smoothing methods were used as was discussed in Chapter 4

Two methods were used for the estimation of the first derivative of simulated drawdown data, namely: the Bourdet method and the Spane and Wurstner method. For the non-leaky aquifer data application of those two methods show no significant differences. However, for the Hantush inflection point method and the DIP method, it is critical that to estimate the inflection points accurately, so derivatives were estimated for observation points at different distances from the pumping well and using different differential intervals.

For demonstration, the different derivation methods were applied to the case of a homogeneous leaky aquifer with Transmissivity T=1 m^2/d, storativity S= 0.0001, vertical conductance C = 0.1, and a discharge rate of 2 m^3/d. Figure 7.2 shows the first derivative of the drawdown estimated using the Bourdet method for different distances and smoothing values. As observed in the figure the same shifting effect in non leaky confined aquifer exists in leaky one. The peak point of the first derivative is needed for the estimation of hydraulic parameters when using the Hantush's inflection point and DIP method. It is seen from the figure that the values of the peak points depend on differentiation interval. Higher differential intervals, such as values 0.1 and 0.2, cause over smoothing. The agreement with the analytic solution of the derivative diminishes when higher smoothing interval is used. Curves also show different responses according to observation distances from the test well. In particular, for observation points located less than 1 m from test well (Figure 7.2 a) larger differences are observed. For later times, all derivative estimates are close to each other. Moreover, at distances greater than 1 m all smoothing techniques give consistent estimates for the time and peak point derivation.

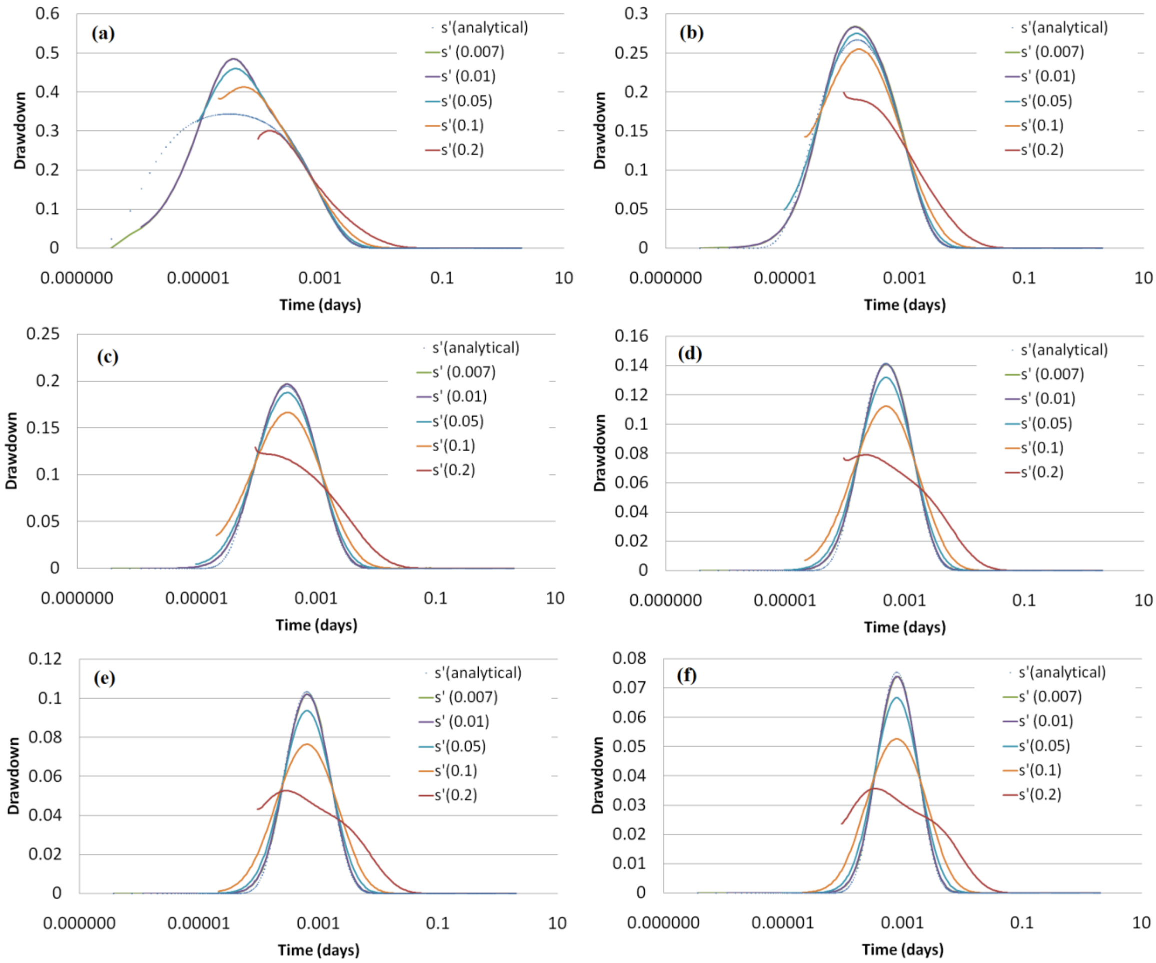

Figure 7.2. First derivatives of the drawdown from a leaky confined aquifer using the Bourdet method and for different smoothing intervals for (a) 0.2 m radius, (b) 1m radius, (c) 2m radius, (d) 3m radius, (e) 4m radius, (f) 5m radius.

Based on these test results, it is decided to use a differentiation interval between 0.001-0.01 for the estimation of the first derivative. For much higher values, such as 0.2, it can be observed from Figure 7.2 that the derivative curve is significantly different that the analytic one with different peak values and loss of data at early times.

Figure 7.3 shows the first derivates for the same problem but calculated using the Spane & and Wurstner method. The results with the Spane & and Wurstner and Bourdet methods are similar to each other. However, there is less data loss in higher differential intervals with the Spane & and Wurstner method than with the Bourdet method.

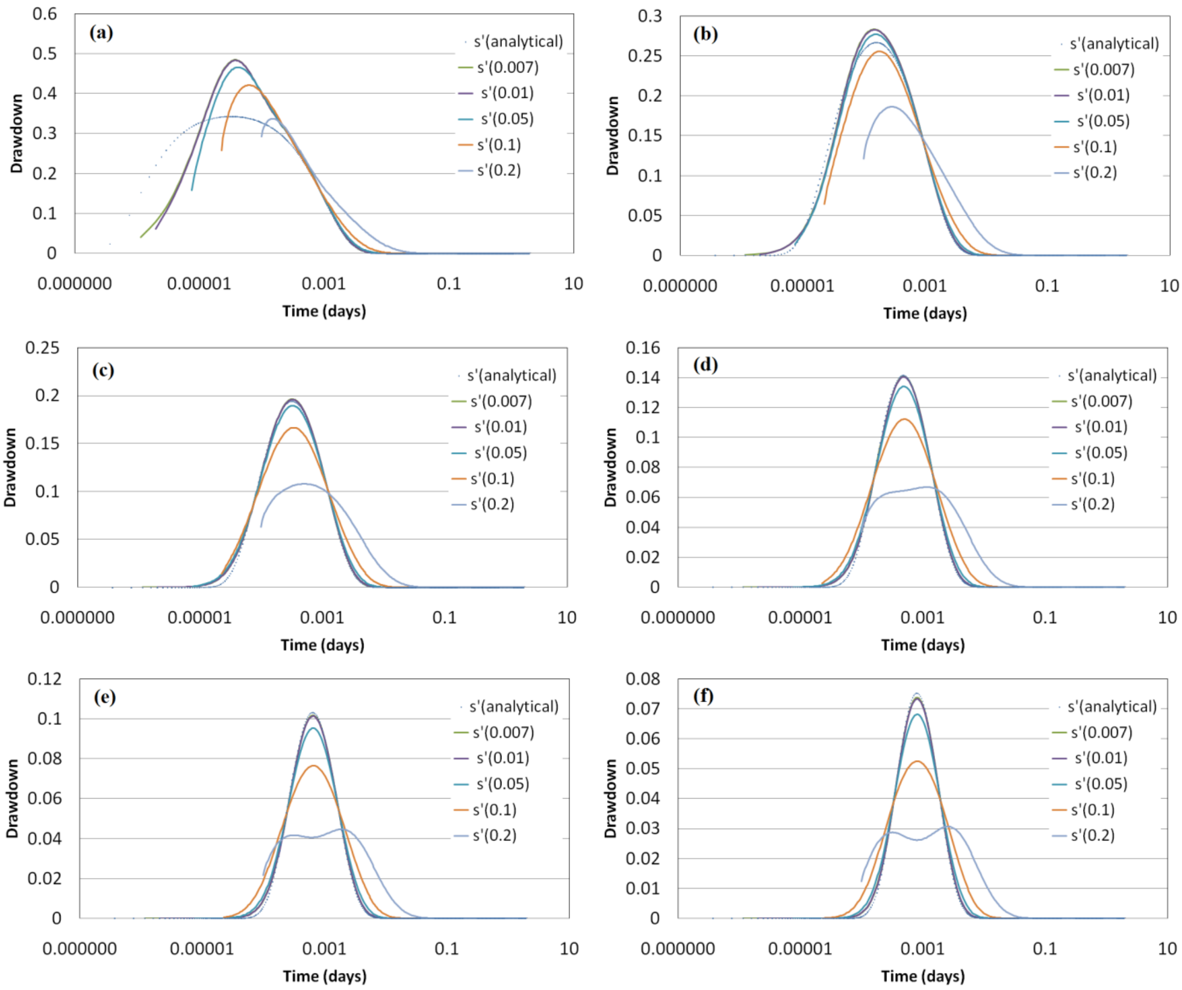

Figure 7.3. First derivatives of the drawdown from a leaky confined aquifer using the Spane & Wurstner method and for different smoothing intervals for A) 0.2 m radius, B) 1 m radius, C) 2 m radius, D) 3 m radius, E) 4 m radius, F) 5 m radius.

Overall, it is seen that the smoothing interval influences the derivative estimation more than the method of estimation. This is further confirmed by examining the mean square error (MSE), presented in Table 7.1, which show that there is no significant difference between Spane & Wurstner and Bourdet methods for the first derivatives of simulation data.

Table 7.1. MSE estimates for comparison of derivation methods

					MSE values		
		Radius (m))	<1	1	2	3	4	5
Bourdet Method	L values	0.007	0.00241	4.76E-05	5.13E-06	2.36E-06	1.06E-06	5.22E-07
		0.01	0.00239	4.74E-05	5.24E-06	2.45E-06	1.11E-06	5.59E-07
		0.05	0.00142	2.49E-05	2.77E-05	2.01E-05	1.34E-05	8.73E-06
		0.1	0.00068	0.00010	0.00020	0.00015	9.56E-05	5.97E-05
		0.2	0.00045	0.00113	0.00101	0.00070	0.00045	0.00027
Spane & Wurstner Method		0.007	0.00244	4.77E-05	5.19E-06	2.44E-06	1.11E-06	5.58E-07
		0.01	0.00240	4.69E-05	5.43E-06	2.77E-06	1.35E-06	7.18E-07
		0.05	0.00170	4.38E-05	1.57E-05	1.31E-05	8.98E-06	5.86E-06
		0.1	0.00077	0.00024	0.00015	0.00013	9.1E-05	5.86E-05
		0.2	0.00066	0.00160	0.00147	0.00089	0.00053	0.00031

It can be seen from the table above that for the small L values, MSEs obtained from the two methods are close to each other. According to previous findings the best fit with the analytic curves are for curves higher than 1 m radius. However, this is mostly due to the discrepancy between the numerically simulated drawdown at the well which depends on the size of the finite difference grid used in the simulation and the analytic solution derived for drawdown at the well. Findings also show that the best results have been adopted from the value L = 0.007 with Bourdet method and L = 0.05 with the Spane and Wurstner method. Below we examine the performance of the different methods for the estimation of the second derivative.

Figure 7.4 shows the estimation of the second derivatives by Bourdet derivation using differential interval of 0.007 and 0.05 which were found to produce optimal results for the first derivative. As seen from the figure, the inflection points (max. and min. points) have different values depending on the interval value used. It can be seen that the inflection points of the derivative for a value of 0.007 are closer to the analytic inflection points. So, it is observed that the first derivatives taken with high differentiation interval causes some discrepancy compared to the homogeneous curves. This discrepancy is most apparent for second derivatives. However, high levels of noise are observed even for a low 0.007 interval,. Thus, derivation with low intervals may cause the second derivative to be noisy especially in field data which are unavoidably corrupted by noise. Also we should note that test data in homogeneous case are the one that have less noise.

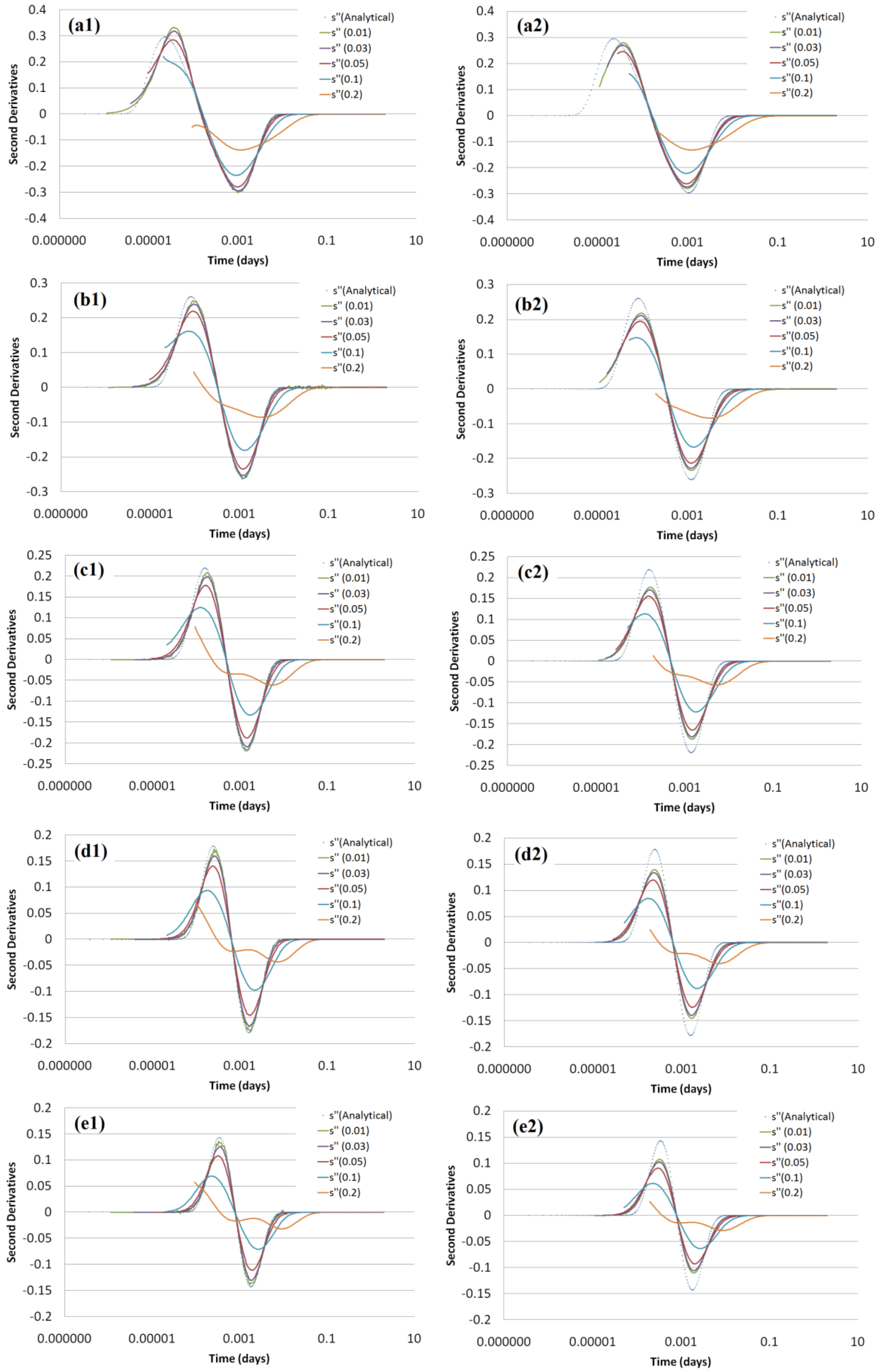

Figure 7.4. Comparison of second derivations calculated with the Bourdet method for (a): 1 m, (b):2 m,(c):3 m, (d):4 m, (e): 5 m radius and. 1) L: 0.007; 2) L: 0.05

The MSE of the second derivative estimated using the Bourdet method is presented in Table 7.2. Two set of data has been used for the second derivatives those are first derivatives smoothed with the L values 0.007 and 0.05.

Table 7.2. MSE values of the second derivates estimated using the Bourdet method

			MSE Values				
		Radius (m)	1	2	3	4	5
L = 0.007 (first derivative)	**L values**	0.01	0.00062	7.97E-05	4.58E-05	2.39E-05	1.43E-05
		0.03	0.00051	0.00010	7.14E-05	4.79E-05	3.43E-05
		0.05	0.00029	0.00028	0.00025	0.00021	0.00017
		0.1	0.00086	0.00163	0.00170	0.00140	0.00103
		0.2	0.00437	0.00755	0.00716	0.00499	0.00323
L = 0.05 (second derivative)		0.01	0.01202	0.00379	0.00101	0.00017	5.58E-07
		0.03	0.01210	0.00381	0.00103	0.00017	7.18E-07
		0.05	0.01246	0.00394	0.00109	0.00019	5.86E-06
		0.1	0.01294	0.00426	0.00128	0.00031	5.86E-05
		0.2	0.01021	0.00508	0.00202	0.00077	0.00031

The results in Table 7.2 suggest that the smallest interval yields estimates that are closer to the analytic second derivative curves. Thus, optimal results were obtained with the values of 0.01 and 0.03. However, from the figures it can be observed that the noise increases when the interval decreases for the derivation. In case of homogeneity drawdown data have minimum noise so derivations with the small differential interval can be acceptable, but, on the other hand, for noisy data (such as those observed in the field for heterogeneous case), higher differentiation interval of first and second derivatives may be needed.

For comparison, the same differential values were used with the Spane & Wurstner method and compared to the results obtained with the Bourdet method and with the analytical solution. Figure 7.5 shows the corresponding curves obtained with the Spane & Wurstner method, while Table 7.3 presents the MSE values for Spane & Wurstner method. As seen from the Figure 7.5 the behavior of the Spane & Wurstner method are similar to that obtained with the Bourdet method. In addition, it can be observed that the noise observed when using the Spane & Wurstner method with lower differential interval tends to be less than that observed with the Bourdet method.

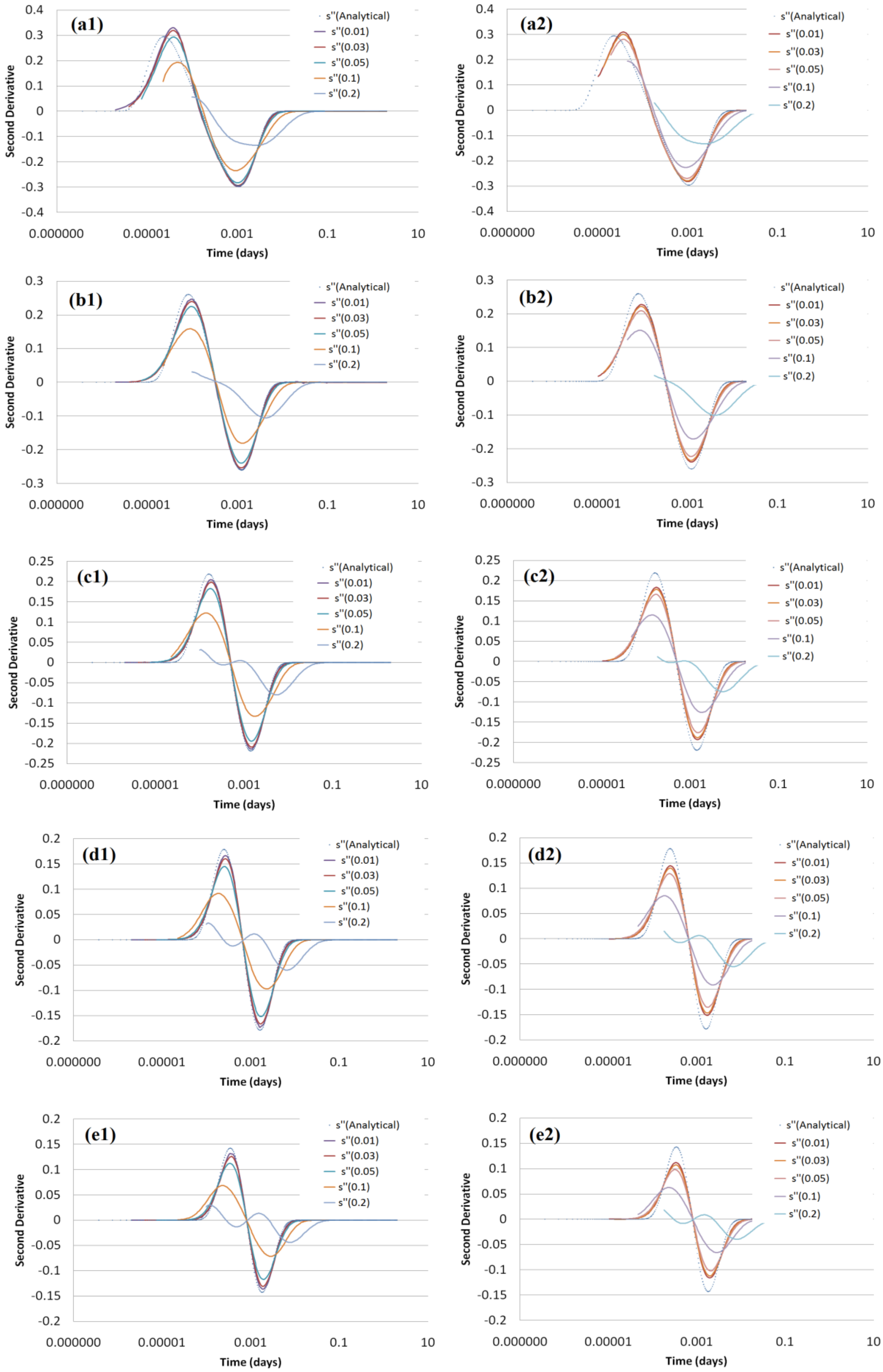

Figure 7.5. Comparison of second derivations calculated with the Spane method for (a):1 m, (b):2 m,(c):3 m, (d):4 m, (e): 5 m radius and. 1) L: 0.007; 2) L: 0.05

Table 7.3. MSE values of the second derivates estimated using the Spane & Wurstner method

			MSE Values				
		Radius (m)	1	2	3	4	5
L = 0.007	L values	0.01	0.00061	7.98E-05	4.84E-05	2.61E-05	1.59E-05
		0.03	0.00058	9.8E-05	6.94E-05	4.62E-05	3.29E-05
		0.05	0.00061	0.00020	0.00018	0.00014	0.00011
		0.1	0.00113	0.00149	0.00148	0.00125	0.00095
		0.2	0.00433	0.00683	0.00710	0.00508	0.00327
L = 0.05		0.01	0.00051	0.00019	0.00018	0.00015	0.00012
		0.03	0.00046	0.00023	0.00023	0.00020	0.00016
		0.05	0.00036	0.00037	0.00040	0.00034	0.00027
		0.1	0.00066	0.00175	0.00172	0.00143	0.00106
		0.2	0.00447	0.00509	0.00534	0.00452	0.00306

Table 7.3 shows that the MSE values are generally low. MSE values corresponding to 0.01-0.03 are lower than the ones in Table 7.2 obtained with the Bourdet method. Moreover, in the case of high differential intervals, the Spane & Wurstner method produces lower MSE, however some reduction in the value of the inflection points remains.

7.1.2. Heterogeneous Case

Drawdown data from heterogeneous aquifers will have an irregular shape that depends on the spatial distribution of the flow parameters and hence differs from that obtained when the aquifer is homogeneous. In this chapter, the estimations of the first and second derivatives have been developed and response behaviors of drawdown data have been observed both in confined and semiconfined aquifer realizations. However, in heterogeneous case it is not possible to measure the accuracy with respect to analytic solution because such a solution does not generally exist.

7.1.2.1. Non-leaky Confined Aquifer. For the evaluation of derivative estimation methods of drawdown data from heterogeneous aquifers, five different transmissivity fields have been generated as explained in section 4.3. In accordance with the findings of differentiation intervals in homogeneous case, we used the optimum L values between 0.001-0.1 for the first derivatives of the heterogeneous synthetic drawdown data as shown in Figure 7.6 Although the distances to the observation points were the same for all 5 realizations, the drawdown and its derivative vary because of the heterogeneity of the transmissivity. It is a unique characteristic for all the heterogeneous non-leaky realizations that there is no fixed point as in the homogeneous case which is confined ideal aquifer.

Overall, the curves with smaller L values tend to produce higher peak values of the derivative. In general, small variability exists between the different estimates. With respect to Bourdet and Spane & Wurstner derivative methods central difference derivation method (CDD) were also applied for the first derivatives. It is however not possible to specify in general terms which methods yields better estimates for the first derivatives.

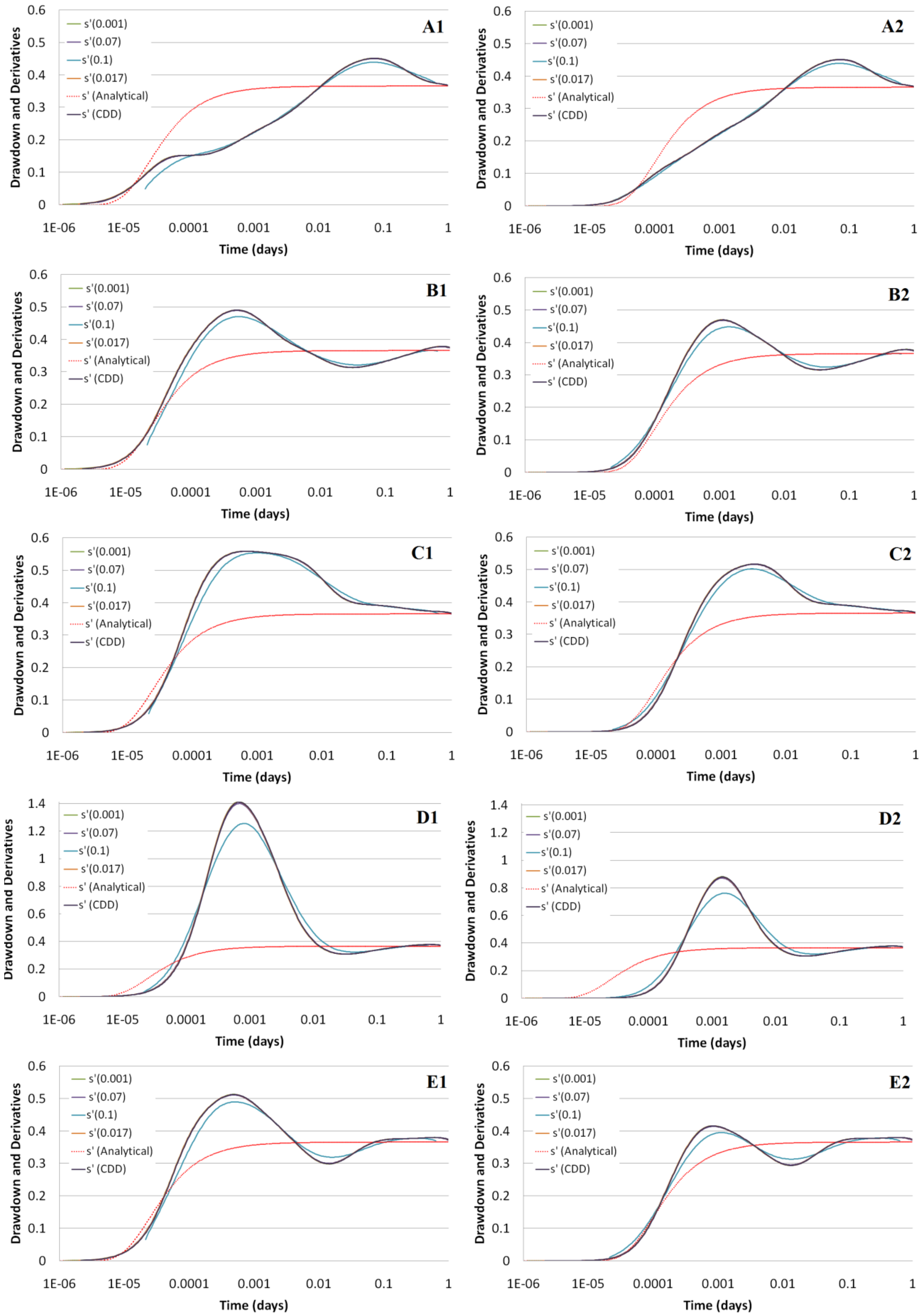

Figure 7.6. Estimates of the first derivative of the drawdown for the case of heterogeneous aquifer using the Spane method and for different L values for 1 m and 2 m radiuses.

7.1.2.2. Leaky Confined Aquifer. The calculation of the derivative was also repeated for the case of heterogeneous leaky confined aquifer. Figure 7.7 shows the first derivative of the drawdown at r=1 and r=2 respectively obtain from the 5 different transmissivity realizations. The Spane & Wurstner method was used to estimate the derivatives using different differentiation intervals. For comparison of the analytic drawdown derivative for the case of homogeneous leaky aquifer system is also shown on these figures. As observed, some of the heterogeneous cases show lower values of the derivative compared to the homogeneous one, while others cases have higher values.

To have an idea how much the first derivatives of the heterogeneous realizations differ from analytical derivative, mean of square differences (MSD) statistic has been used and results tabulated in Table 7.4. From Figure 7.7. the MSD value close to the zero is considered as also closer to homogeneous case. It can be observed that the L values of 0.007 and 0.01 gives best results for this case as shown in homogeneous case.

Table 7.4. MSD statistics for the degree of difference from homogeneous case in realizations for first derivatives

		Realizations					
		A		B		C	
	Radius (m)	1	2	1	2	1	2
L Values	0.007	0.884	0.236	0.520	0.247	0.688	0.115
	0.01	0.886	0.237	0.515	0.244	0.675	0.112
	0.05	0.914	0.255	0.443	0.205	0.585	0.084
		Realizations					
		D		E			
	Radius (m)	1	2	1	2		
L Values	0.007	14.007	1.302	0.682	0.115		
	0.01	13.914	1.287	0.675	0.112		
	0.05	12.648	1.091	0.585	0.084		

The MSD results in the table above suggest that realization D is highly variable; on the other hand realization B has the lowest variation of transmissivity parameter among others. So, it can be said that the realization D has higher a variation with respect to analytical homogeneous case based on the first derivatives.

Table 7.5. MSD statistics for the degree of difference from homogeneous case in realizations for second derivatives

			Realizations					
			A		B		C	
		Radius (m)	1	2	1	2	1	2
L = 0.007	L Values	0.007	1.855	0.884	1.243	0.740	2.359	0.688
		0.01	1.858	0.891	1.218	0.718	2.316	0.664
		0.05	1.941	0.993	0.937	0.459	1.794	0.392
			Realizations					
			D		E			
		Radius (m)	1	2	1	2		
	L Values	0.007	63.910	10.518	2.359	0.688		
		0.01	62.959	10.299	2.316	0.664		
		0.05	50.791	7.6300	1.794	0.392		

			Realizations					
			A		B		C	
		Radius (m)	1	2	1	2	1	2
L = 0.05	L Values	0.007	1.855	0.884	1.243	0.740	2.359	0.688
		0.01	1.858	0.891	1.218	0.718	2.316	0.664
		0.05	1.964	1.444	0.452	0.203	0.709	0.198
			Realizations					
			D		E			
		Radius (m)	1	2	1	2		
	L Values	0.007	63.910	10.518	2.359	0.688		
		0.01	62.959	10.299	2.316	0.664		
		0.05	22.907	2.860	0.709	0.198		

The analysis of the second derivatives for the 5 heterogeneous test cases is presented in Appendix A. As an example Figure 7.8 shows the second derivative for realization A for the distances of 1 m and 2 m (in which first graphs shows 1 m distance second ones shows 2 m distance from the test well). The derivative curves which were computed with L=0.007 show less variability than the curves with L=0.05. In addition, minimal differences are observed in the values of the inflection points and the times were they occur when different L values are considered. However, it should be noted that field data which will invariably be noisier than the synthetically simulated drawdown used in this exercise.

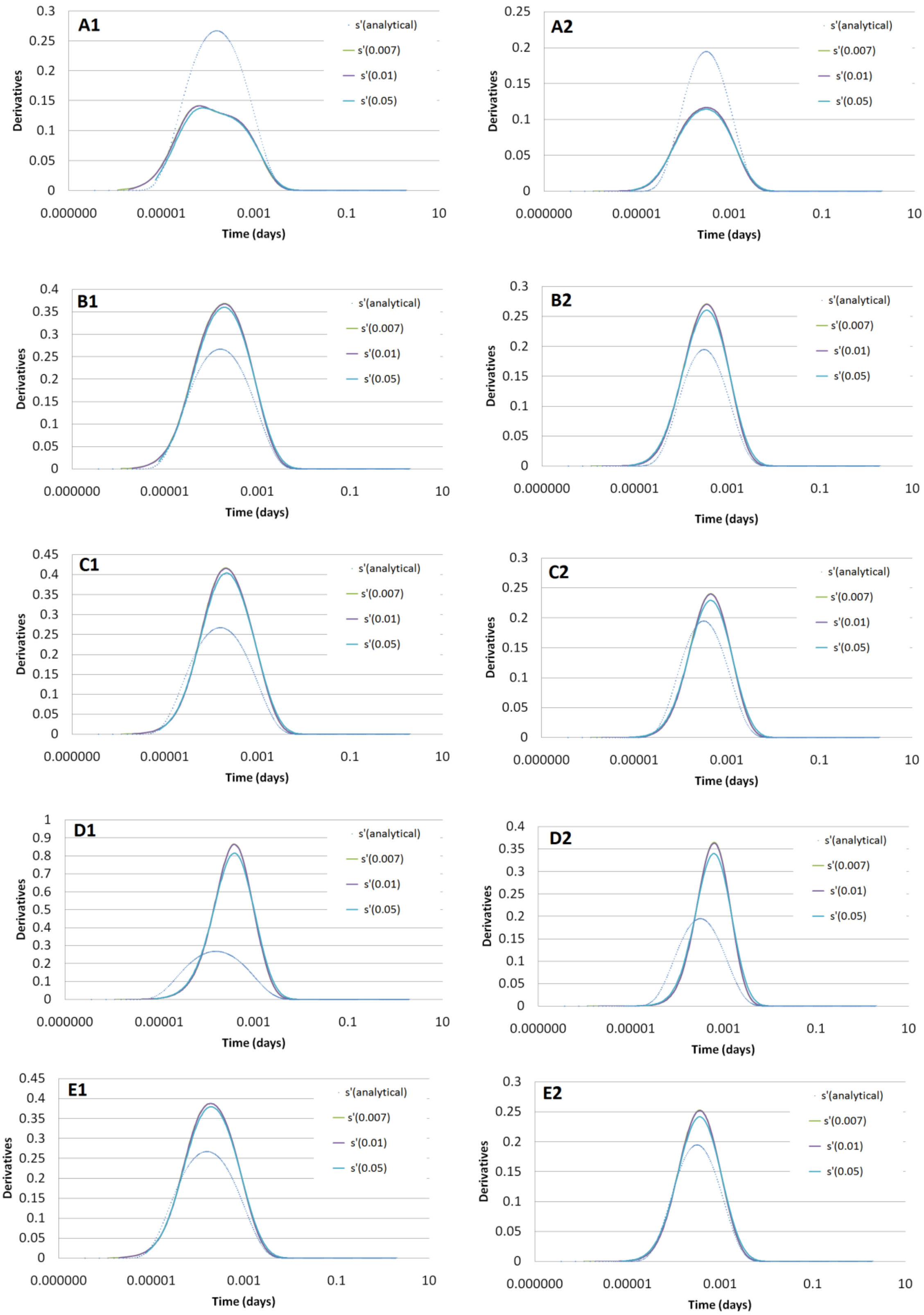

Figure 7.7. First derivatives of the drawdown data for 5 randomly generated heterogeneous field realizations, (each letter denotes different realizations. First row of graphs shows 1 m radius while second column shows 2 m radius)

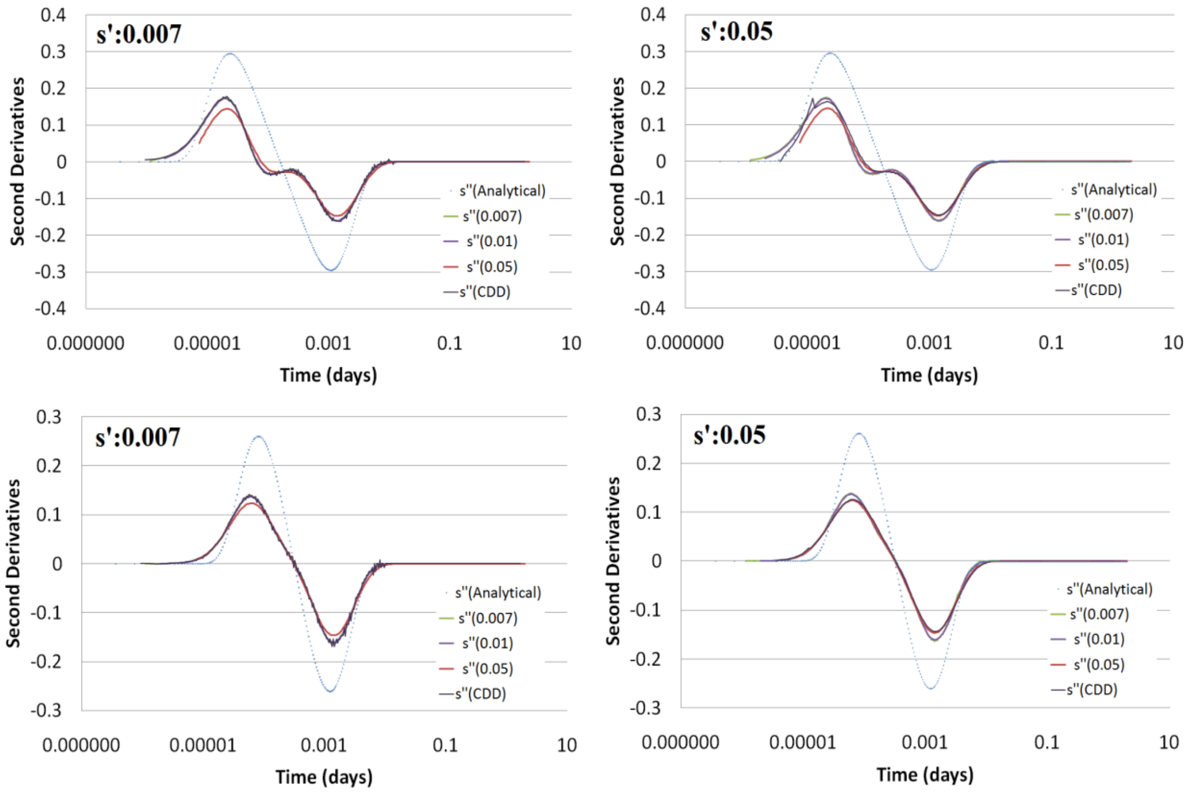

Figure 7.8. Second derivatives of the drawdown data for realization A, using different intervals by Spane and CDD methods. First row of graphs shows 1 m radius while second row shows 2 m radius)

Figure 7.8 also shows that the derivatives calculated with Central Difference methods have poorer data quality. Same L values was used for each method for comparison, however, it is observed that derivatives computed from the central differences are prone to noise.

7.2. Estimation of Flow Parameters- Synthetic Data from Confined Aquifers

In this section the pumping test interpretation methods described in Section 4.1 are applied to synthetically generated pumping test data. Three methods are applicable to pumping tests conducted in confined aquifers: Cooper-Jacob, Theis and CD-Confined methods. The latter is a novel recently developed method that has not been tested previously, because conventional methods (Cooper-Jacob, Theis) are based on the assumption of homogeneity, they provide a single “representative” value when applied to pumping tests conducted in heterogeneous aquifers. By applying these methods to synthetically generated drawdown data obtained solutions can be compared to the underlying hydrological parameters that were used in the data simulation.

Different from the estimations of the conventional methods, the CD method repetitively calculates estimates of the flow parameters yielding time and distance dependent spectrum of the heterogeneous parameter estimates. Conventional methods were used not only for the estimation of the hydrological parameters but also for the comparison of the findings of CD method.

When applying standard interpretation methods to a hydraulic test we obtain a parameter value that is somehow “representative”. The difference here is that the value obtained depends on the interpretation method. In field applications, hydrogeologists typically interpret pumping tests using conventional methods (such as the Theis or Cooper-Jacob methods) to obtain a value that they would later use in flow and contaminant transport models or calculations.

7.2.1. Conventional Methods

Conventional methods (Theis, Cooper-Jacob) have been applied as explained in section 4.1.1. These methods require no derivative data. Table 7.6 presents the estimates of the transmissivity and storativity obtained with the Theis method for 5 randomly generated realizations marked A through E. Table 7.7 presents the results obtained with the Cooper-Jacob method. In these realizations the transmissivity was assumed to be spatially variable with geometric mean of 1 m^2/day, while the storativity was assumed to be uniform equal to 0.0001. The FORTRAN computer code used for the interpretation of the data is listed in Appendix E.

Table 7.6. Estimates of Hydrological parameter using Theis Method

		Transmissivity				
	Distance (m)	0.2	1	2	3	4
Realizations	A	1.20	1.00	0.90	0.90	0.90
	B	0.90	0.90	0.90	0.90	0.90
	C	0.70	0.70	0.80	0.80	0.80
	D	0.10	0.40	0.60	0.80	1.00
	E	0.80	0.90	1.00	1.10	1.10
		Storativity				
	Distance (m)	0.2	1	2	3	4
Realizations	A	0.00099	0.00039	0.00028	0.0002	0.00016
	B	0.00013	0.00006	0.00006	0.00007	0.00007
	C	0.00016	0.00009	0.00009	0.00009	0.00008
	D	0.00026	0.00006	0.00008	0.00008	0.00009
	E	0.00013	0.00006	0.00007	0.00011	0.00015

Table 7.6 shows that the estimated transmissivity is close to the geometric mean of the data (T = 1 m^2/day). The estimates tend to approach the mean with increase in distance for the well. Although a uniform storativity of S=0.0001 was used for all realizations, the estimated storativity values show wider fluctuations between the different realizations and as a function of distance. This suggests that the spatial variability of the transmissivity is influencing the estimation of the storativity to a larger degree than the estimation of the transmissivity.

Table 7.7. Estimates of hydrological harameters using the Cooper-Jacob Method

		Transmissivity				
	Distance (m)	0.2	1	2	3	4
Realizations	A	0.572	0.572	0.572	0.572	0.573
	B	0.592	0.592	0.591	0.591	0.591
	C	0.586	0.586	0.586	0.587	0.587
	D	0.587	0.586	0.586	0.586	0.586
	E	0.580	0.579	0.579	0.579	0.579
		Storativity				
	Distance (m)	0.2	1	2	3	4
Realizations	A	0.1604	0.0123	0.0044	0.0025	0.0017
	B	0.0162	0.0032	0.0019	0.0016	0.0013
	C	0.0032	0.0012	0.0013	0.0011	0.0009
	D	0.0000	0.0001	0.0007	0.0013	0.0018
	E	0.0095	0.0033	0.0029	0.0032	0.0028

The results obtained with the Cooper-Jacob method (Table 7.7) are in general similar to those obtained with the Theis method. The transmissivity values are close to the geometric mean. The storativity on the other hand shows larger fluctuations.

7.2.2. CD – Confined Method

The CD method has a different logic than the conventional method because it provides continuous values of the parameters. Therefore, comparison of the CD method with the conventional methods cannot be done exactly because conventional methods cannot explain the variability of the field data. Nevertheless, some qualitative comparison between the two sets of estimates is possible.

Figure 7.9 shows the estimates of the transmissivity and storativity estimated using the CD method and drawdown data from observation points at 1m and 2 m from the pumping wells.

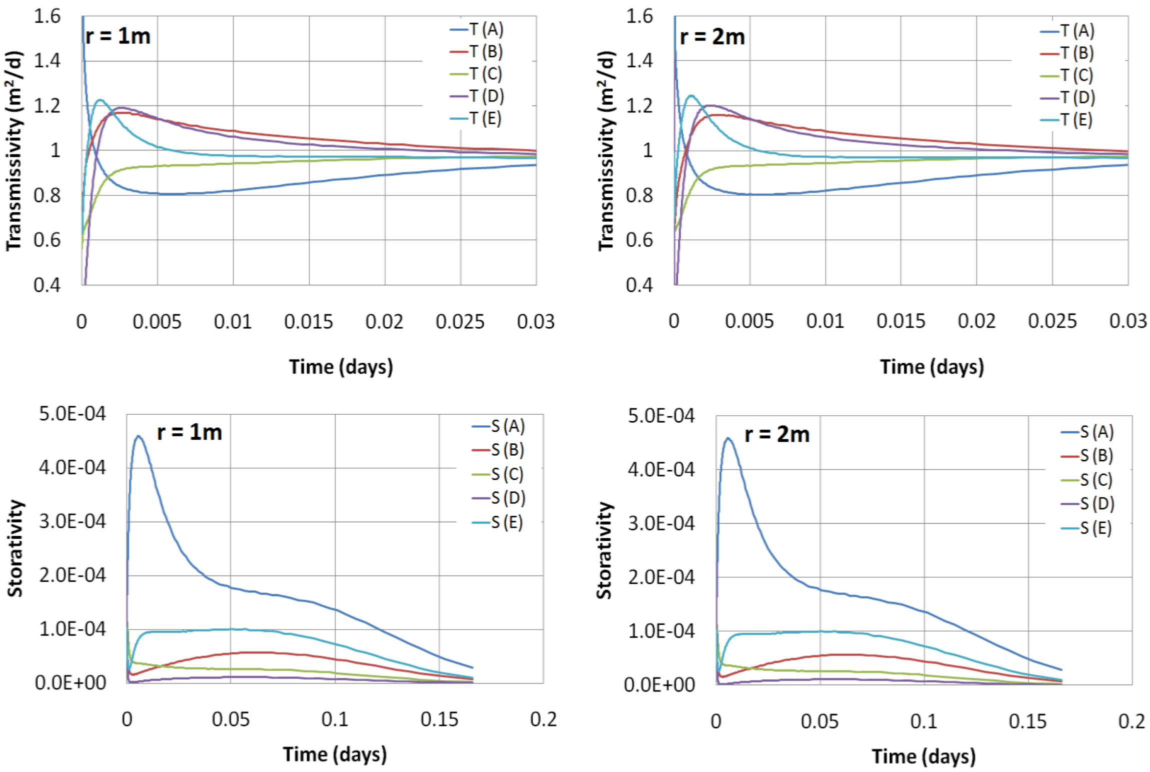

Figure 7.9. Estimated transmissivity and Storativity data as a function of time (every line corresponds to a different realization)

At early times, the transmissivity estimates obtained for the different realizations are very different. At later times, however, the transmissivity estimates tend to approach tends to approach the geometric mean (1 m^2/day). The behaviors of the curves are different due to the heterogeneity that they have. If we compare the findings of the conventional method with CD-Confined method, findings of the transmissivity data are consistent for all methods, however, we can infer that the Theis method gives average results corresponding to the late CD-Confined method estimates. Storativity estimates again exhibit more variability as was also shown with the conventional methods.

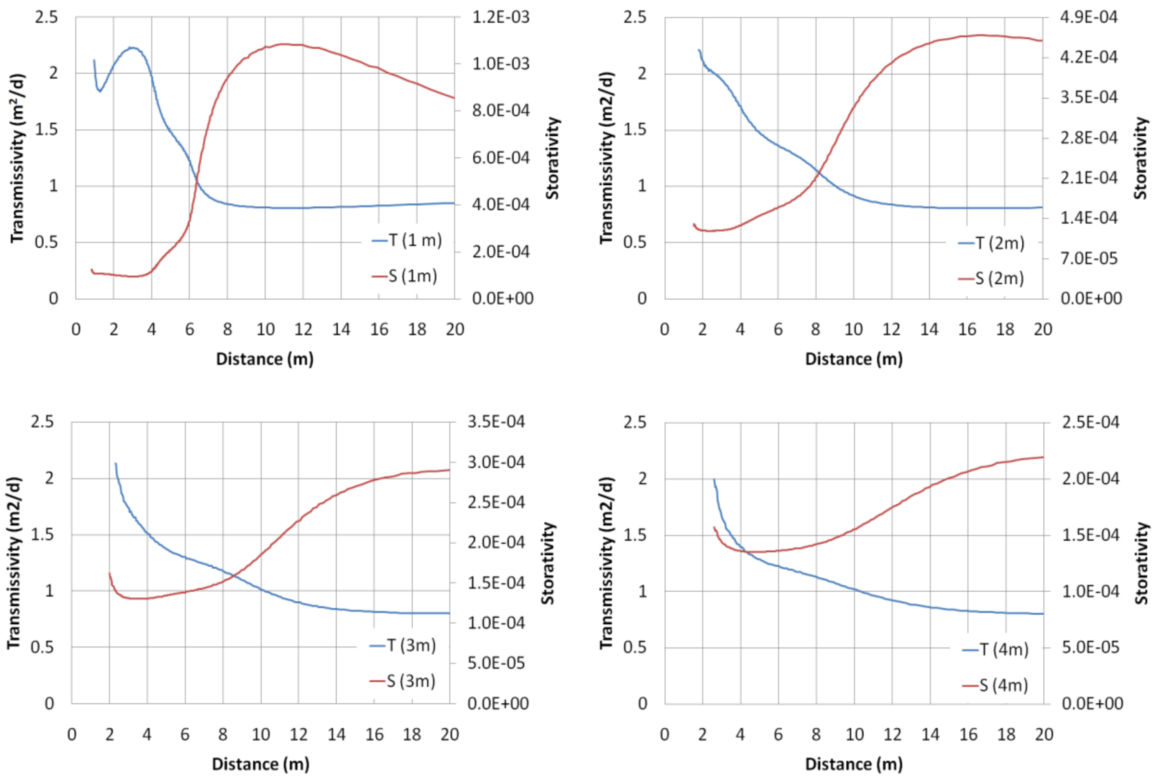

Figure 7.10. Transmissivity and Storativity data as a function of distance for the realization A, estimated from different observation points (1m to 4 m from the pumping test)

Figure 7.10 shows the plot of the transmissivity and storativity estimates with the x axis converted to distance as described in Section 5.1. Only the results for realization A are shown. Estimates in Figure 7.10 shows that the transmissivity estimates are inversely proportional to storativity. Transmissivity values show a slight change based on where the drawdown data has been taken. On the other hand, storativity estimates show different results in first 20 m distance over a continuously increasing circle centered at the pumping well. These results are consistent with previously reported findings (e.g., Trinchero et al., 2008). The estimates of the parameters as a function of distance are also consistent with the single representative estimates from conventional methods, All estimates by CD-Confined method for all other realizations can be found over Appendix B.

As the pumping test progresses in time a larger portion of the aquifer starts to influence the pumping test. Hence, the interpreted transmissivity gradually varies from the transmissivity at the well to the geometric mean of the entire domain at late times. Beyond this time, the aquifer starts to behave as a homogeneous aquifer with transmissivity equal to the geometric mean of the entire domain which was assumed to be 1 for these five cases.

7.3. Estimation of Flow Parameters- Synthetic Data from Leaky Aquifers

In this section the interpretation methods for leaky aquifer system (described in Section 4.1.2) are applied to synthetically generated pumping test data. Two conventional methods are considered: the Walton's Type Curve and Hantush's Inflection Point, and the novel Double Inflection Point (DIP) method. Because Walton's Type Curve and Hantush's Inflection Point are based on the assumption of homogeneity, they provide a single "representative" value when applied to pumping tests conducted in heterogeneous aquifers. The DIP method on the other hand provides two estimates. Results from all methods are compared to each other and to the underlying parameters used in the simulation of the drawdown data.

As explained in the methodology section, the DIP method requires the estimation of the first and second derivatives (first and second inflection points), while the Hantush inflection point method requires the estimation of the first derivative. One disadvantage of Hantush method to estimate parameters accurately steady-state drawdown value should be apparent to point out the inflection point. On the other hand, In DIP method instead of the estimation of slope as in Hantush's method, [see. Figure 4.9 and Equation(4.8)] second derivatives are used for estimation of leakage factor.

7.3.1. Conventional Methods

The parameter estimates obtained with the Walton and Hantush inflection point methods are presented in Tables 7.8 and 7.9, respectively. The results are for 5 randomly generated realizations assuming a uniform storativity value S=0.0001 and uniform vertical conductance C= 0.1. The calculations were repeated for drawdown data from different observation points (r=0.2 m, 1 m, 2 m, 3 m, and 4 m). The FORTRAN program used for the interpretation of the drawdown data is listed in Appendix E.

Table 7.8. Estimates of hydrological parameters using the Walton's Type Curve method with synthetic heterogeneous data

		Transmissivity (m^2/day)				
	Distance (m)	0.2	1	2	3	4
Realizations	**A**	2.10	2.10	2.10	1.90	1.90
	B	0.80	0.80	0.70	0.90	0.50
	C	0.70	0.70	0.80	1.00	0.40
	D	0.10	0.20	0.40	0.50	0.60
	E	0.50	0.80	0.70	0.80	0.90
		Storativity				
	Distance (m)	0.2	1	2	3	4
Realizations	**A**	0.00021	0.00011	0.00012	0.00014	0.00015
	B	0.00021	0.00008	0.00008	0.00009	0.00007
	C	0.00019	0.00010	0.00012	0.00012	0.00007
	D	0.00024	0.00011	0.00012	0.00012	0.00014
	E	0.00030	0.00009	0.00009	0.00011	0.00013
		B (m)				
	Distance (m)	0.2	1	2	3	4
Realizations	**A**	0.06	0.20	0.40	0.70	1.00
	B	0.09	0.30	0.65	0.85	1.60
	C	0.09	0.35	0.70	0.90	1.90
	D	0.40	0.80	1.00	1.40	1.80
	E	0.20	0.30	0.75	1.20	1.60

Estimations for the Walton's type curve method were based on the curve fitting principle as in Theis method, but with an additional parameter, *B*. As tabulated in Table 7.8 transmissivity values of realization A is higher and realization D is lower consistent with the estimations of confined methods. On the other hand storativity values are consistent for every realization and there are no extreme values. Also it can be seen that leakance shows variation as a distance. As noted earlier, although constant C and S values were used in the simulation of the drawdown, the estimates show some variability showing that the spatial variability of the transmissivity influences the estimation of all parameter.

Table 7.9. Estimates of hydrological parameters using the Hantush's Inflection Point Method

		Transmissivity (m^2/day)				
	Distance (m)	0.2	1	2	3	4
Realizations	**A**	1.856	2.287	2.065	1.783	1.571
	B	0.646	0.693	0.695	0.735	0.734
	C	0.520	0.551	0.686	0.696	0.711
	D	0.086	0.172	0.292	0.338	0.356
	E	0.500	0.614	0.665	0.926	1.109
		Storativity				
	Distance (m)	0.2	1	2	3	4
Realizations	**A**	0.00024	0.00010	0.00012	0.00014	0.00014
	B	0.00028	0.00009	0.00008	0.00009	0.00008
	C	0.00029	0.00011	0.00012	0.00011	0.00010
	D	0.00028	0.00011	0.00011	0.00010	0.00010
	E	0.00029	0.00010	0.00009	0.00012	0.00015
		B (m)				
	Distance (m)	0.2	1	2	3	4
Realizations	**A**	0.084	0.173	0.418	0.748	1.132
	B	0.152	0.363	0.666	0.999	1.304
	C	0.173	0.466	0.802	1.159	1.438
	D	0.439	0.904	1.238	1.695	2.230
	E	0.199	0.429	0.779	1.095	1.436

The estimates obtained with the Walton method and Hantush's inflection point methods are highly correlated, but transmissivity values are slightly less than the ones in Walton's type curve method. In general the differences between two methods are not significant. The storativity and leakance values obtained with the two methods are in general quite close to each other.

7.3.2. DIP Method

Estimates obtained with the DIP estimates are shown in Tables 7.10 and 7.11, respectively. As a characteristic of DIP method there are two estimates of flow parameters due to early and late data with respect to inflection points.

Table 7.10. Estimates of hydrological parameters using DIP method for early data for synthetic heterogeneous data

		Transmissivity (m^2/sec.)				
	Distance (m)	0.2	1	2	3	4
Realizations	**A**	0.358	0.599	2.157	1.626	0.898
	B	0.211	0.545	0.573	0.569	0.737
	C	0.177	0.321	0.462	0.496	0.498
	D	0.041	0.090	0.232	0.400	0.201
	E	0.153	0.400	0.341	0.717	0.948
		Storativity				
	Distance (m)	0.2	1	2	3	4
Realizations	**A**	1.32E-05	8.634E-05	0.00354	0.00207	0.00083
	B	2.48E-05	0.00043	0.00053	0.00056	0.00089
	C	2.49E-05	0.00016	0.00037	0.00046	0.00045
	D	1.69E-05	5.024E-05	0.00021	0.00045	0.00015
	E	1.69E-05	0.0002204	0.00019	0.00062	0.00095
		B (m)				
	Distance (m)	0.2	1	2	3	4
Realizations	**A**	0.227	1.128	5.060	3.714	2.577
	B	0.285	2.048	2.536	2.538	3.076
	C	0.279	1.264	1.864	2.126	2.332
	D	0.220	0.729	1.420	1.920	1.476
	E	0.241	1.480	1.608	2.338	2.570

Table 7.11. Estimates of hydrological parameters using DIP method for late data for synthetic heterogeneous data

				Transmissivity (m^2/sec.)		
	Distance (m)	0.2	1	2	3	4
Realizations	**A**	2.741	2.92915	1.71738	1.67392	1.20739
	B	0.756	0.60163	0.57810	0.61627	0.60700
	C	0.653	0.50954	0.64754	0.47549	0.37996
	D	0.028	0.12737	0.22204	0.13956	0.19466
	E	0.680	0.63354	0.55979	0.99966	1.28022
				Storativity		
	Distance (m)	0.2	1	2	3	4
Realizations	**A**	0.00367	0.00373	0.00215	0.00218	0.00131
	B	0.00059	0.00054	0.00054	0.00064	0.00065
	C	0.00062	0.00041	0.00067	0.00044	0.00031
	D	0.00001	0.00009	0.00020	0.00010	0.00015
	E	0.00060	0.00057	0.00042	0.00107	0.00151
				B (m)		
	Distance (m)	0.2	1	2	3	4
Realizations	**A**	8.26941	9.98055	3.86312	3.80382	3.01678
	B	1.86932	2.30000	2.55429	2.66875	2.76299
	C	1.89177	1.96214	2.38301	2.07742	2.07014
	D	0.17058	0.89763	1.38590	1.24078	1.46035
	E	1.91925	2.42389	2.24112	2.88106	3.01325

Conventional methods use limited part of drawdown data; Walton's method estimates according to part of the data which comes over a specific curve, Hantush's inflection point method estimates the parameters according to inflection point which cannot represent early and late data. On the other hand, DIP method uses three distinctive points of drawdown data with their derivatives. From Tables 7.10 and 7.11, estimations also show that variation in three parameters with respect to distances (radiuses) is more apparent. The first DIP estimates tends to put more weight on the transmissivity near the well, while the second DIP estimates put more weight on the later data. Variability of parameters shows that DIP method is better tool for representation of heterogeneity and gives information about a larger portion of the leaky aquifer.

In summary, the application of the different interpretation methods to heterogeneous media indicates that different methods may produce different estimates that may differ from the actual parameters of the system (defined by the constant input values for *S*, *C*, and some average value of *T*). It is obvious that all findings from different methods show high consistency in storativity and transmissivity values but we may not say parameters have increasing or decreasing trend according to monitoring point radiuses.

7.4. Estimation of Flow Parameters-Field Data from Confined Aquifer Approach

In this section the different pumping test interpretation methods are applied to field data. A description of the site, the pumping test, and the structure of test data were presented in Chapter 6. The data that will be used in this analysis are the constant rate pumping tests as explained in more detailed in section 6.1.1.

The analytic methods used with the synthetic data were also used for the field data. Often in the field the nature of the aquifer, (leaky vs. confined) may not be known prior to conducting the pumping test as seen from the Figure 6.5 in which drawdown data do not reach steady state because of the end of constant tests. However, the shape of the drawdown data can provide some information on the aquifer type. In this section the interpretation results of the aquifers tests that have been classified as confined are presented.

The application of the conventional methods (Theis and Jacob-Cooper) and CD-Confined method were applied to the field data in a similar manner to the application to the synthetic data. In the application of synthetic data, drawdown data from multiple observation points were present and comparisons of the estimates for different realizations have been made from different observations points. A similar approach was taken with the field data where data from several observation points are present for the same pumping test. This comparison has been made also with the CD-confined method which yields a continuous estimate of the flow parameters.

7.4.1. Fitting and Derivation on Field Data

To use the CD-confined method, an estimate of the derivative is needed. This section presents the results of this step, which is similar to what was used with the synthetic data. However, unlike the synthetic data, real field data, even preliminary corrections made (Tidal and Barometric corrections), have noisier characteristic as explained in previous sections which makes field data more challenging to analyze accurately.

The same procedure for derivation in synthetic data has been followed for the real field data. The chosen technique of Spane & Wurstner method was applied to the drawdown data Different from the application to synthetic data, fitting techniques (Described in Section 4.2.2) were also applied to the field data, in order to provide some comparison between the derivation techniques.

For the field data application, the chosen observation points for the test well 2A are monitoring wells 2A, 2B, 2C and 2D; for the test well 2B the observation points are 2B, 2C, 2E, 2F and 2H and for the last group of the test well 5A monitoring wells are 1, 5B, 5, 7, 8 and borehole 68-80.

To exemplify some of the difficulty typically encountered with field data, the data collected at test well 2A and related observation points are analyzed here in detail. The decision of which method can produce workable as well reliable derivative estimates were made according to these four observation points. The results of the Spane & Wurstner method to the real data are presented in Figure 7.11.

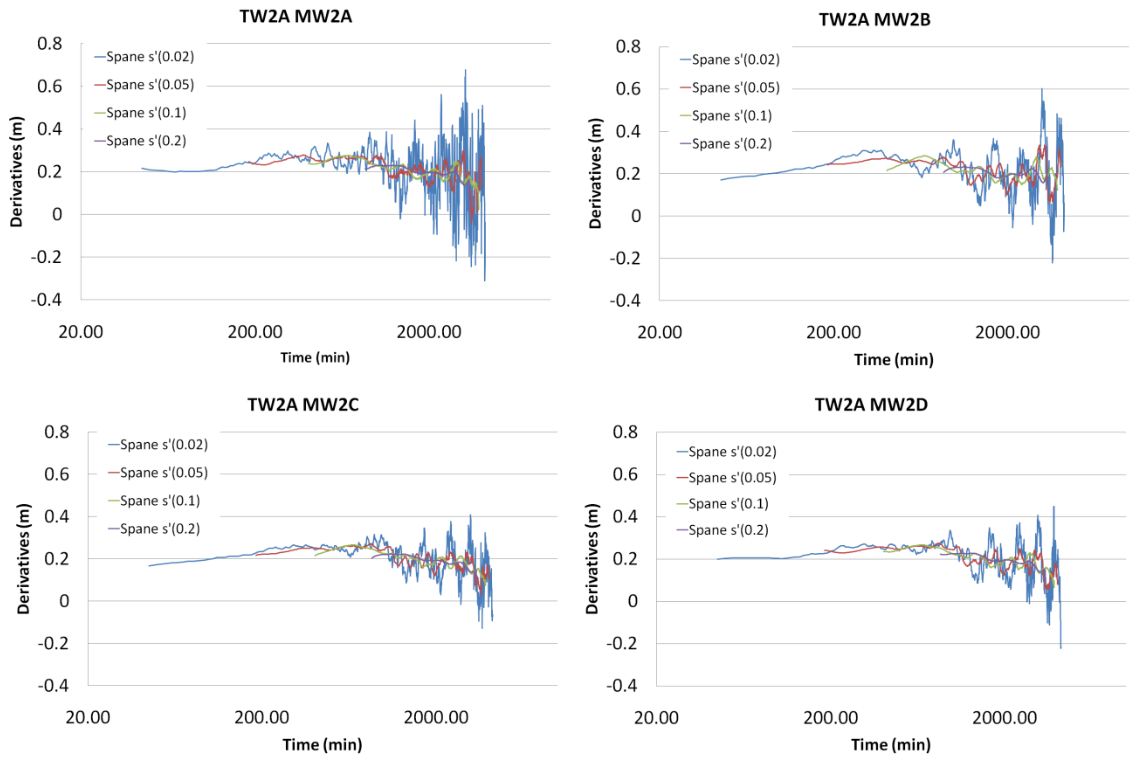

Figure 7.11. First derivatives of drawdown at four different monitoring points as a function of time due to pumping from TW2A for real field data.

As seen from Figure 7.11, although the general pattern of the drawdown curve is somewhat visible, the level of noise is substantial and, as a result, it is impossible to use derivatives in any interpretation method reliably. The noise of the curves increases through the late drawdown data, in part because the change in the drawdown towards the end of the test slows down and due to the small time intervals between data points, which is further diminished due to the logarithmic scale of the time. Therefore, it was decided to apply smoothing methods to the raw field data to reduce the fluctuations and the high noise level in the data.

<u>7.4.1.1. Smoothing of the Field Drawdown Data.</u> The smoothing techniques explained in section 4.2 were applied to the second derivatives of synthetic data. The second derivatives were generated via central difference derivation with the time intervals of the collected drawdown data (approximately 4500 min). As a result, the derivative estimates were highly noisy (see Figure 4.13). To compare the smoothing methods Figure 7.12 was plotted using synthetic heterogeneous data.

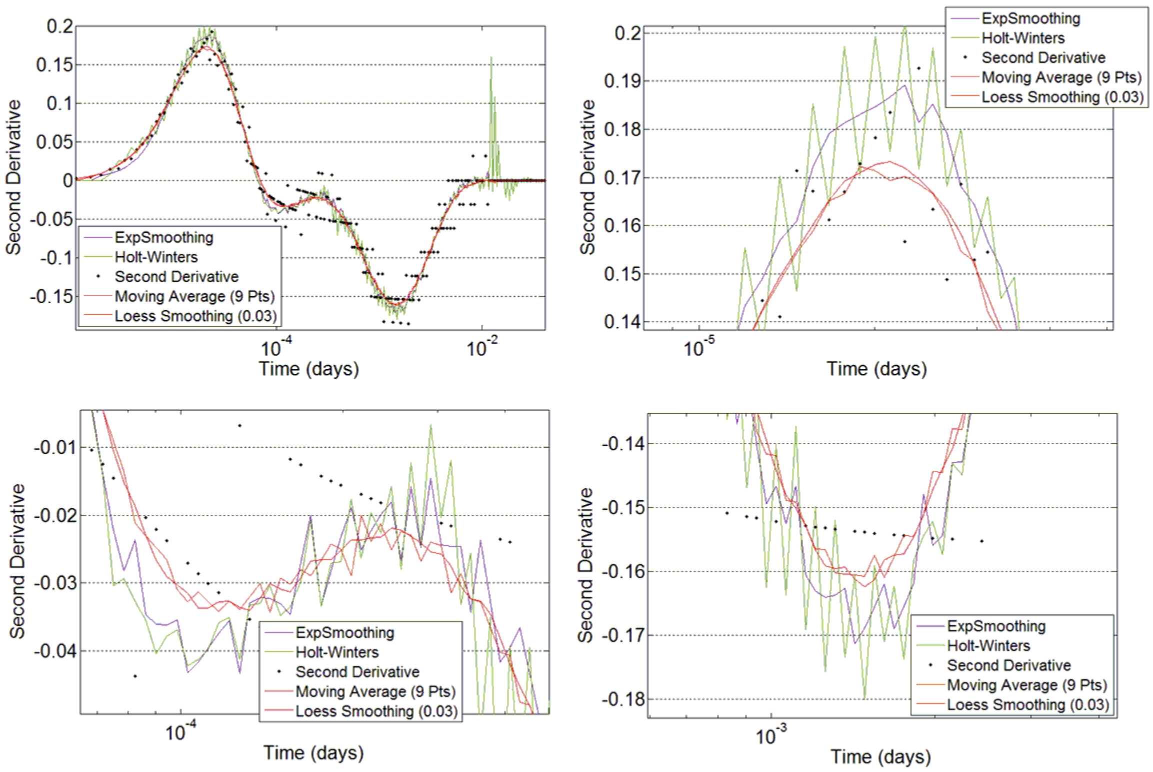

Figure 7.12. Application of different smoothing techniques to the second derivative of the synthetic heterogeneous drawdown at observation point in 1 m radius due to pumping

All methods were applied to the field data at the same smoothing power according to the application results for synthetic heterogeneous drawdown; the smoothest results were obtained when using moving average and Loess smoothing methods. For instance in this case the moving average method was applied using a 9-point interval so the Loess method was also applied with an alpha (α) value of 0.04 which corresponds to the value for 9 data point interval for this data set.

<u>7.4.1.2. Derivation of Smoothed Curves.</u> The field drawdown data were smoothed prior to the estimation of the drawdown derivatives Smoothing was tested for different smoothing coefficient (alpha value for the Loess method). Alpha values ranging from 0.3 to 0.9 were considered. For each smoothing value the derivative of the smoothed drawdown data was estimated using the Spane method for distinct differential intervals.

The first derivative of the drawdown due to pumping from TW 2A as a function of time for different smoothing parameters are presented in Figure 7.13. The results show that alpha values 0.3 and 0.5 gives smoothed results for the early data. The value of the derivative at the inflection point is about 0.25 m occurring around 620 minutes for all cases, indicating that the estimated derivative curves are consistent with each other. This information would be sufficient to apply the Hantush's inflection point Cooper–Jacob methods. The late data which is used in the CD methods have exhibit a break in the curve. These problems appear to be solved by considering higher values of the smoothing parameter. Moreover, no drastic difference between the derivatives for alpha values 0.8 and 0.9.

If the derivatives are estimated with the differential interval approach, a shifting problem in the early data, as the case with synthetic data, may develop. For all cases differential interval 0.02 (Corresponds to 20 data points for each interval for this data set) gives best results and is least skewed one with respect to other curves. However, although the problem is alleviated with a differential interval of 0.2, significant early data loss in the early data is observed.

The other conspicuous character of the curves is ambiguity of the derivatives to define the type of the aquifer. There is a decreasing trend in the curves for all cases but it cannot be certainly said what is the dominant cause for this decrease, which can be either leakance or heterogeneity of the field (Similarity can be observed from the Figure 7.6 which shows confined heterogeneous realizations). Different than other confined aquifer examples derivatives are not starting from zero, therefore, early character of the drawdown cannot be observed.

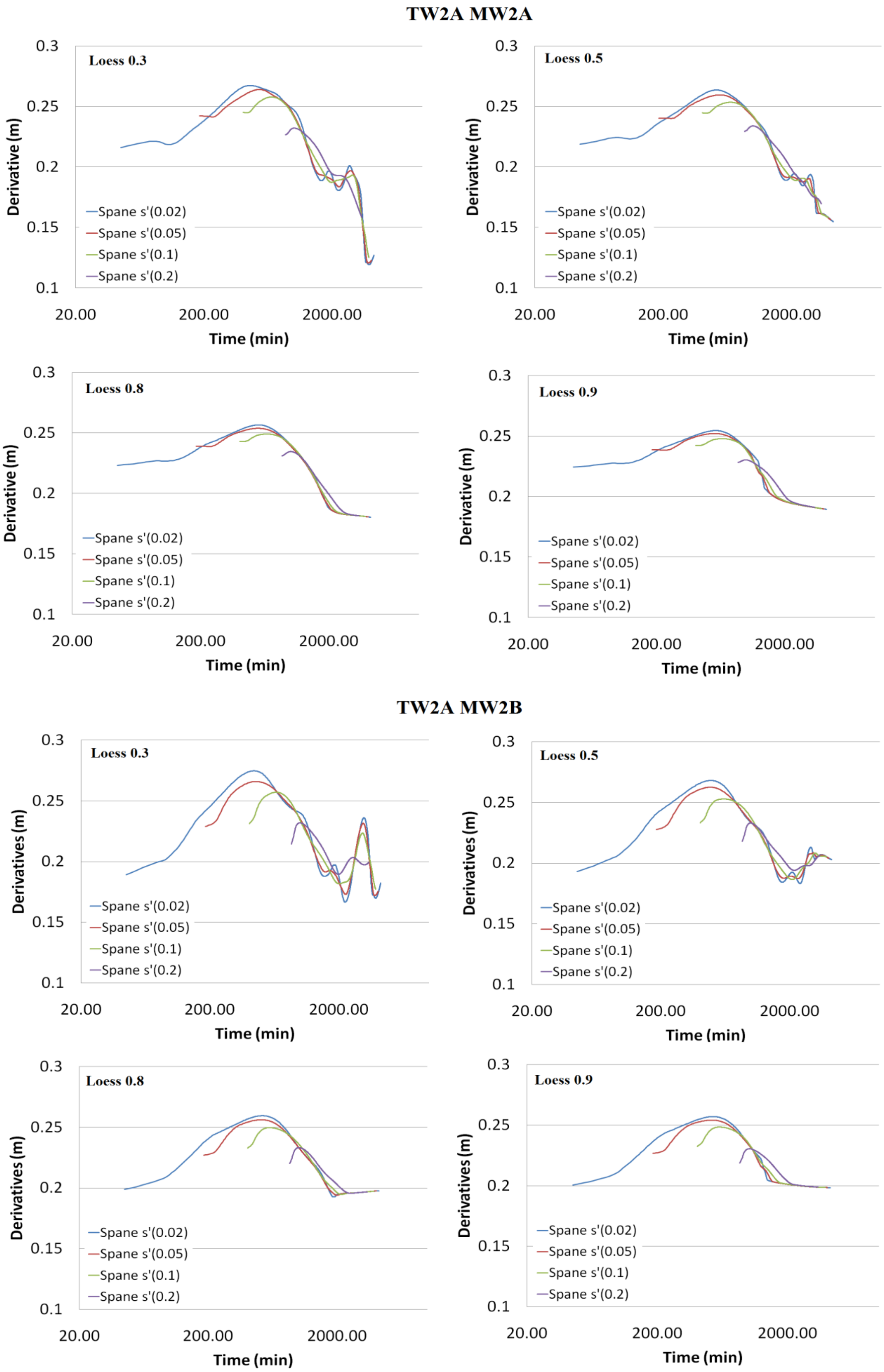

Figure 7.13. First derivatives of smoothed real drawdown data for monitoring wells 2A and 2B

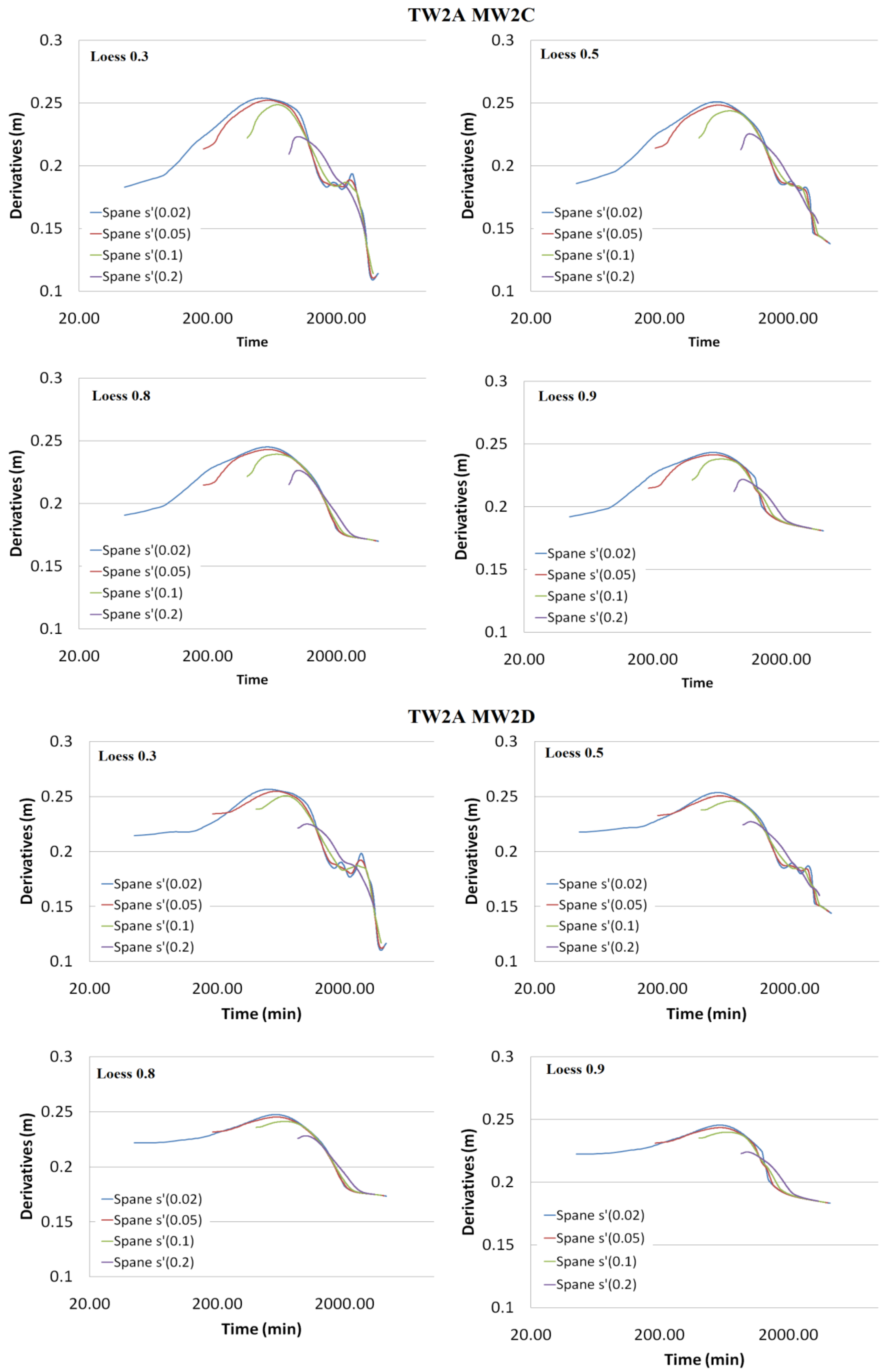

Figure 7.14. First derivatives of smoothed real drawdown data for monitoring wells 2C and 2D

<u>7.4.1.3. Fitting Procedure and Derivations of Fitting curves.</u> Because of the ambiguity of the derivatives, the polynomials fitting methods and Spline interpolation methods explained in section 4.2.2 were applied. Figure 7.15 shows the different fitted polynomials and Splines applied to the Field drawdown data. The residual, defined as the difference between the observed and interpolated values are also shown.

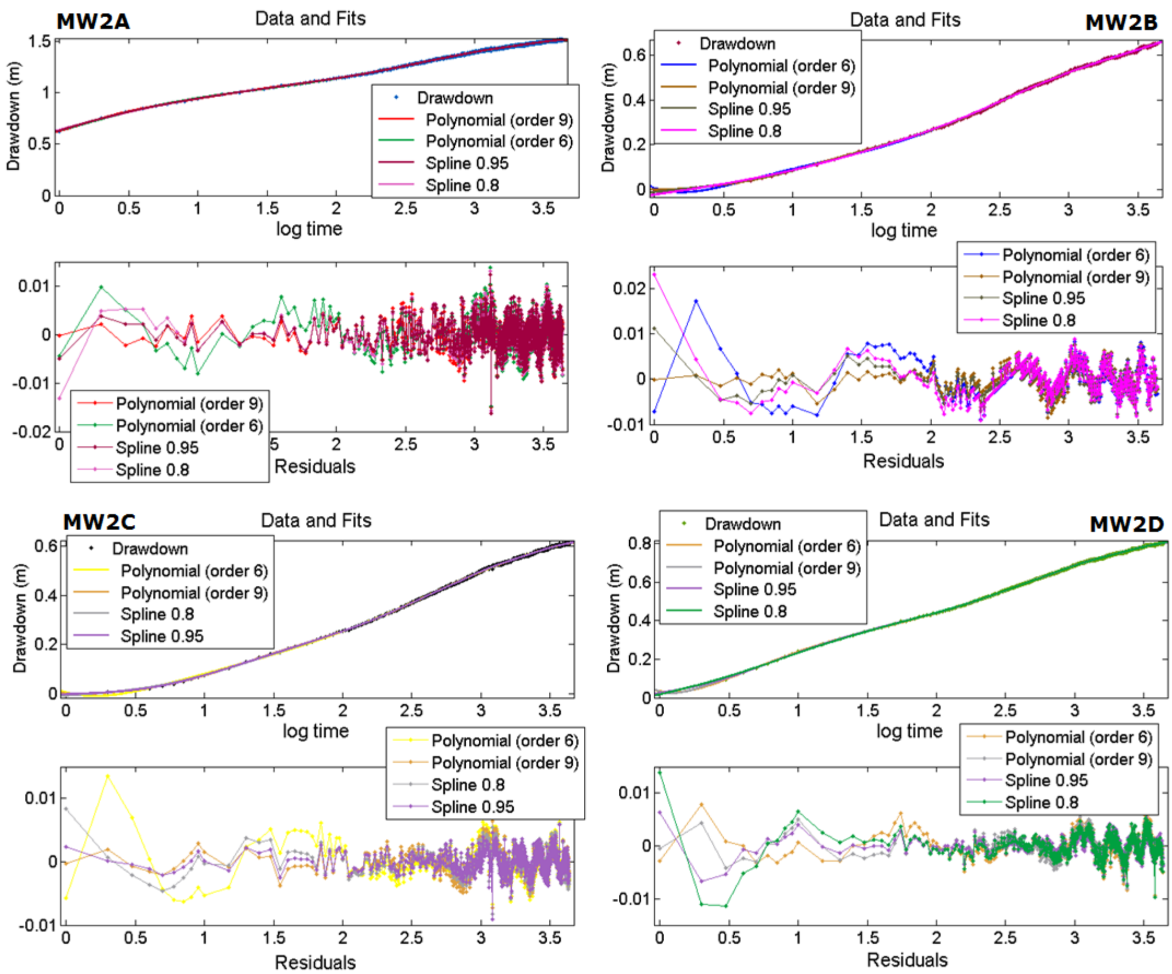

Figure 7.15. Drawdown fitted polynomials/Splines and residuals

As seen from Figure 7.15, residual demonstrations according to fitting curves were observed and analyzed. The residual values designate closeness of fit of the data to the assumed model. Small residuals mean the correction of the noise in the base data, on the other hand big residuals as shown in MW2B figure is overestimating which leads inaccurate estimation of aquifer parameters. The quality of each fit was also evaluated in terms of goodness of fit some statistics (Table 7.12).

Table 7.12. Goodness of Fit Statistics

		SSE	R-square	Adjusted R-square	RMSE
MW2A	Poly 4	0.167	0.9986	0.9986	0.0139
	Poly 6	0.138	0.9988	0.9988	0.0126
	Poly 9	0.126	0.9989	0.9989	0.0121
	Spline 0.8	0.124	0.9989	0.9989	0.0120
	Spline 0.95	0.138	0.9988	0.9988	0.0127
MW2B	Poly 4	0.186	0.9983	0.9983	0.0146
	Poly 6	0.102	0.9991	0.9991	0.0109
	Poly 9	0.085	0.9992	0.9992	0.0099
	Spline 0.8	0.103	0.9991	0.9991	0.0110
	Spline 0.95	0.083	0.9993	0.9992	0.0098
MW2C	Poly 4	0.054	0.9995	0.9995	0.0079
	Poly 6	0.054	0.9995	0.9995	0.0079
	Poly 9	0.041	0.9996	0.9996	0.0069
	Spline 0.8	0.062	0.9994	0.9994	0.0084
	Spline 0.95	0.030	0.9997	0.9997	0.0059
MW2D	Poly 4	0.130	0.9988	0.9988	0.0122
	Poly 6	0.060	0.9995	0.9995	0.0083
	Poly 9	0.053	0.9995	0.9995	0.0078
	Spline 0.8	0.053	0.9995	0.9995	0.0079
	Spline 0.95	0.042	0.9996	0.9996	0.0070

The above table shows the results of the residual analysis for the goodness of fit values. It includes sum of squared errors (SSE) for measuring the total deviation of the response values; R-square to show how successful the fit is in explaining the variation of the data, in short it is the square of the correlation coefficient, adjusted R-square is based on the degrees of freedom; root mean squared error which is also known as the fit standard error and the standard error of the regression.

The statistics show that nearly all fits explain about 99% of the total variation in the data about the average, suggesting that all fitting curves represents the real data well. SSE, RMSE statistics indicates that 9th order polynomials and Spline in smoothing value (p) 0.8 and 0.95 have smaller random error component, and that the fits may be more useful for the prediction.

However, the main goal of this analysis is to see which curve provides smooth and representative derivatives of the data, not to find accurate predictions. So, from the residual statistics it can be inferred that 4th and 6th order polynomial fits partially on the field data, thus they are not giving reliable representations. After residual diagnostics, the derivatives of fitting are presented in Figure 7.16.

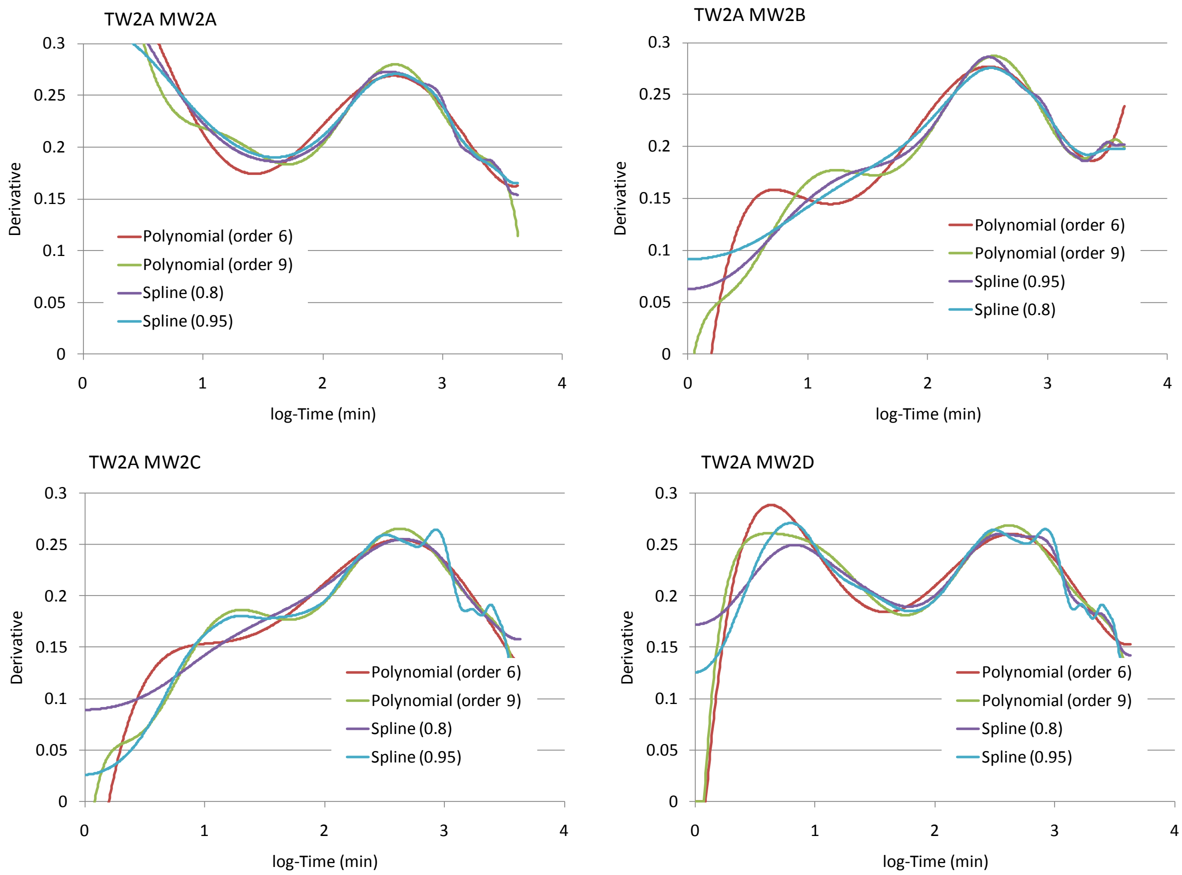

Figure 7.16. Derivatives of fitting curves for the field data from test well 2A and monitoring wells 2A, 2B, 2C and 2D

The results of the derivatives show consistent values with smoothed derivatives in Figure 7.13. and Figure 7.14. Comparing to the smoothed derivatives inflection points are viable, but different than smoothed derivatives, fitted derivatives provide us early data information. It can be seen that for the cases of MW2A and MW2B Spline 0.95 gives smooth and useable results; for cases MW2C and MW2D there are fluctuations which makes hydrological parameter estimation more uncertain. Although the statistics indicated that the 9th order polynomial is useful for the prediction; the derivative graphs show that it contains unrealistic fluctuations that may have stemmed from barometric fluctuations. On the other hand, observations show that Spline 0.8 curve has no fluctuation and appears to be good representation for hydrological parameter estimation. Plots of the derivatives of other observation points computed with the Spline method using *p* values 0.8 and 0.95 are presented in Appendix C.

7.4.2. Conventional Methods

In this section two conventional methods will be applied to the field data: the Cooper-Jacob method for non-leaky aquifers and Walton's method for leaky aquifers.

In real subsurface systems completely non-leaky aquifer may not be present; aquifer with very small leakance can be considered as non-leaky aquifer. In case of very high leakage factor (*B*) the aquifer is classified as non-leaky confined. Unlike synthetic data applications for confined aquifer, the type of aquifer may not be known with certainty in real pumping test data applications. Therefore, Walton's method can be used also for non-leaky aquifer, in case of very small *r/B* curve (specified in Walton's curve family as $r/B < 0.001$) the parameter estimations will be similar to Theis method.

Table 7.13. Estimated Parameters using the Walton and Theis methods for real data

	Pumping well	Observation point	T(m^2/s)	S	B(m)	r(m)	r/B
Walton's and Theis's Type Curve	TW2A	MW2B	0.0096	0.10813	8423	8.42	0.001
		MW2A	0.0083	0.00004	4724	9.45	0.002
		MW2C	0.0096	0.00067	108953	108.95	0.001
		MW2D	0.0093	0.00012	113386	113.39	0.001
	TW2B	MW2E	0.0072	0.00039	5944	11.89	0.002
		MW2F	0.0089	0.00027	2906	87.17	0.03
		MW2H	0.0093	0.00007	5385	161.54	0.03
		MW2C	0.0097	0.00001	7742	232.26	0.03
		MW2B	0.0084	0.00022	14712	294.25	0.02
	TW5A	BH68-80	0.0111	0.00562	163	4.88	0.03
		ST8	0.0128	0.00105	427	8.53	0.02
		MW5B	0.0138	0.00021	6309	126.19	0.02
		NW05	0.0266	0.00019	12771	255.42	0.02
		ST7	0.0226	0.00016	11931	417.58	0.035
		MW1	0.0328	0.00010	27081	541.63	0.02

Tables 7.13 and 7.14 list the parameter estimates using the Walton method and the Cooper-Jacob method respectively. The results suggest all of the drawdown data aquifers being tested exhibit some leaky aquifer characteristics. Drawdown data from monitoring wells (especially MW2C and MW2D) have higher leakage factors proportional to radius of the monitoring points. Overall, the curves are close to the Theis's (no leaky) curve but none of them fall exactly on to it.

Table 7.14. Parameter Estimations of Cooper-Jacob method for real data

	Pumping well	Observation point	T (m^2/s)	S	r(m)
Cooper - Jacob Method	TW2A	MW2B	0.010	8.62E-06	8.42
		MW2A	0.011	7.63E-02	9.45
		MW2C	0.010	1.03E-04	108.95
		MW2D	0.010	1.03E-04	113.39
	TW2B	MW2E	0.008	1.91E-04	11.89
		MW2F	0.009	2.22E-04	87.17
		MW2H	0.010	7.96E-05	161.54
		MW2C	0.010	7.96E-05	232.26
		MW2B	0.011	6.71E-05	294.25
	TW5A	BH68-80	0.015	1.52E-03	4.88
		ST8	0.016	6.58E-04	8.53
		MW5B	0.017	1.46E-04	126.19
		NW05	0.031	1.29E-04	255.42
		ST7	0.026	8.59E-05	417.58
		MW1	0.033	1.58E-04	541.63

The transmissivity values obtained with the Cooper-Jacob methods is generally consistent with the values obtained with the Walton method. Because the Cooper-Jacob method does not include the effect of leakance, there is a tendency to calculate higher transmissivity values and lower storativity values. This exercise also exemplifies the high level of uncertainty in its estimates; the difference in the storativity for each observation point is apparent. On the other hand, storativity estimations for each method are comparable.

In summary, the results obtained from each method for each observation point are generally consistent. The aquifers where the pumping tests were conducted can be considered as slightly leaky, but the leakage is sufficiently low such that using non-leaky aquifer interpretation methods may yield acceptable results, particularly the transmissivity estimates. Therefore, it was decided that both leaky and non-leaky methods will be applied and the results will be compared to each other.

7.4.3. CD Method

In this section, application of the new method titled as Continuous Derivation method for non-leaky confined aquifer is discussed. The method was described in section 5.1 and applied to the synthetic data in section 7.2.2. Conventional methods provide single representative estimates of hydrological parameters and types of the aquifers; they cannot give variability of parameters as a function of time and distance.

In addition to the estimation of flow parameters, the CD method provides a method for the identification of the type of aquifer present as described in the following section

7.4.3.1. Identification of Aquifer type. As shown in the Figure 5.2 which was developed for the Hantush leaky aquifer system, shows that γ_L should increase with time. Depending on the value of r/B, γ_L increases rapidly at late times as the drawdown approaches steady state. In general, the γ_L curves depicted in Figure 7.17 exhibit a relatively shaper increase in γ_L at late times suggesting that the aquifer system is slightly leaky. Test well 5A appears to have the highest increase in γ_L at the end of pumping tests and, hence, has relatively higher leakage (r/B value). Moreover, variations between different individual γ_L may reveal important information about the aquifer conditions. For example the response at MW2A and MW2B which are both less than 10 m away from TW2A are significantly different, demonstrating the complexity of the geologic conditions. MW2A exhibits a larger drawdown at early times, resulting in a larger initial γ_L value compared to MW2B. Because both monitoring wells are at the same distance from the test well, the smaller γ_L value of MW2B corresponds to a lower value of 1/u (Figure 5.2).

This may be an indication of a higher "apparent" storativity value for MW2B caused by poorer connectivity to the pumping well. This is indeed consistent with the geology within the vicinity of TW2A. Monitoring well MW2A is completed at the same elevation and within the same sand/gravel layer as TW2A and, hence, is well connected to the pumping well. MW2B is completed in a hydraulically connected sand/gravel above the elevation of the test well, with less connectivity to the pumping well. The lower connectivity to MW2A manifests itself as a higher storativity value.

Unlike the transmissivity, the estimated storativity varies significantly from about 10^{-6} to as high as 10^{-1} for TW2A-MW2B (which was predicted qualitatively based on the shape of the γ_L curves). The variation in the estimation of the storativity stems in part from its dependence on the point-to-point connectivity of the heterogeneous transmissivity field (e.g., Sanchez-Vila et al., 1999).

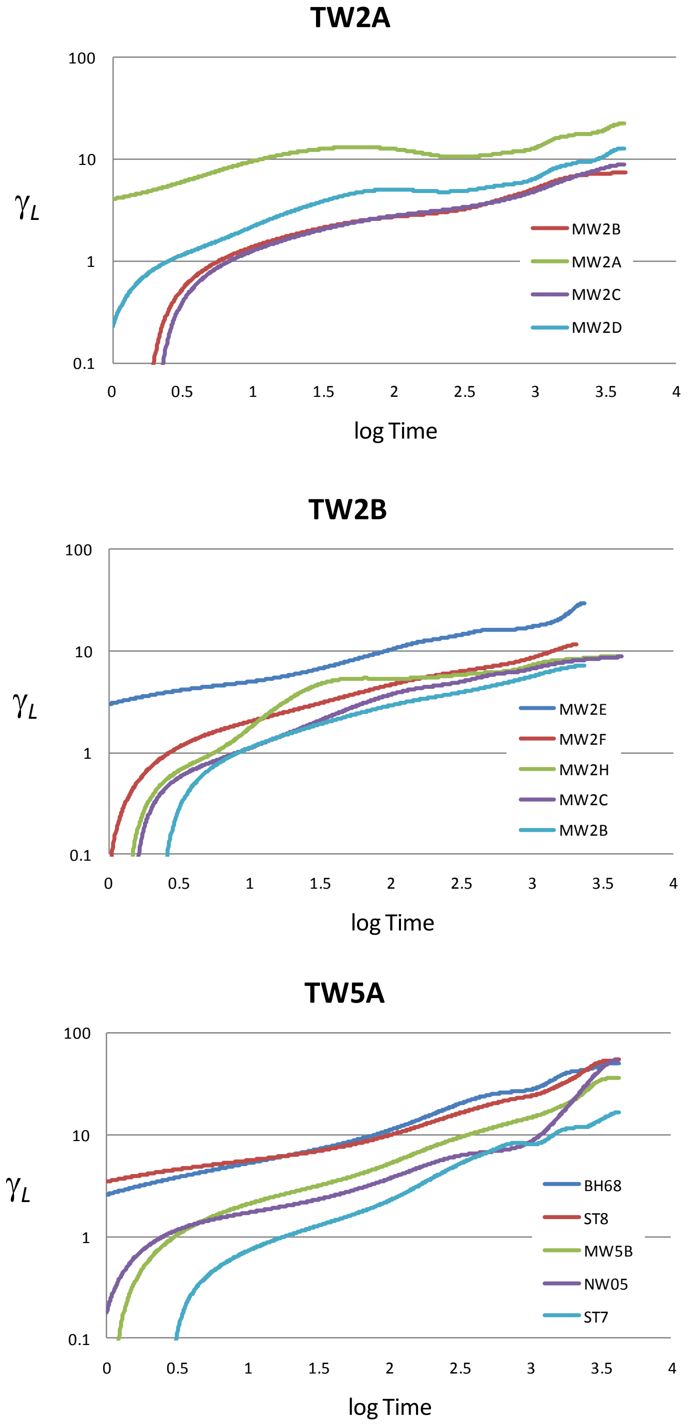

Figure 7.17. $\gamma_L = \dfrac{2.3s}{s'}$ estimated from the drawdown data and its time derivative

7.4.3.2. Estimation of Flow Parameters. Figure 7.18 and Figure 7.19 show the results of different fitting curves. Each interpolation curve was denoted in terms of the fitting method applied to drawdown data and will serve as input to the CD-Confined computer program (see Appendix G). The flow parameters are first estimated as a function of time and the x-axis is later converted to distance as described in Section 5.1.

The results show in general that, for any particular test, the estimated parameters as a function of time or distance do not vary much irrespective of the interpolation method used. This suggests that the results are not very sensitivity to the considered interpolation method. The spread in the estimates at any particular time (or distance) is a measure of the uncertainty in the definition of the drawdown derivatives.

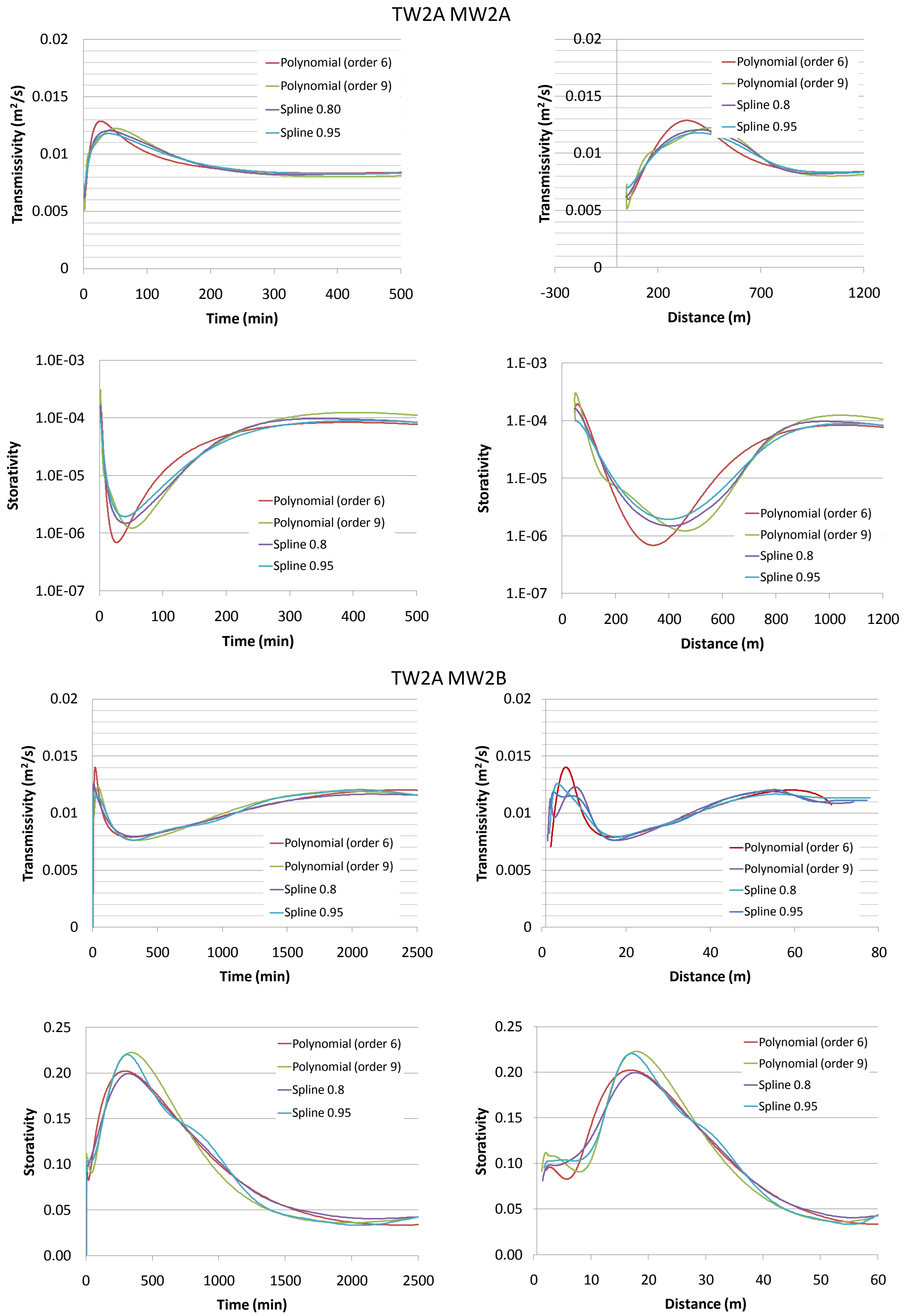

Figure 7.18. Estimation of flow parameters using the CD–Confined method for test wells 2A and 2B and for different drawdown fitting methods

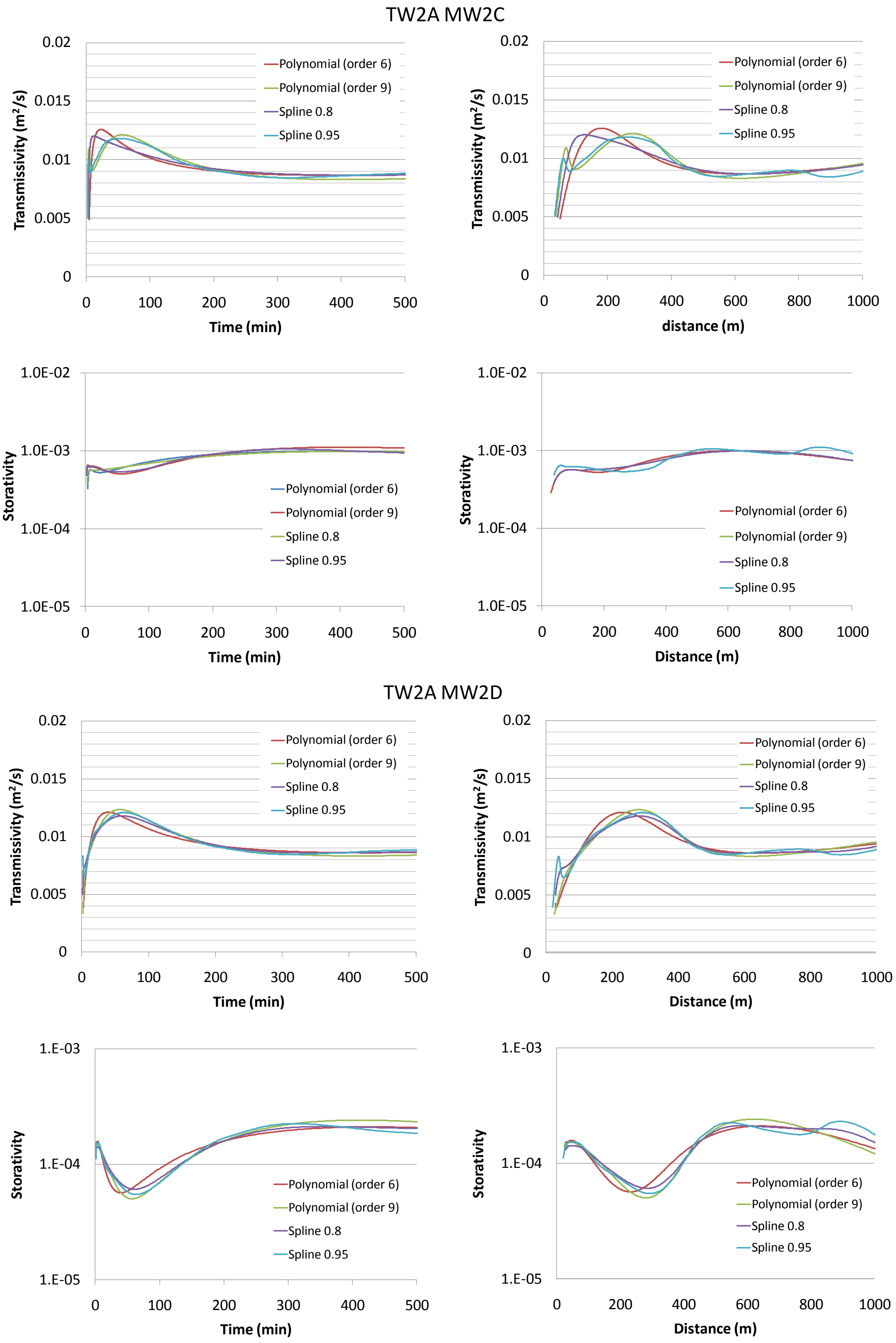

Figure 7.19. Estimation of flow parameters using the CD-Confined method for test wells 2C and 2D and for different drawdown fitting methods

Different than the field data, synthetic data estimates for CD-Confined method was not affected by real pumping test conditions such as skin effect, head losses due to plugging of the aquifer with drilling mud, head losses in the gravel pack, and head losses in the screen. Consequently, calculations of early data in synthetic fields can be interpreted as storativity values are relatively close to the real value at early times and distance. In real applications, however, estimation of storativity is error prone since the interpreted values are also affected by a number of processes such as well storage or well development, among others. Therefore, estimates at early times, unlike the case with synthetic data were mainly excluded, as seen from solutions (Figure 7.18, Figure 7.19 and for other cases in Appendix C)

From the figures it can be observed that the relative variation of the storativity is higher than the variation in the transmissivity estimations. This again shows that pumping tests generally yield more reliable transmissivity estimates than storativity estimates. Another feature of the results that the transmissivity and storativity estimates exhibit negative correlation; for high transmissivity estimates, the storativity estimates are low and vice versa. Transmissivity and storativity values appear consistence in spite of the differences in some cases, for instance MW2B from the test well 2A have approximately closer transmissivity estimate with respect to other cases, however storativity estimates are very high. In test well 2A group, estimates of cases are alike except MW2B solutions, which probably stem from the low quality of the data.

Nearly all of the cases show decreasing storativity behavior after steady storativity estimation between specific range, after that range transmissivity values tend to increase, which is probably due to the derivatives of the late drawdown data. This further indicates that some leakage may be as discussed in section 5.2. In addition, according to these interpretations CD method allows us to define what the types of the aquifers are. We can also diagnose at what time and distance the effect of leakage is evident. For the test well 2A the effect of leakage is active between time ranges 21000–40000 seconds, and distances between 10–650 m; observations of the test well 2B indicate that active leakage time range is 600–20000 seconds, distance range is 50–800 m; for TW5A leakage becomes significant for range between <100–4500 seconds and 10–300 m. The minimum values estimated from the monitoring points those have the smallest radius and maximum values from the monitoring points those have highest radius. According to findings to see the parameter variations in furthest distance, the monitoring point with the highest radius should be analyzed. In order to understand the characteristics of the aquifer, the drawdown data set obtained from the constant rate pumping test, which was conducted for maximum 12 hours of duration, is sufficient for this case.

Comparison of the estimates obtained with the CD–Confined method and the estimates obtained with the conventional methods indicates that the transmissivity estimates are generally consistent. However, the CD method provides estimates as a function of distance from the pumping test, whereas the Walton and CJ methods give single estimates only. The storativity estimates on the other hand shows that the values estimated by Walton's and Cooper-Jacob methods as implied before corresponds to different times of CD method parameter curves, however in late data there is decrease in storativity parameters especially in test well 5A cases, which proves the effect of leakage is higher or in other words leakage factor is smaller in this case.

For pumping test TW2A, the Walton method predicted a transmissivity of about 0.01 m^2/s, and a storativity of about 0.0001 at all wells except for TW2A-MW2B where the storativity was about 0.1). Similar storativity and transmissivity values were also obtained with the CD method (See Figure 7.18). However, the estimated parameters obtained with the CD method exhibit some variation particular at early distance (or time). At later times, the transmissivity estimate tends to stabilize suggesting that the aquifer system is behaving close to a homogeneous system. This corresponds to a distance of about 600 to 800 m for monitoring wells MW2A, MW2C and MW2D. For MW2B, which has a much higher apparent storativity value due to its lower connectivity to the test well, the aquifer system starts to behave as a homogeneous aquifer. These distances are representative of the characteristic length scale of the heterogeneous transmissivity field. Furthermore, the estimated transmissivity values at the very early times are mostly dependent on the transmissivity values in the immediate vicinity of the test well. Therefore, the variability of the transmissivity values at early times can be indicative of the transmissivity variance of the aquifer system provided that a sufficient number of tests is available to satisfy the ergodicity requirement.

For applications with scales larger than the characteristic length of the the transmissivity field, a conventional deterministic approach may be appropriate. However, for applications of smaller scales the results of this approach may be inaccurate a stochastic approach would be required to quantify the uncertainty in any predictions of the response of the system to future changes and stresses.

Inspection of the observed data also indicates that the selected different derivatives estimation techniques do not yield significantly different estimates of the flow parameters, suggesting that the results of the pumping test analysis method are not too sensitive to the methods selected for derivative estimation.

7.5. Estimation of Flow Parameters- Field Data from Leaky Aquifers

The examples presented in section 7.3 focused on synthetic data analysis from leaky aquifer data and showed that in a heterogeneous system, different interpretation methods provide different parameter estimates as in the analysis from synthetic non-leaky confined aquifer data. Thus using all methods may provide insight into the actual spatial variability of flow parameters.

In this section, one conventional (Hantush's Inflection Point) and one novel (DIP) method were applied to the field data. As another conventional method Walton's type curve method had been used in section 7.4.2 because this method is a generalized version of Theis's method that can also account for leakance; that is, Theis method is for the special case of $r/B = 0$. However, it was observed that all real field data have slight leaky aquifer features. Estimations in Table 7.13 were also compared with the findings of the methods applied in this section.

7.5.1. Conventional Method

As explained previously the Hantush inflection point method requires that the steady-state drawdown at the end of the pumping test has been reached (see section 4.1.2.2), however, when the pumping test data do not extend up to the steady state, previously used fitting methods have been used to extrapolate until the curve reaches steady state (see Figure 7.19). One disadvantage of extrapolation is the high level of uncertainty in the value of the maximum (steady-state) drawdown. The best fitting techniques to extrapolate were chosen as polynomial and rational fittings.

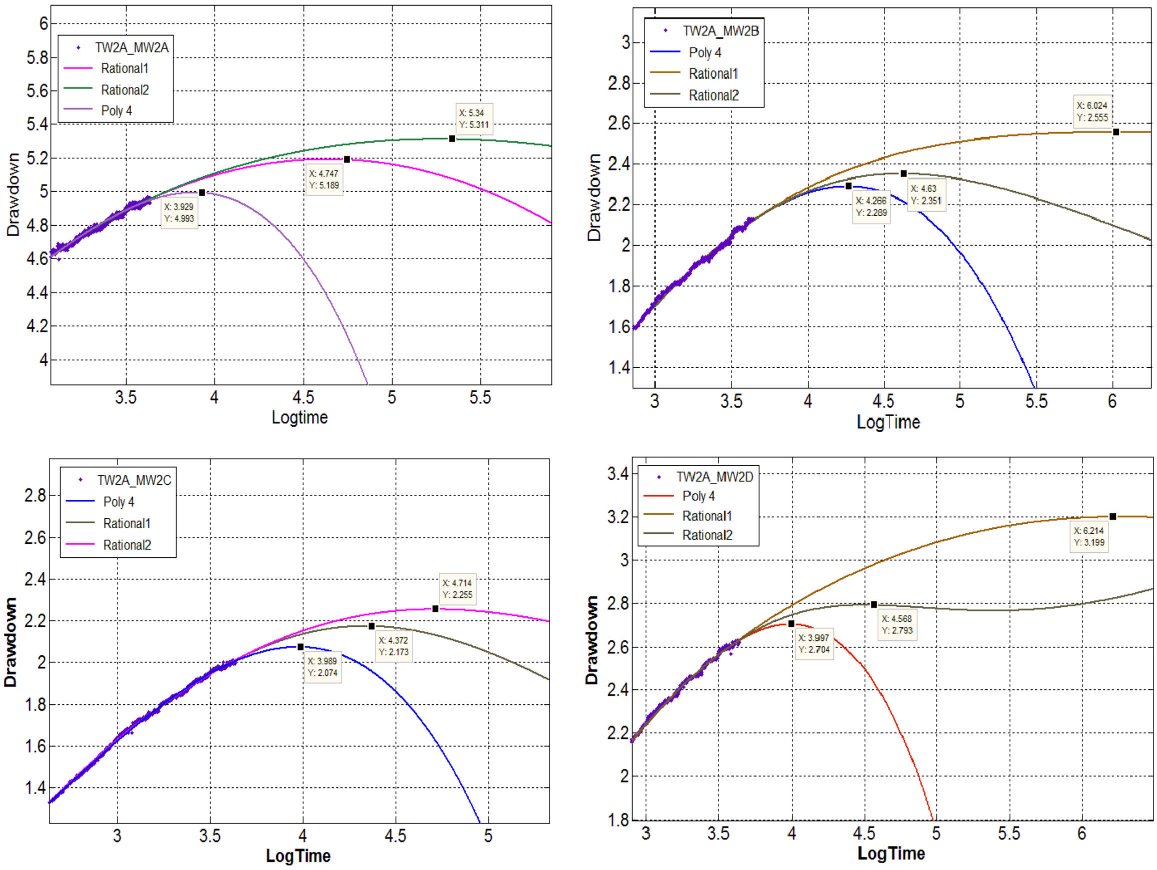

Figure 7.20. Different extrapolation of the drawdown data for the determination for the maximum drawdown points (four monitoring wells data of test well 2A)

Approximation to steady-state drawdown, s_m, obtained from different extrapolation methods are shown in Figure 7.20. The uncertainty of the definition of the steady state will invariably affect the estimate of the leakance factor. However the analysis will be guided by the results of previous analysis methods which indicated low r/B values.

Table 7.15. Parameters estimated with the Hantush's Inflection Point method with extrapolation

	Pumping well	Observation point	T(m^2/s)	S	B(m)	r(m)	r/B
Hantush's Inflection Point Method	TW2A	MW2B	0.0089	0.00002648	179	8.42	0.01433
		MW2A	0.0090	0.00000106	8765	9.45	0.00033
		MW2C	0.0089	0.00000018	1717	108.95	0.01934
		MW2D	0.0086	0.00000010	4295	113.39	0.00805
	TW2B	MW2E	0.0135	0.00000014	88710	11.89	0.00004
		MW2F	0.0112	0.00000011	8072	87.17	0.00329
		MW2H	0.0117	0.00000004	10160	161.54	0.00485
		MW2C	0.0102	0.00000003	7420	232.26	0.00954
		MW2B	0.0100	0.00000003	6875	294.25	0.01305
	TW5A	BH68-80	0.0130	0.00003087	387	4.88	0.00384
		ST8	0.0141	0.00000850	837	8.53	0.00311
		MW5B	0.0123	0.00000019	1361	126.19	0.02825
		NW05	0.0240	0.00000005	2683	255.42	0.02902
		ST7	0.0162	0.00000003	2047	417.58	0.06218
		MW1	0.0181	0.00000002	2238	541.63	0.07376

The hydrological parameters estimated with the Hantush inflection method are shown in Table 7.15. The transmissivity values are consistent with the estimates from Walton's method (see Table 7.13) and early estimates of CD-Confined method. However, it can be seen that there is wide variability in leakage factors which were underestimated along with the storativity values in comparison with the values from other leaky aquifer methods especially in test well 5A case. So, it can be interpreted, instead of using extrapolation the last data point could be used as the maximum drawdown value for inflection method.

Table 7.16. Parameters estimated with the Hantush's Inflection Point method assuming the steady-state drawdown is equal to the drawdown at the end of test

	Pumping well	Observation point	$T(m^2/s)$	S	B(m)	r(m)	r/B
Hantush's Inflection Point Method	TW2A	MW2B	0.0089	0.0000257	179	8.42	0.01433
		MW2A	0.0090	0.0000018	8749	9.45	0.00033
		MW2C	0.0089	0.0000028	1717	108.95	0.01934
		MW2D	0.0085	0.0000019	3395	113.39	0.01018
	TW2B	MW2E	0.0135	0.0000002	78205	11.89	0.00005
		MW2F	0.0112	0.0000009	6272	87.17	0.00424
		MW2H	0.0117	0.0000012	8925	161.54	0.00552
		MW2C	0.0089	0.0000028	6543	232.26	0.01082
		MW2B	0.0100	0.0000011	5626	294.25	0.01594
	TW5A	BH68-80	0.0130	0.0005589	387	4.88	0.00384
		ST8	0.0141	0.0002944	837	8.53	0.00311
		MW5B	0.0123	0.0000545	1361	126.19	0.02825
		NW05	0.0240	0.0000453	2683	255.42	0.02902
		ST7	0.0141	0.0000292	2047	417.58	0.06218
		MW1	0.0130	0.0005589	2067	541.63	0.07986

Estimations of Hantush inflection point method indicate that there is no remarkable difference between extrapolated data and maximum points of non-fitted drawdown data. Even there is consistency in synthetic data estimates of inflection point method comparing to other conventional and new methods, unapparent steady-state drawdown value culminated with inaccurate leakage factor estimations and underestimated storativity values. These observations point to the difficulty of interpreting field data particularly at a complex site such as the one considered in this study.

7.5.2. DIP Method

In this section the drawdown data from the field pumping tests were interpreted with the double inflection point (DIP) method. The FORTRAN computer code used for this purpose is listed in Appendix H.

The DIP method requires the estimation of the second derivative in the application of the CD method; fitting curves of the drawdown were developed. So the second derivatives were determined by differentiation of the fitted curves. As indicated earlier the

Spline method was used for curve fitting unlike the second derivatives of synthetic data the heterogeneity in the field data is apparent. As explained in methodology part three distinctive inflection points were determined to estimate leaky aquifer parameters.

The behavior of second and first derivatives can be observed from Figure 7.20. In general, the shape of the curves differs significantly from the analytic solution developed for homogeneous conditions. However, locations of the maximum and minimum points (inflection points) of second derivatives are sufficiently distinct for parameter estimation.

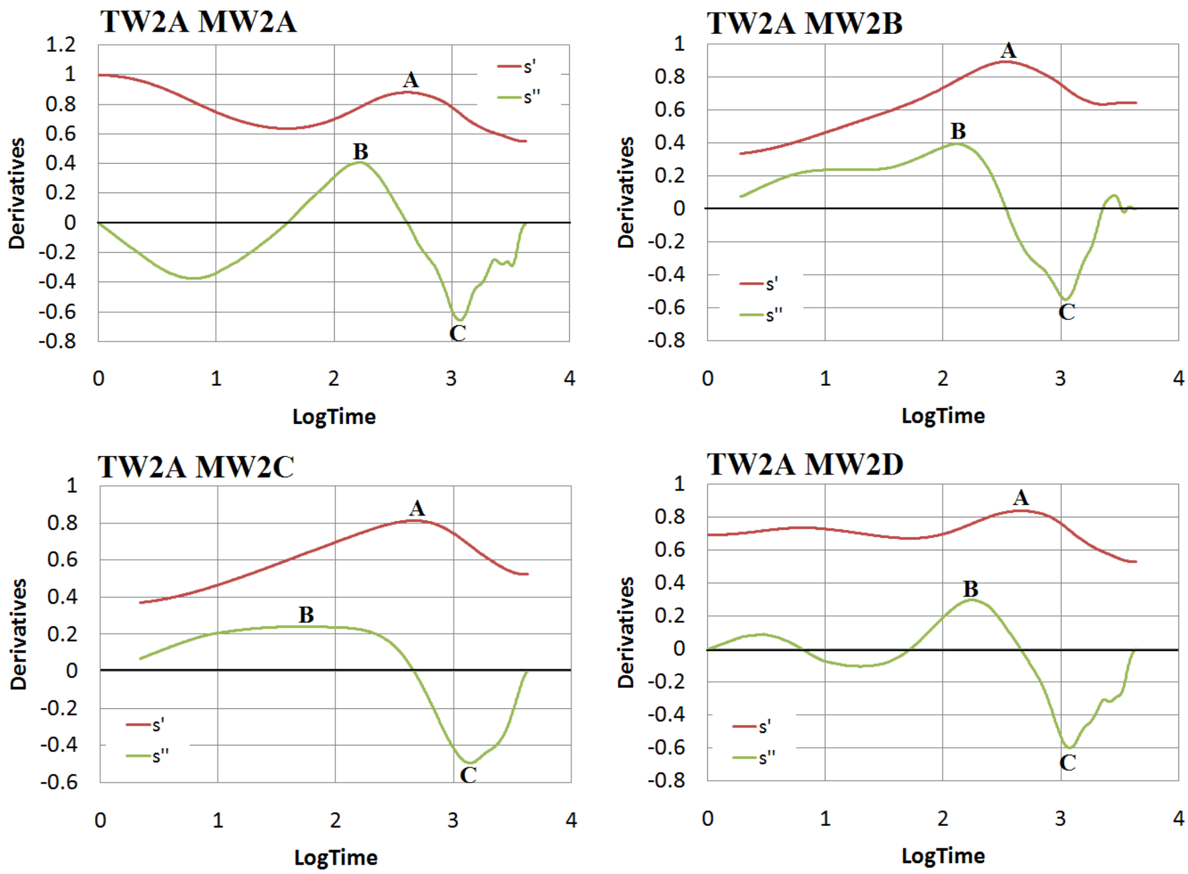

Figure 7.21. First and second derivatives of drawdown using LOESS smoothing and Spline fitting method, A is inflection point, t_p, B and C are t_{s1} and t_{s2}

The DIP method first gives an estimate of the leakance, which is then used to estimate the storativity and transmissivity. That approach is based on using the first inflection point (t_{s1}, denoted as B in Figure 7.20) that is based mostly on the early portion of the drawdown data and second inflection point (t_{s2}, denoted as C in Figure 7.20) uses the late and intermediate portions of the drawdown curve. Hence, the DIP method provides two sets of estimates can be determined depending on whether the first or second inflection point is used, thereby, providing some information about the heterogeneity of the aquifer.

Table 7.17. Parameters estimated using the DIP the field data based on the first inflection point and second inflection point of the second derivatives

			(First Inflection Point)t_{s1}			
Pumping well	**Observation point**	**r (m)**	**B(m)**	**r/B(early)**	**T(m^2/s)**	**S**
TW2A	MW2B	8.42	7.2	1.16	0.00131	0.20630
	MW2A	9.45	7.4	1.27	0.00037	0.08181
	MW2C	108.95	529.8	0.21	0.00522	0.00140
	MW2D	113.39	97.5	1.16	0.00081	0.00124
TW2B	MW2E	11.89	3.1	3.88	0.00002	0.00017
	MW2F	87.17	129.9	0.67	0.00239	0.00017
	MW2H	161.54	38.2	4.23	0.00003	0.00101
	MW2C	232.26	419.4	0.55	0.00462	0.00004
	MW2B	294.25	6638.1	0.04	0.01026	0.00006
TW5A	BH68 80	4.88				
	ST8	8.53	12.9	0.66	0.00228	0.01423
	MW5B	126.19	155.3	0.81	0.00307	0.00019
	NW05	255.42	1082.4	0.24	0.01683	0.00009
	ST7	417.58	927.8	0.45	0.01075	0.00008
	MW1	541.63	618.9	0.88	0.00701	0.00006
			(Second Inflection Point)t_{s2}			
Pumping well	**Observation point**	**r (m)**	**B(m)**	**r/B(Late)**	**T(m^2/s)**	**S**
TW2A	MW2B	8.42	10.0	0.84	0.002070	0.236451
	MW2A	9.45	9.0	1.05	0.000509	0.301456
	MW2C	108.95	125.9	0.87	0.001447	0.005362
	MW2D	113.39	93.2	1.22	0.000755	0.003961
TW2B	MW2E	11.89	62.8	0.19	0.002856	0.003819
	MW2F	87.17	99.6	0.88	0.001743	0.000539
	MW2H	161.54	28.5	5.67	0.000006	0.000001
	MW2C	232.26	158.0	1.47	0.001223	0.000102
	MW2B	294.25	395.9	0.74	0.001957	0.000637
TW5A	BH68 80	4.88	73.4	0.07	0.008175	0.002741
	ST8	8.53	24.0	0.36	0.003942	0.043529
	MW5B	126.19	152.5	0.83	0.003005	0.000614
	NW05	255.42	559.5	0.46	0.010550	0.000369
	ST7	417.58	433.1	0.96	0.004704	0.000237
	MW1	541.63	323.9	1.67	0.002380	0.000128

In Table 7.17, estimations of DIP method for field data are presented, for DIP method two distinct group of estimates are exist, one is the estimate based on the t_{s1} and t_p , and the other is based on t_{s2} and t_p (see Figure 4.10). The change of the flow parameters between specific times can be observed with this characteristic of DIP method.

Specifically, the critical parameter is to focus on the estimation of the leakage factor, which is subsequently used in the estimation of the other flow parameters. Transmissivity values of DIP method are not changing drastically and findings are close to the estimations of previous methods. It is observed that the analysis of time-drawdown data of observation points located closer to the test wells gives lower transmissivity estimates than of interpretation methods for confined aquifer. Also compared to the Hantush's inflection point method, the DIP method produces lower leakage factor in other words high leakance. With respect to CD-confined method, late data, especially second inflection point, estimates do not show decreasing storativity and estimations from the observation points located at large distances from the pumping test are consistent with estimates from nearby observation points. For the second estimates of DIP, it can be said that *r/B* values, which corresponds to late data, show increasing trend which was also seen from CD-confined estimations curves as leakage effect.

A measure of the variability of the parameters can be viewed by the comparing the estimations of DIP method based on the first and second inflection points. It has been reported in the literature that the local transmissivity at the well is positively correlated with the DIP estimate based on t_{s1} and negatively correlated with the DIP estimate based on t_{s2} (Trinchero et al., 2008).

Finally, because each of the used methods gives weight to different parts of the time drawdown data, some information of the heterogeneity of the site can be determined by the synthesis of all the data obtained with the different methods and using drawdown data from different pumping test. Such estimates can then be used in a numerical model to simulate groundwater flow and contaminant transport in support of groundwater field investigations, remedial investigations or remedial feasibility studies.

8. CONCLUSIONS AND RECOMMENDATIONS

Groundwater flow and contaminant transport are strongly influenced by the heterogeneity of the subsurface and the spatial variability of the flow parameters such as the hydraulic conductivity. Although heterogeneity of subsurface parameters is often encountered in the field, most existing pumping test analysis techniques are based on the assumption of homogeneity. The purpose of this study is to apply different interpretation methods to pumping test data in order to provide some information about the spatial variability of the flow parameters.

Two types of aquifer systems were considered: confined aquifers whereby the upper and lower boundaries do not allow flow and semi-confined (leaky) where the boundaries allow some leakage. Analytical methods for the interpretation of pumping tests have been applied according to aquifer types to estimate flow parameters, namely: the transmissivity, the storativity, and the leakage factor (for leaky aquifer systems only).

The pumping test interpretation methods that were evaluated in this study can be grouped into two categories: conventional methods and novel methods. Conventional methods are based on the assumption of homogeneity and include the type-curve approach developed by Walton (1962) and the inflection point method developed by Hantush (1956) for leaky aquifer, and Theis (1935) and Cooper and Jacob (1946) methods for confined aquifers. Such methods, which are often used in practice, provide a single estimate of the flow parameters, although the real aquifer system may be heterogeneous. The two novel methods examined in this study are the DIP (Double Inflection Point) method which was proposed for leaky aquifer (Trinchero at al., 2008) and the CD (Continuous Derivation) method which was recently developed by Copty et al. (2011). The CD method attempts to provide information about the spatial variability of flow parameters rather than estimating a single representative value of the perturbed aquifer with respect to conventional methods. The method uses the ratio of the drawdown to the drawdown derivative at a single point in time to estimate the transmissivity and storativity at the considered time. The time-dependent interpreted transmissivity is then expressed as a function of radial distance from the well. The DIP method uses the time at the inflection points (where the second derivative peaks positive or negative) of the second derivative to estimate the flow parameters. A common characteristic of these methods, including Hantush's inflection point method, is that they need the first and (in some cases) the second derivatives of time-drawdown data.

Two kinds of pumping tests were evaluated in this work; synthetic pumping test data and real field data. The advantage of the synthetic pumping tests is that the spatial distribution of the parameters is known, unlike the case in real aquifer systems. The synthetic pumping tests were developed by first generating transmissivity fields using the turning bands method (Mantoglou and Wilson, 1982). Using the generated transmissivity field the drawdown due to pumping was simulated using the MODFLOW (Harbaugh et al., 2000) computer program for both confined and semi-confined aquifer systems. Interpretation of the drawdown data using conventional methods shows that each method is influenced differently by the transmissivity of the aquifer volume surrounding the well. The methods that use mainly the first part of the drawdown curve provide an estimated value which is close to the actual value at the well, while those that analyze the late transient part of the curve give an estimate that provides a representative average value of the entire aquifer. This average value is shown to be equal to the geometric mean of the transmissivity field. The results of conventional methods indicate that different interpretation methods yield similar results at large distances from the well. Moreover the heterogeneity of the transmissivity field influences the estimation of the other parameters such as the storativity.

Different derivation methods have been applied to the drawdown data from synthetic pumping tests. It was observed that the Bourdet (Bourdet et al., 1989) and Spane & Wurstner methods (Spane and Wurstner, 1993) give similar results when the drawdown data are slightly noisy. In general, depending on the parameters used in smoothing, over smoothing of the drawdown may results, particularly at locations near the well, leading to some distortion of the derivative curve.

The synthetically generated time-drawdown data were also analyzed using the novel CD method. The estimates obtained with the CD method based on early data generally exhibited large variability. On the other hand, estimates calculated from the end of the parameter curves, which represents the late data, exhibit less variability and were highly correlated with the spatial average of the flow parameters *S, C* and *T* used in the data generation. The information provided by the observation points located near the well is most useful in the characterization of these contrasts in flow parameters. Also with using the CD method, it was observed that each conventional method (Cooper-Jacob, Theis) gives more emphasis to different portion of pumping test data.

Although the generated transmissivity field was the same in confined and semi-confined cases; the results indicate that confined aquifer interpretation methods gave closer estimations relative to leaky aquifer method estimations to the defined input flow parameters. Calculations showed that storativity parameter gives higher response to the heterogeneity than transmissivity parameter in heterogeneous field. Also flow parameters in leaky aquifer exhibit higher variability because of the continual change in leakage factor.

The different interpretation methods were also applied to field pumping test data. The first step in the interpretation of the real data was to remove the effect of barometric and tidal variations on the drawdown. To get better representation of drawdown data and to reduce the noise in the data differentiation, various fitting methods were applied. The Spline method was chosen as the optimal fitting method and LOESS smoothing method was used in some cases as an initial smoothing procedure. To identify the type of aquifer system present, Walton's type curves method was applied and the estimates indicate that time-drawdown data of real pumping test show slightly leaky aquifer characteristics.

According to the findings of conventional methods, the transmissivity was estimated to be about 0.01 m^2/s for test wells 2A and 2B, and around 0.02 m^2/s for test well 5A. However, the different interpretation methods did not yield a single storativity value because of the variability according to distance and monitoring point. The estimated storativity ranged from 0.0001 – 0.00008 for test wells 2A and 2B (excluding MW2B which was screened in a different layer), and 0.0001 – 0.001 for test well 5A, demonstrating the difficulty of estimating a reliable estimate of the storativity. It can be implied from the interpretation of conventional methods that two different aquifer zones exist, one in the vicinity Test wells 2A and 2B and the other around test well 5A. Both aquifers have similar transmissivity values, however, the leakage is higher in the vicinity of test well 5A.

Findings of CD- method indicate that variability in transmissivity data is lower than the variability in storativity data. The effect of leakage can easily be observed from the parameter curves. Due to the slightly leaky characteristics $S_i(t)$ and $T_i(t)$ values were estimated up to a distance of 1 km from the pumping well. This study demonstrates that, with appropriate data fitting, the CD-confined method can be applied to the real data from non-leaky or slightly leaky aquifers. However, it is important to collect frequent (automated) high quality data.

The application of DIP method demonstrated that the difference between early and late data estimations is not always apparent. The transmissivity and storativity values are close to the estimates obtained from other methods. However, it is seen from the estimation tables for each method, *r/B* or Leakage factor is hard to diagnose. In general DIP method demonstrated lower leakage factor (higher leakance) estimations than conventional leaky aquifer methods. Diagnoses of the flow parameters according to analytical methods demonstrated that storativity and transmissivity parameters are inversely proportional. Moreover, with DIP method it was observed that lower leakage factor results in a decrease in the transmissivity and storativity estimates. The main difficulty of the application of the DIP method is that steady-state conditions are needed (or need to be extrapolated) and that second derivatives are prone to error. On the other hand, the method is simple to use once the inflection points and state-steady have been estimated.

In summary, the results presented in this study show that additional information about the spatial variability of transmissivity can be derived from time-drawdown data. While conventional single-well pumping test interpretation methods use time-drawdown data to estimate a single representative estimate of the transmissivity, other newly developed methods can provide additional information. Through the combination of all methods a better interpretation of the subsurface system is achieved.

Future research related to this study could focus on:

- Combining data from different pumping tests into the parameter estimation problem, instead of using data from each well independently and then combining the results,
- Testing the novel methods at other sites and compare results to other types of field data such as slug tests, geologic maps and geophyically derived data. This will provide a good tool to evaluate the performance of these novel methods.
- Estimation of the transmisisivty spatial structure, spficically, the transmisisivty variance and integral scale
- Incorporate the estimates of the flow parameters in a groundwater flow and contaminant transport model. For the development of realistic flow and transport models, information on the spatial variability of the flow parameters must be identified and included in the model. These models can then be used to different problems such as prediction of contaminant transport, evaluation of different remedial alternatives, and identification of effective monitoring strategies.

REFERENCES

Amin, I. (2005), Determination of the rate and volume of leakage using the slopes of time-drawdown data, Environmental Geology, 47(4), 558–564.

Apostel, L. (1961), Formal study of models. In: The Concept and the Role of the Model in Mathematics and Natural and Social. Edited by Hans Freudenthal. Springer. p. 8-9.

ASTM International (2002c), Designation D 4050-96 (Reapproved 2002), Standard Test Method (Field Procedure) for Withdrawal and Injection Well Tests for Determining Hydraulic Properties of Aquifer Systems.

Bakr, A.A., L.W. Gelhar, A.L. Gutjahr, and J.R. MacMillan (1978), stochastic analysis of spatial variability in subsurface flows. Comparisons of one and three-dimensional flows. Water Resources Research 14, no. 2: 263-271.

Barker, J., and R. Herbert (1982), Pumping tests in patchy aquifers, Ground Water, 20(2), 150–155.

Batu, V. (1998), Aquifer Hydraulics: A Comprehensive Guide to Hydrogeologic Data Analysis. Wiley-Interscience; 1 edition (February 27, 1998).

Bear, J., Dynamics of Fluids in Porous Media. New York: Elsevier, 1972.

Bourdet, D., T. M. Whittle, A. A. Douglas, and Y. M. Pirard (1983), A new set of type curves simplifies well test analysis, World Oil, 196(6), 95–106.

Bourdet D, Ayoub JA, Pirard YM (1989), Use of pressure derivative in well-test interpretation. SPE Reprint Ser 4:293–302.

Bourdet, D. (2002), Well test analysis: The use of advanced interpretation models, 426 pp. Elsevier, Amsterdam.

Box, G.E.P., and G.M. Jenkins (1976), Time Series Analysis: Forecasting and Control. San Francisco: Holden-Day.

Butler, J. J. (1988), Pumping tests in non-uniform aquifers the radially symmetric case, Journal of Hydrology, 101(1-4), 15–30.

Butler, J. J., and W. Z. Liu (1993), Pumping tests in non-uniform aquifers the radially asymmetric case, Water Resources Research, 29(2), 259–269.

Central Area Guideway, Pumping Test Data Report. Issued for Use, June 3, 2008

Copty, Nadim K. and Findikakis, Angelos N. (2004), stochastic analysis of pumping test drawdown data in heterogeneous geologic formations, Journal of Hydraulic Research, 42: S1, 59-67.

C. Rolland and C. Thanos Pernici (1998), A Comprehensive View of Process Engineering. In: Proceedings of the 10th International Conference CAiSE'98, B. Lecture Notes in Computer Science 1413, Pisa, Italy, Springer, June 1998.

C. Kechavarzi, K. Soga, T.H. Illangasekare (2005), Two-dimensional laboratory simulation of LNAPL infiltration and redistribution in the vadose zone. Journal of Contaminant Hydrology 76, 211-233.

Chapellier, D. (1992). Well logging in hydrogeology, A.A. Balkema Publishers, Brookfield, MA.

Chow VT (1952), On the determination of transmissibility and storage coefficients from pumping test data. Trans Am Geophys Union 33:397–404.

Cleveland, W.S. (1979) Robust Locally Weighted Regression and Smoothing Scatterplots, Journal of the American Statistical Association, Vol. 74, pp. 829-836.

Cleveland, W.S. and Devlin, S.J. (1988) "Locally Weighted Regression: An Approach to Regression Analysis by Local Fitting," Journal of the American Statistical Association, Vol. 83, pp. 596-610.

Cooper, H., and C. Jacob (1946), A generalized graphical method for evaluating formation constants and summarizing well-field history, Transaction American Geophys Union, 27(4), 526–534.

Copty, N. K., Trinchero P., Sanches-Vila, X. (2011). Inferring spatial distribution of radially integrated transmissivity from pumping tests in heterogeneous confined aquifers, Water Resour. Res., 47, doi: 10.1029/2010WR009877.

Copty, N., P. Trinchero, X. Sanchez-Vila, M. S. Sarioglu, and A. Findikakis (2008), Influence of heterogeneity on the interpretation of pumping test data in leaky aquifers, Water Resour. Res., 44, doi: 10.1029/2008WR007120.

Copty, N. K., M. S. Sarioglu, and A. N. Findikakis (2006), Equivalent transmissivity of heterogeneous leaky aquifers for steady state radial flow, Water Resources Research, 42(4),W04,416.

D.N.H. Beach, J.E. McCray, K.S. Lowe, R.L. Siegrist, 2005. Temporal changes in hydraulic conductivity of sand porous media biofilters during wastewater infiltration due to biomat formation. Journal of Hydrology 311:230-243.

Dagan G Flow and Transport in Porous Formations, New York: Springer, 1989.

Dagan, G. 1976. Stochastic conceptual analysis of one-dimensional groundwater flow in non-uniform homogeneous media. Water Resources Research 12, no. 3: 567 - 567.

Darcy, H.P.G (1856). Les fontaines Publiques de la Ville de Dijon. Paris: Victor Dalmont.

Dawson KJ, Istok JD (1991) Aquifer testing. Lewis, Boca Rataon, FL.

Delhomme, J.P. 1979. Spatial variability and uncertainty in groundwater flow parameters. Water Resources Research 15, no. 2: 281 - 290.

Electric Analog Model Study of Aquifer in Krishni-Hindon Interstream Region, U.P., India C. P. Gupta, M. Thangarajan, V.V.S. Gurunadha Rao Article first published online: 6 JUL 2006 DOI: 10.1111/j.1745-6584.1979.tb03322.

Farrel, D. A., A. D. Woodbury, E. A. Sudicky, and M. O. Rivett (1994), Stochastic and deterministic analysis of dispersion in unsteady flow at the Borden Tracer-Test site, Ontario, Canada, J. of Contaminant Hydrology, 15, 159-185.

Freeze, R.A. (1977), A stochastic-conceptual analysis of one dimensional groundwater flow in non uniform homogeneous media .Water Resources Research 13, no. 2: 480.

Freeze, R. A. (1975), A stochastic conceptual analysis of one dimensional groundwater flow in non – uniform homogeneous media. Water Resources Research, 11(5), 725 – 741.

G.P. Kruseman and N. A.de Ridder: Analysis and Evaluation of Pumping Test Data (second edition, completely revised, 1994).

Gelhar, L.W., A.A. Bakr, A.L. Gutjahr, and J.R. MacMillan (1977), Stochastic-conceptual analysis of 1-dimensional groundwater flow in non-uniform homogeneous media. Water Resources Research 13, no. 2: 477 - 479.

Gilham, R. W., Klute, A., Herman, D. F. (1976), Hydraulic properties of a porous medium. Measurements and empirical representations. Soil Science Society of America Journal, 40.

Hantush, M., and C. Jacob (1955), Non-steady radial flow in an infinite leaky aquifer, Trans., Am. Geophys. Union, 36(1), 95–100.

Hantush, M. (1956), Analysis of data from pumping tests in leaky aquifers, Trans Am Geo-phys Union, 37(6), 702–14.

Harbaugh, A., E. Banta, M. Hill, and M. McDonald (2000), Modflow-2000: The US Geological Survey modular ground-water model—user guide to modularization concepts and the ground-water flow process. USGS Open-File Report 00-92. Reston, Virginia: USGS.

Horne, R. (1995), Modern Well Test Analysis: A Computer-aided Approach, 257 pp., 2nd edn. Petroway, Inc., Palo Alto.

Hunter, J. S. (1986), "The Exponential Weighted Moving Average," Journal of Quality Technology, 18, 203–210.

Illman, W. A.; Zhu, J.; Craig, A.; Yin, D (2008), Can a Groundwater Flow Model BE Validated? Encouraging, Positive Evidence from Laboratory Hydraulic Tomography Experiments. American Geophysical Union, Fall Meeting 2008.

Illman, W. A., and S. P. Neuman (2001), Type-curve interpretation of a cross-hole pneumatic test in unsaturated fractured tuff, Water Resources. Research*., 37*(3), 583- 604, doi: 10.1029/2000WR900273.

J.E. McCray, S.L. Kirkland, R.L. Siegrist, G.D. Thyne (2005), Model parameters for simulating fate and transport of onsite-wastewater nutrients. Groundwater 43(4):628-639.

JLW MS thesis (1972): Collins, Gelhar & Wilson, Hele-Shaw model of Long Island aquifer system, J. Hydrau. Div., ASCE, 98(9), 1701-1714.

Journal Bulletin of National Pingtung University of Science and Technology (2000) Vol. 9 No. 2 pp. 133-142.

Kazemi, H. (1969), Pressure transient analysis of naturally fractured reservoirs with uniform fracture distribution, Trans. Soc. Pet. Eng. AIME.

Kernodle, J.M., McAda, D.P., and Thorn, C.R. (1995), Simulation of ground-water flow in the Albuquerque Basin, central New Mexico, 1901-1994, with projections to 2020: U.S. Geological Survey Water-Resources Investigations Report 94-4251, p. 114.

Kernodle, J.M., Miller, R. S., and Scott, W.B. (1987), Three-dimensional model simulation of transient ground-water flow in the Albuquerque-Belen Basin, New Mexico: U.S. Geological Survey Water-Resources Investigations Report 86-4194, 86 p.

Kernodle, J.M., and Scott, W.B., (1986), Three-dimensional model simulation of steady-state ground-water flow in the Albuquerque-Belen Basin, New Mexico: U.S. Geological Survey Water-Resources Investigations Report 84-4353, 58 p.

Konikow, L.F., and Reilly, T.E. (1999), Seawater intrusion in the United States. In: Bear J, Cheng AHD, Sorek S, Ouazar D, Herrera I (eds) Seawater intrusion in coastal aquifers—concepts, methods and practices. Kluwer Academic Publishers, pp 463–506.

Lunati, I., and P. Jenny (2006), Multiscale finite-volume method for compressible multiphase flow in porous media. Journal of Computational Physics 216, no. 2: 616-636.

Mantoglou, A., and J. l. Wilson (1982), The turning bands method for simulation of random-fields using line generation by a spectral method, Water Resources. Research., 18(5), 1379–1394.

McAda, D.P., and Barroll, Peggy (2002) Simulation of ground-water flow in the Middle Rio Grande Basin between Cochiti and San Acacia, New Mexico: U.S. Geological Survey Water-Resources Investigations Report 02-4200.

McDonald, M.G., and Harbaugh, A.W. (1988), A modular three-dimensional finite-difference ground-water flow model: Techniques of Water-Resources Investigations of the United States Geological Survey, book 6, chap. A1, 586 p.

Meier, P. M., J. Carrera, and X. Sanchez-Vila (1998), An evaluation of Jacob's method for the interpretation of pumping tests in heterogeneous formations, Water Resources Research, 34(5), 1011–1025.

Meinzer, O. E. (1932), Outline of Methods for estimating ground – water supplies. Water Supply Paper 638c, U.S. Geological Survey.

Mualem Y. (1976), A new model for predicting the hydraulic conductivity of unsaturated porous media. Water Resources Research, 12, 513 – 522.

Ogilvy, A. A., Ayed, M. A. and Bogolovsky, V. A. (1969), Geophysical Studies Of Water Leakages From Reservoirs. Geophysical Prospecting, 17: 36–62.

P.J. Green and B.W. Silverman (1994), Nonparametric Regression and Generalized Linear Models. London: Chapman & Hall

Pumping test data report, (2008), Silicon Valley Rapid Transit Project-Central Area Guide Way. June 3, 2008; HMM/Bechtel.

R.L. Siegrist, J.E. McCray, K.S. Lowe (2004), Wastewater infiltration into soil and the effects of infiltrative surface architecture. Small Flows Journal 5(1):29-39.

Renard, P. Glenz, D. M, Mejias (2009), Understanding diagnostic plots for well-test interpretation, Hydrogeology Journal, volume: 17, Issue: 3, Publisher: Springer, Pages: 589-600.

Renard P. (2007) Stochastic Hydrogeology: What Professionals Really Need? Vol. 45, No.5 GROUNDWATER September - October 2007 (pages 531 - 541).

Sagar, B. (1978), Analysis of dynamic aquifers with stochastic forcing function. Water Resources Research 14, no. 2: 207 - 216.

Sanchez-Vila, X., A. Guadagnini, and J. Carrera (2006), Representative hydraulic conductivities in saturated groundwater flow. Review s of Geophysics 44, no. 3: Art. No.RG3002.

Sanchez-Vila, X., P. M. Meier, and J. Carrera (1999), Pumping tests in heterogeneous aquifers: An analytical study of what can be obtained from their interpretation using Jacob's method, Water Resources Research, 35(4), 943–952.

Sanford, W. E., Plummer, L. N., McAda, D. P., Bexfield, L. M., and Anderholm, S. K. (2001), Estimation of hydrologic parameters for the ground-water model of the Middle Rio Grande Basin Using carbon-14 and water-level data, in Cole, J. C., ed., U.S. Geological Survey Middle Rio Grande Basin Study-Proceedings of the Fourth Annual Workshop, Albuquerque, New Mexico, February 15-16, 2000: U.S. Geological Survey Open-File Report 00-488, p. 4-6.

Sudicky, E. A., W. A. Illman, I. K. Goltz, J. J. Adams, and R. G. McLaren (2010), Heterogeneity in hydraulic conductivity and its role on the macro scale transport of a solute plume: From measurements to a practical application of stochastic flow and transport theory, Water Resour. Res., 46, W01508, doi: 10.1029/2008WR007558.

Sudicky, E. A. (1986) A natural gradient experiment on solute transport in a sand aquifer: Spatial variability of hydraulic conductivity and its role in the dispersion process, Water Resour. Res., 22(13), 2069-2082.

Temples, T.J., and Waddell, M.G. (1996), Application of petroleum geophysical well logging and sampling techniques for evaluating aquifer characteristics. Ground Water, 34(3), 523-531.

Theis, C.V. (1935). The relation between the lowering of the piezometric surface and the rate and duration of discharge of a well using groundwater storage. Transactions of the American Geophysical Union, 2, 519-524.

Theis, C.V. (1967), Aquifers and Models. In Proceedings of the Symposium on Groundwater Hydrology, ed. M. A. Marino. Minneapolis: American Water Resources Associations, p. 138.

Toll NJ, Rasmussen TC (2007) Removal of barometric pressure effects and earth tides from observed water levels. Ground Water 45:101-105.

Trinchero (2009), Characterization of spatial heterogeneity in groundwater applications. PhD Thesis Department of Geotechnical Engineering and Geo-Sciences (ETCG) Technical University of Catalonia, UPC.

Trinchero et al. (2008), A New Method for the Interpretation of Pumping Tests in Leaky Aquifers. GROUND WATER 46, no. 1: 133–143.

Veneruso AF, Spath J (2006), A digital pressure derivative technique for pressure transient well testing and reservoir characterization. Paper presented at the 2006 SPE Annual Technical Conference and Exhibition, San Antonio, TX, 24-27 September 2006.

Walton, W. (1962), Selected analytical methods for well and aquifer evaluation, in Illinois State Water Survey.

Warren, J. E., Root, P.J (1963), The behavior of naturally fractured reservoirs, Society of Petroleum Engineers Journal, Trans., AIME.

Winter, C.L. (2004), stochastic hydrology: Practical alternatives exist. Stochastic Environmental Research and Risk Assessment 14, no. 8: 271 - 273.

YiLung, Y., TingChien, C., YuMin, W. (2007), Hydraulic conductivity identification of groundwater sandbox model.

APPENDIX A: SECOND DERIVATIVES OF SYNTHETIC HETEROGENEOUS DATA

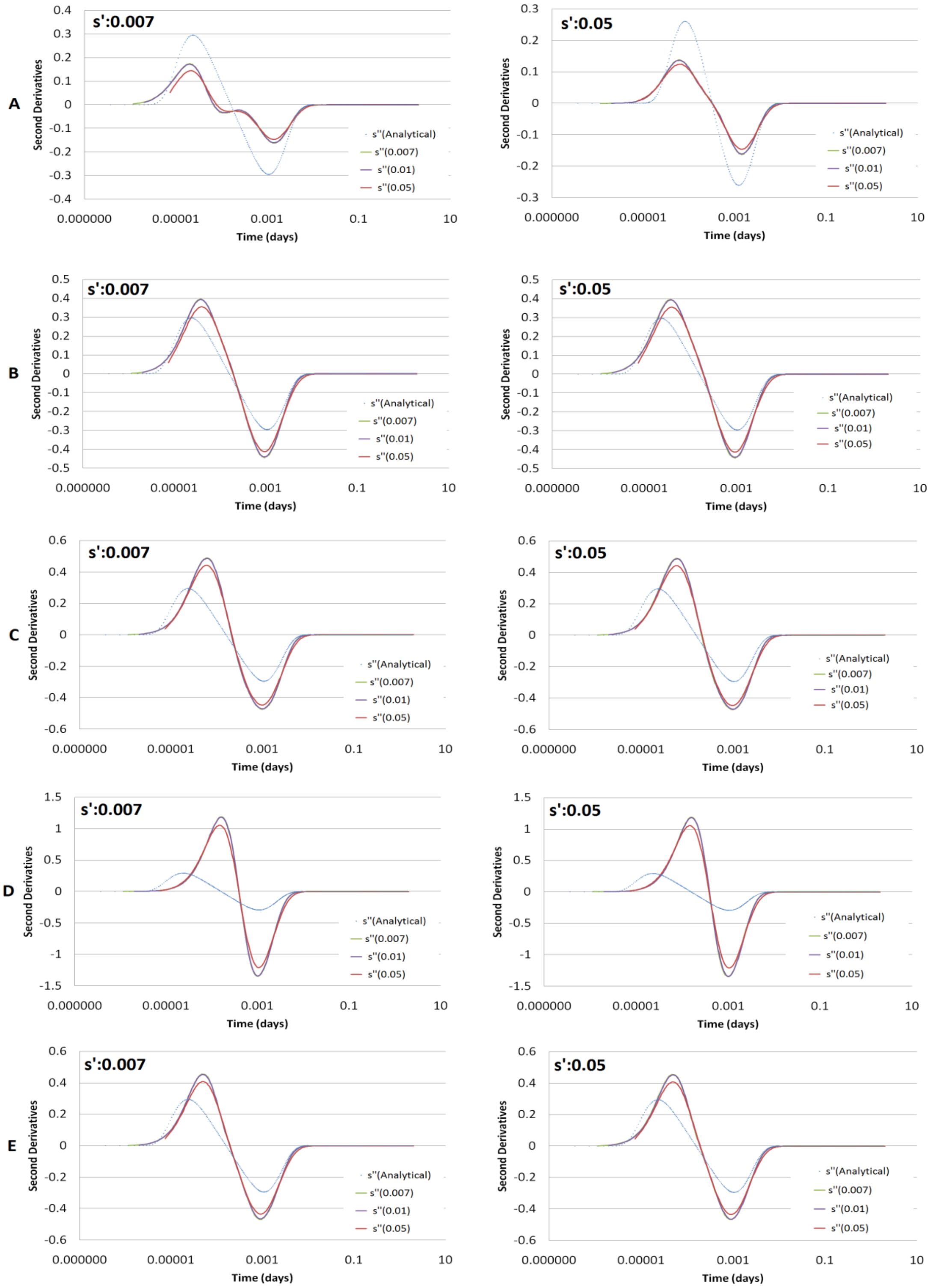

Figure A. 1. Second derivatives of synthetic pumping test data for each realization for 1m radius

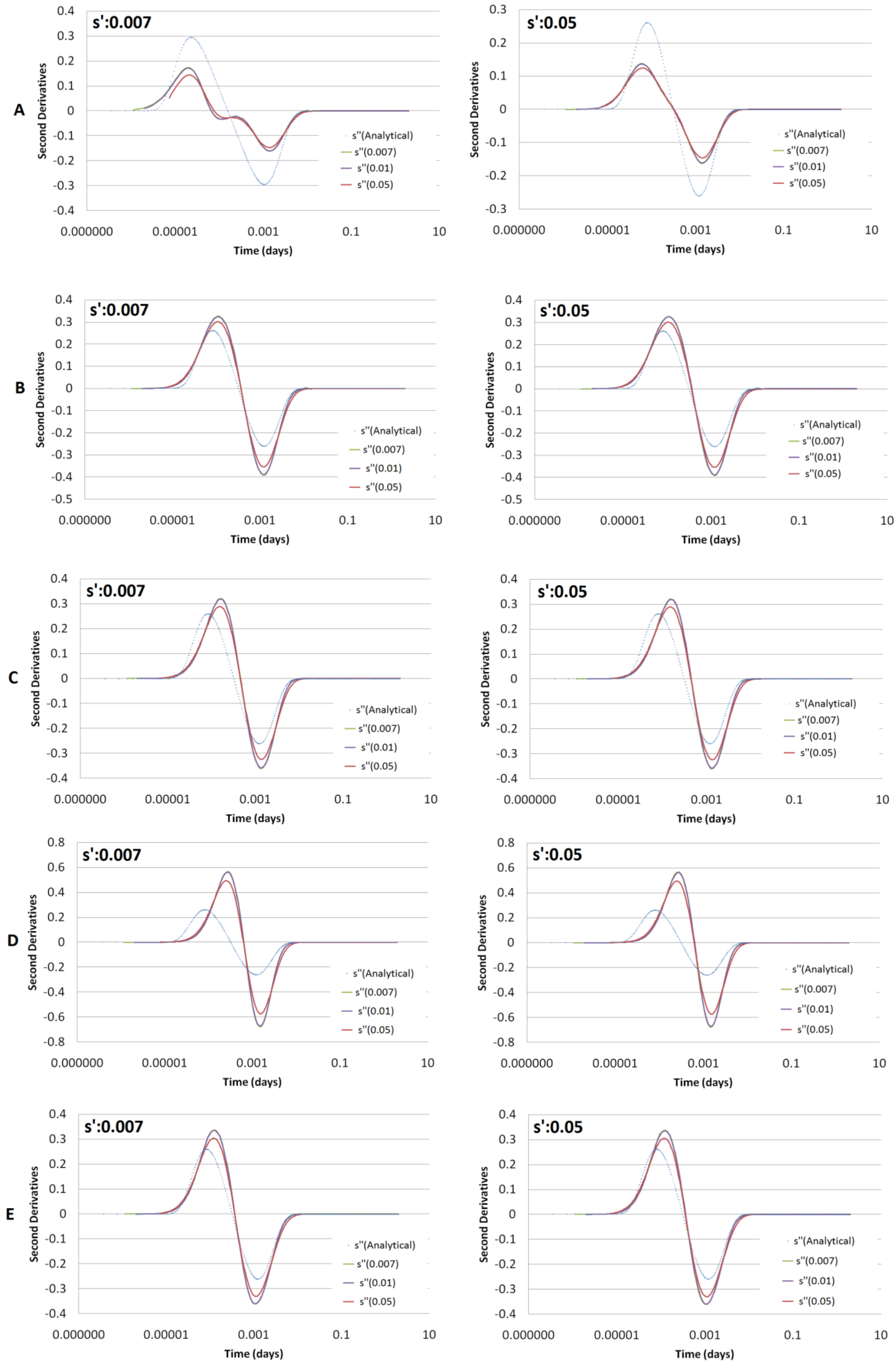
A
B
C
D
E
s':0.007
s':0.05
Second Derivatives
Time (days)
0.000000
0.00001
0.001
0.1
10
s''(Analytical)
s''(0.007)
s''(0.01)
s''(0.05)

m

radius

APPENDIX B: CD-CONFINED METHOD ESTIMATIONS FOR SYNTHETIC HETEROGENEOUS DATA

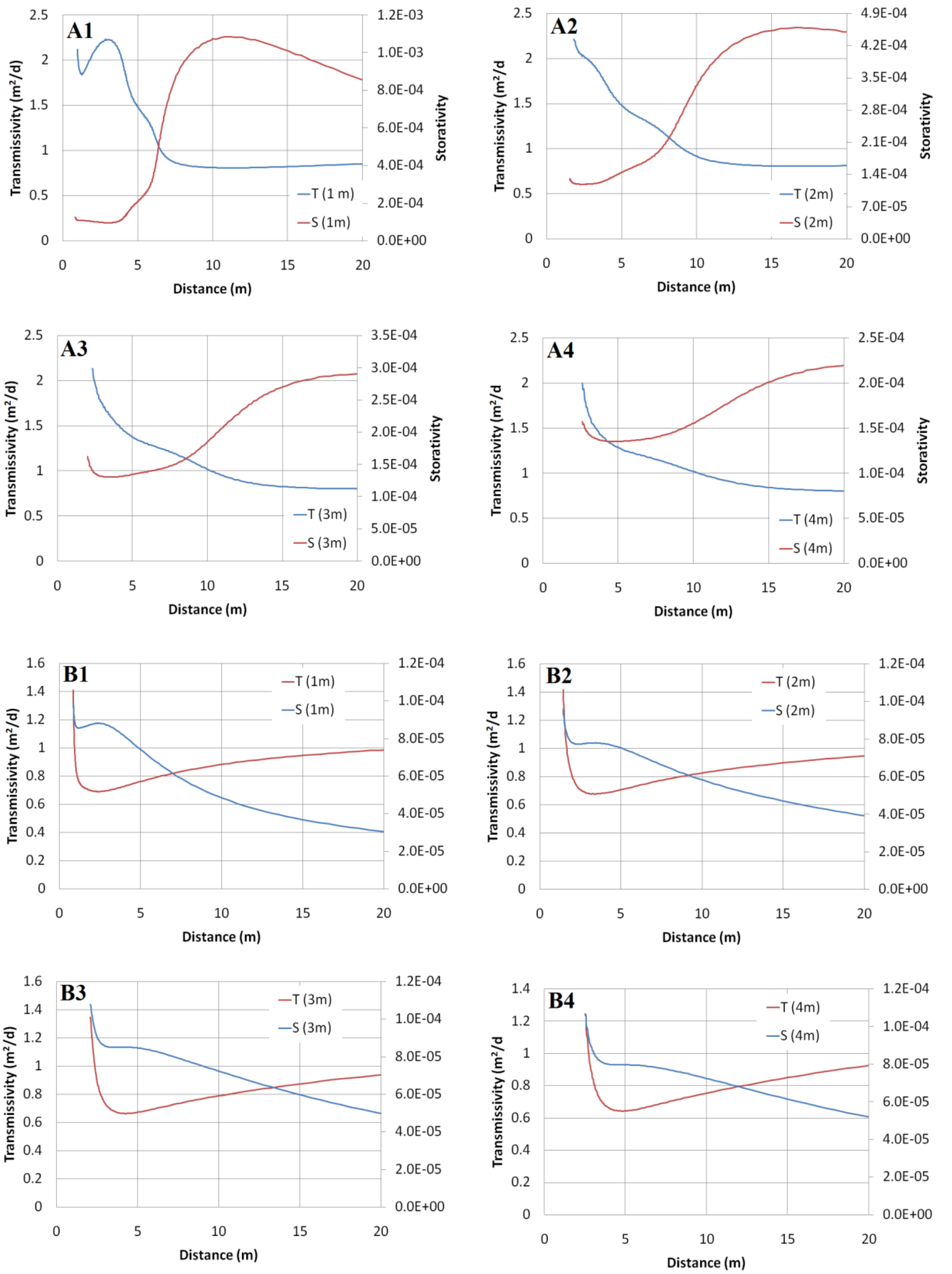

Figure B. 1. Estimations of CD-confined method from synthetic data for realizations A and B

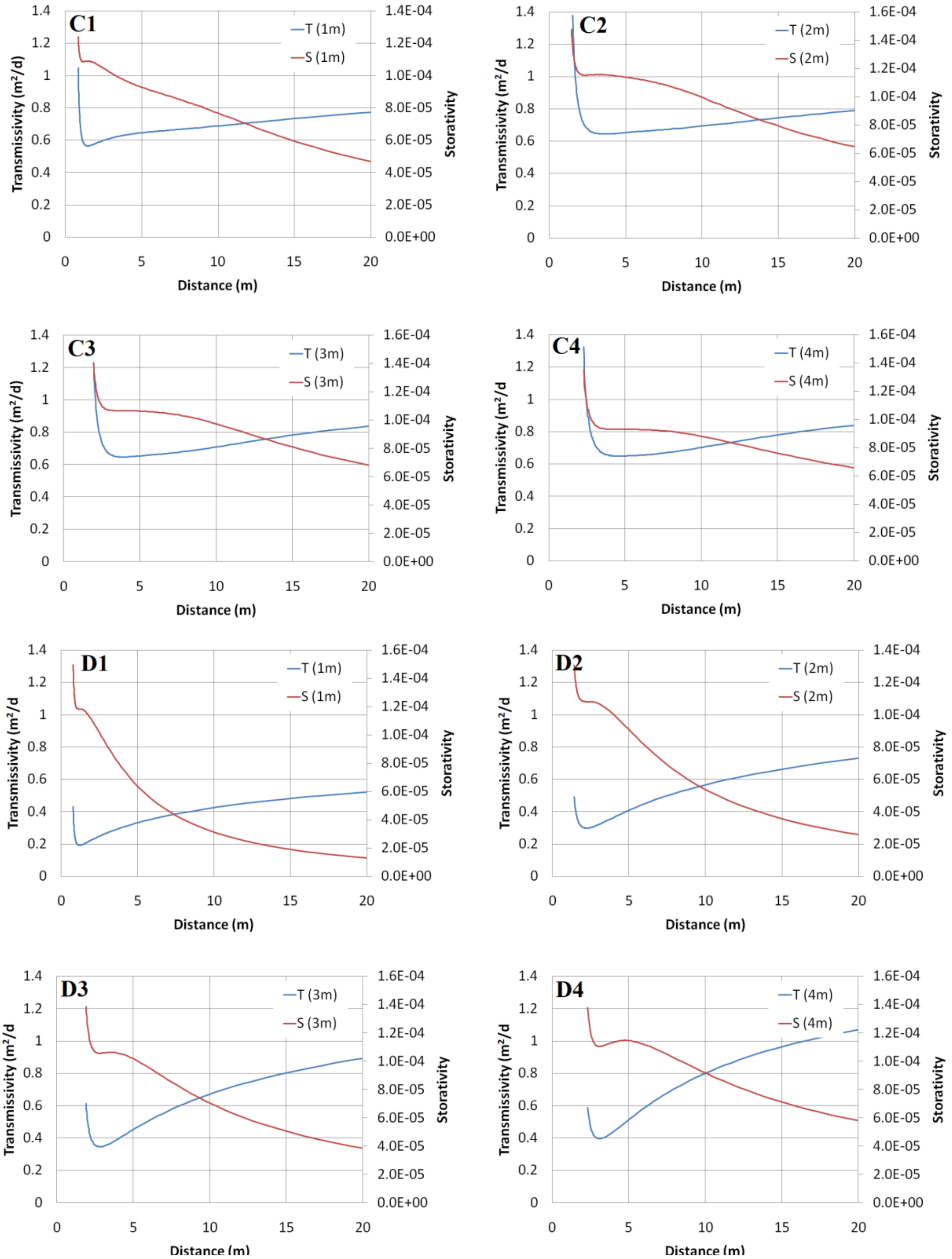

Figure B. 2. Estimations of CD-confined method from synthetic data for realizations C and D

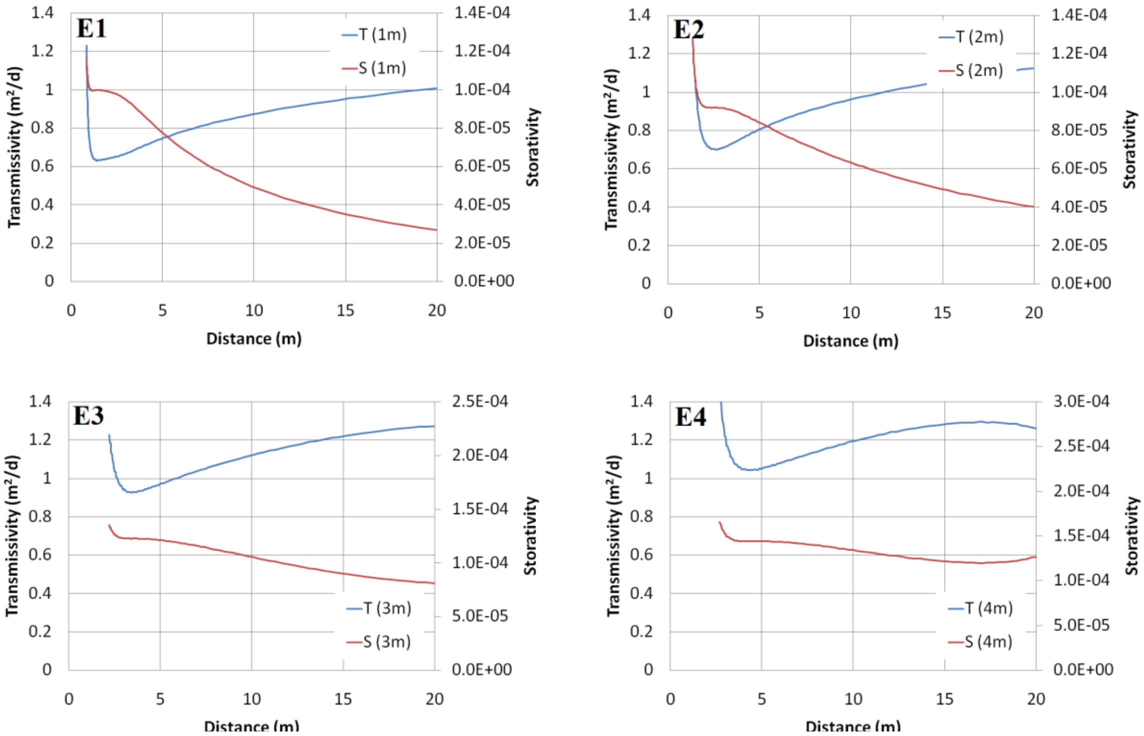

Figure B. 3. Estimations of CD-confined method from synthetic data for realization E

APPENDIX C: CD-CONFINED METHOD ESTIMATIONS FOR FIELD DATA

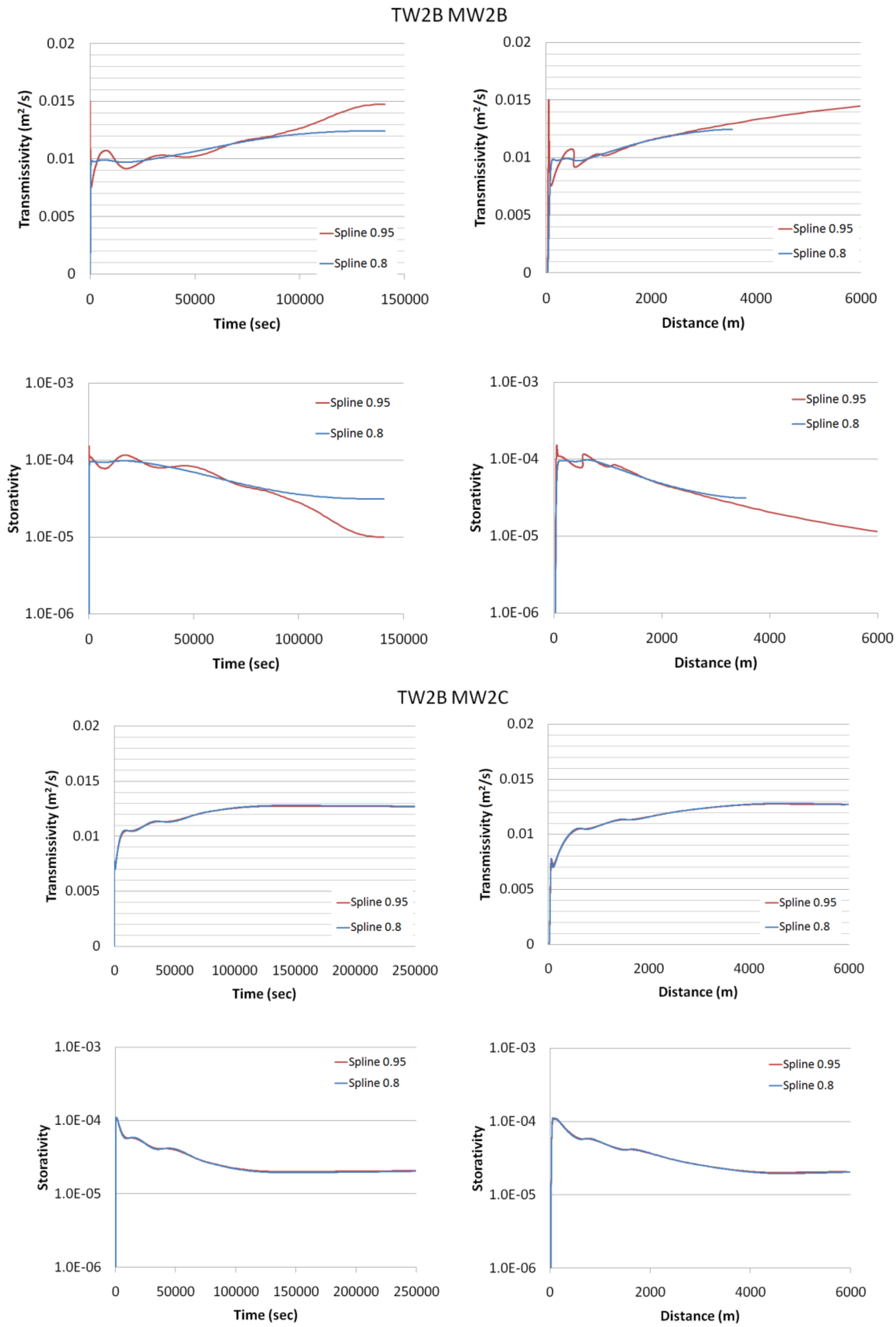

Figure C. 1. Estimations of CD-confined method from real data for MW2B and MW2C

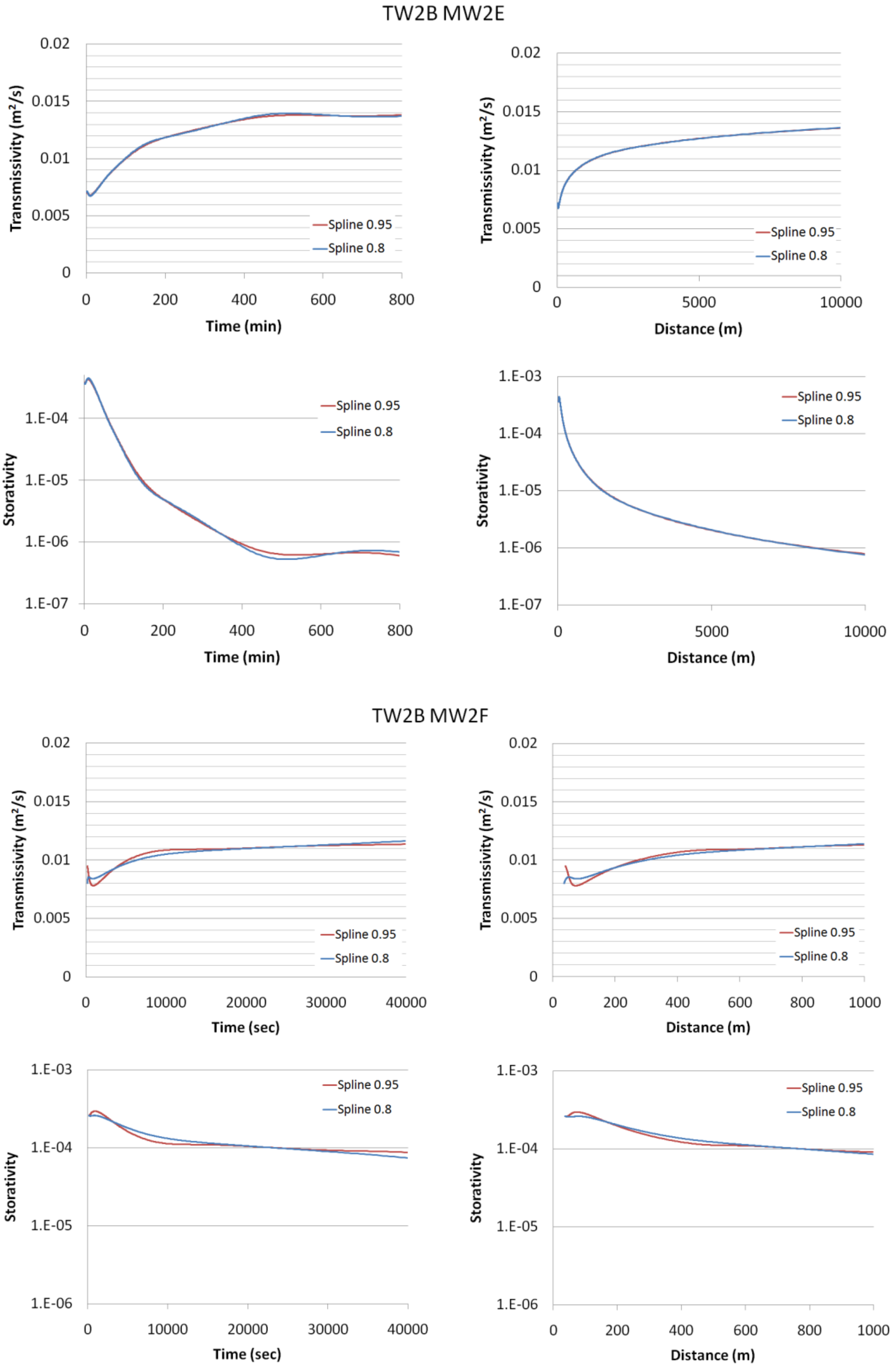

Figure C. 2. Estimations of CD-confined method from real data for MW2E and MW2F

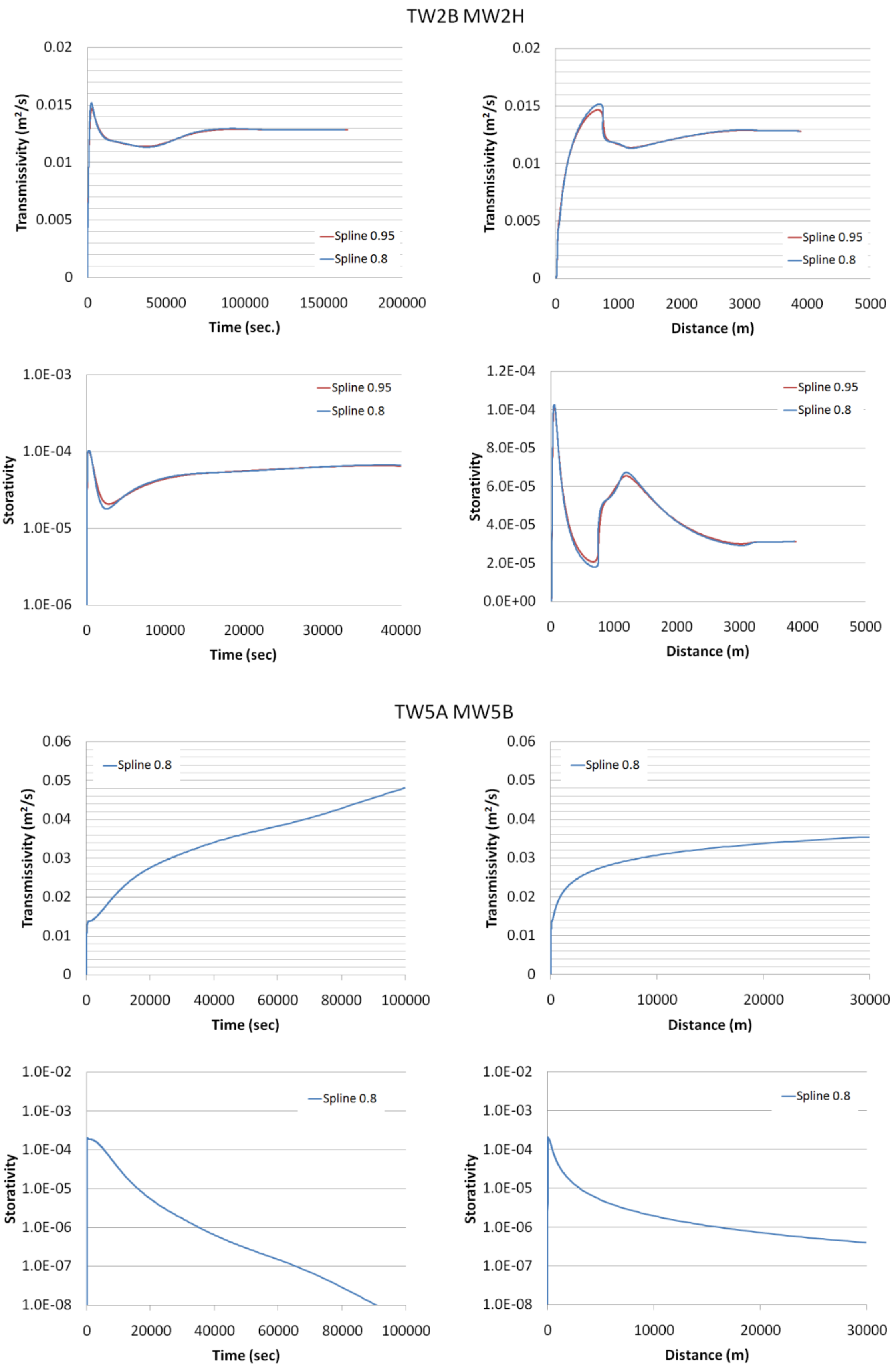

Figure C. 3. Estimations of CD-confined method from real data for MW2H and MW5B

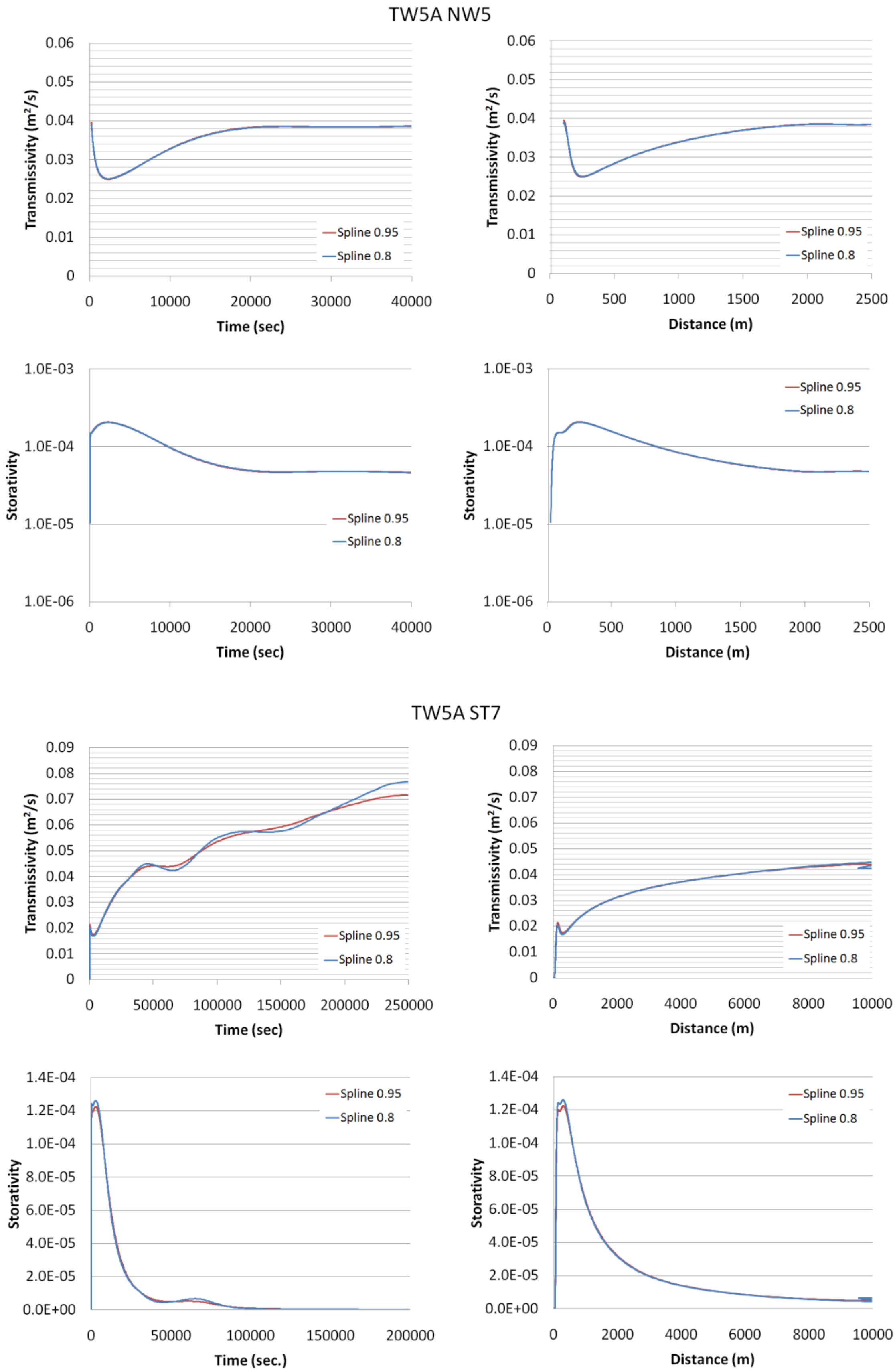

Figure C. 4. Estimations of CD-confined method from real data for NW5 and ST7

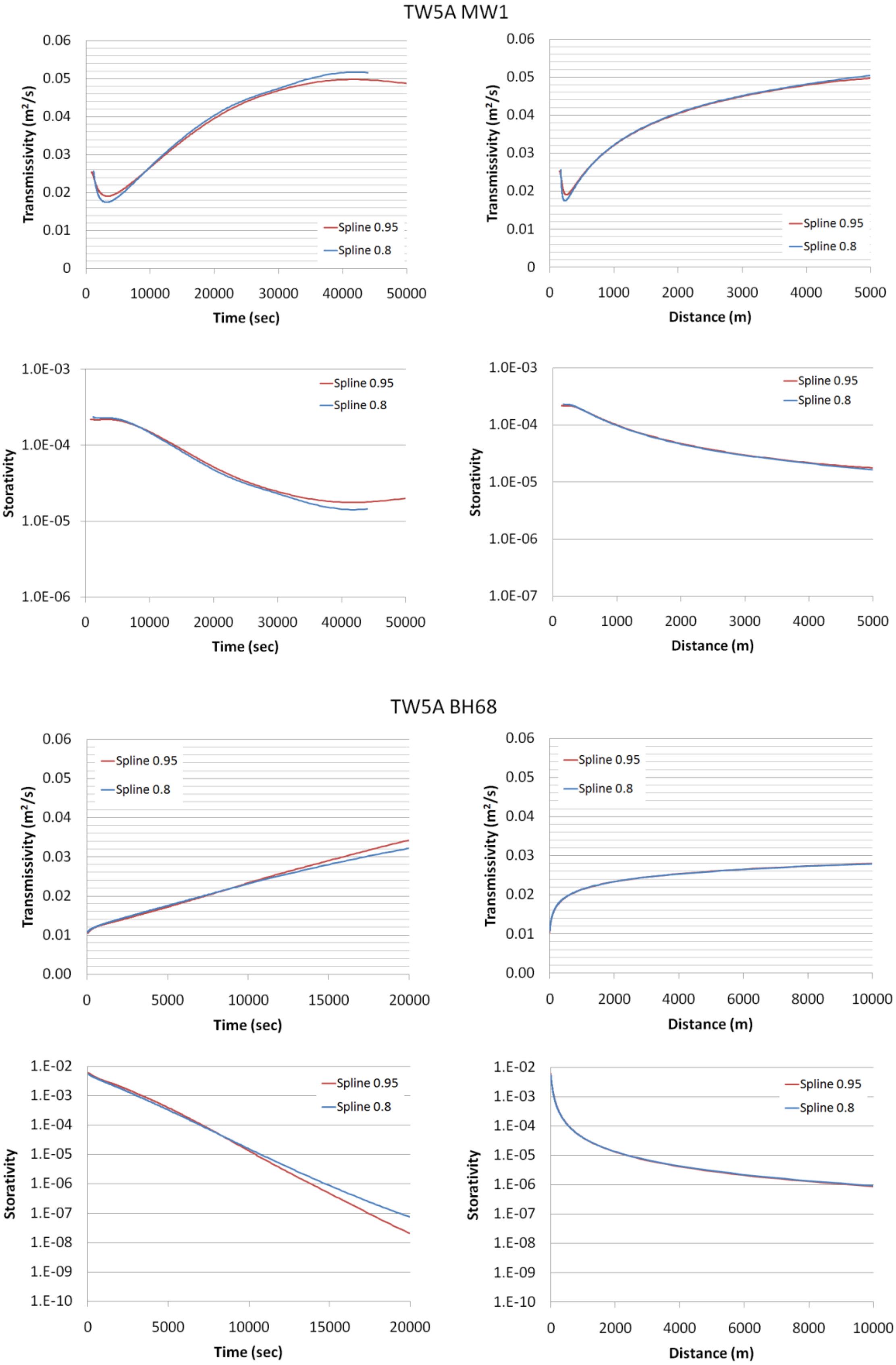

Figure C. 5. Estimations of CD-confined method from real data for MW1 and BH68

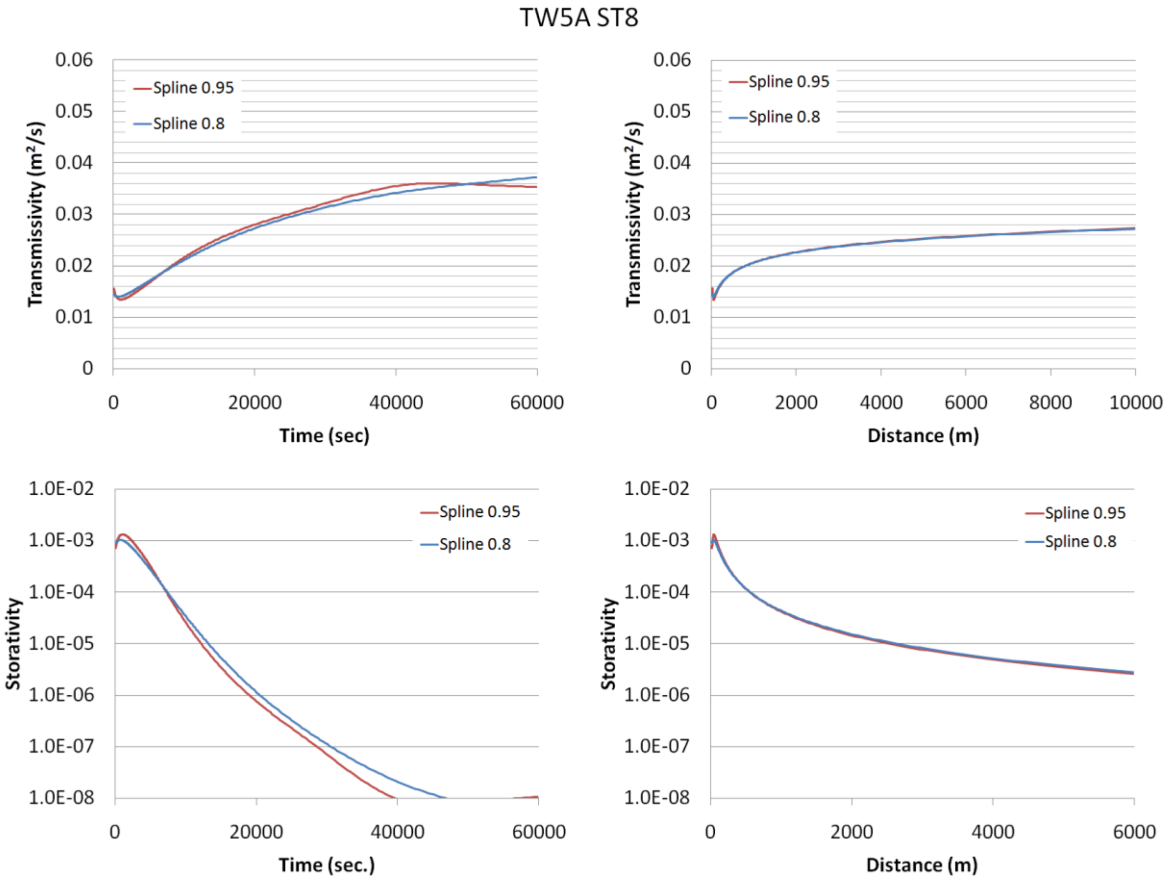

Figure C. 6. Estimations of CD-confined method from real data for ST8

APPENDIX D: PROGRAM FOR SIMULATED DATA READING

```
c    post1.for
c    reads the output head file of MODFLOW-2000 and writes the head
c    as a function of time at selected observation points.
c    The output is written to file: xxx.obs
c    ***********************************************************
      implicit double precision (a-h,o-z)
      Parameter (nstep0=300, nx0=481, ny0=481)
      dimension h(nx0,ny0)
      open(4,file='xxx.hds',status='old')
      open(5,file='xxx.obs',status='unknown')
c    read the head data
      do 20 n=1,nstep0
      read(4,*) ndummy
      do 30 i=1,nx0
      read(4,*) (h(i,j),j=1,ny0)
30    continue
c    write at well, then every cell for 4I, every 2 cells for 4I and every 4 cells for 8I
c    Therefore, farthest point is 16I: 128 m from well
c    observation points are along SOUTH direction
      write(5,1)ndummy,h(241,241),
     &h(241,240),h(241,239),h(241,238),h(241,237),
     &h(241,236),h(241,235),h(241,234),h(241,233),
     &h(241,232),h(241,231),h(241,230),h(241,229),
     &h(241,228),h(241,227),h(241,226),h(241,225),
     &h(241,224),h(241,223),h(241,222),h(241,221),
     &h(241,220),h(241,219),h(241,218),h(241,217),
     &h(241,216),h(241,215),h(241,214),h(241,213),
     &h(241,212),h(241,211),h(241,210),h(241,209),

     &h(241,207),h(241,205),h(241,203),h(241,201),
     &h(241,199),h(241,197),h(241,195),h(241,193),
     &h(241,191),h(241,189),h(241,187),h(241,185),
     &h(241,183),h(241,181),h(241,179),h(241,177),

     &h(241,173),h(241,169),h(241,165),h(241,161),
     &h(241,157),h(241,153),h(241,149),h(241,145),
     &h(241,141),h(241,137),h(241,133),h(241,129),
     &h(241,125),h(241,121),h(241,117),h(241,113)
c    write at well, and 1, 4, 8, 12, 16, 32, 48, 64 cells away (including the diagonals)
c    observation points start at NORTH and rotate clockwise
c     write(5,1)ndummy,h(241,241),
c    &h(241,242),h(242,242),h(242,241),h(242,240),h(241,240),h(240,240),
c    & h(240,241),h(240,242),
c    &h(241,245),h(245,245),h(245,241),h(245,237),h(241,237),h(237,237),
c    & h(237,241),h(237,245),
c    &h(241,249),h(249,249),h(249,241),h(249,233),h(241,233),h(233,233),
```

```
c     & h(233,241),h(233,249),
c     &h(241,253),h(253,253),h(253,241),h(253,229),h(241,229),h(229,229),
c     & h(229,241),h(229,253),
c     &h(241,257),h(257,257),h(257,241),h(257,225),h(241,225),h(225,225),
c     & h(225,241),h(225,257),
c     &h(241,273),h(273,273),h(273,241),h(273,209),h(241,209),h(209,209),
c     & h(209,241),h(209,273),
c     &h(241,289),h(289,289),h(289,241),h(289,193),h(241,193),h(193,193),
c     & h(193,241),h(193,289),
c     &h(241,305),h(305,305),h(305,241),h(305,177),h(241,177),h(177,177),
c     & h(177,241),h(177,305)
c      write(5,1) ndummy, h(241,225),h(241,229),h(241,233),
c     &          h(241,237),h(241,241)
1     format(i5,65f12.7)
20    continue
      stop
      end
```

APPENDIX E: PROGRAM FOR THE APPLICATION OF CONVENTIONAL AND DIP METHOD ANALYSIS TO THE SYNTHETIC DATA

```
c    Calculates:
c    i)   effective leakance vL_eff, transmissivity T_eff, and storativity S_eff
c         of a leaky confined aquifer using the
c           a) Cooper-Jacob for non-leaky aquifers (ileak=0)
c           b) Hantush (1956) inflection point method (ileak=1)
c           c) Walton (1962) Type curve method (ileak=2)
c          and for steady state flow, effective transmissivity using
c           d) The Double Inflection Point Method (DIPM)  (ileak=4)
c    ii)  calculates the cummulative distribution function (CDF) for each of the effective
parameters
c    iii) calculates the probability density function (pdf) for each of the effective parameters
c ******************************
          implicit double precision (a-g,o-z)
     parameter(nreal=5,ngroup=1,nobs=5,nsim=nreal*ngroup,nstep=300
    &  ,xmin1=0.,xmax1=1.,xmin2=0.,xmax2=10.
    &  ,xmin3=0.,xmax3=0.001,xmin4=0.,xmax4=100.,nbin=50,q=2.,h0=20.
    &  ,ileak=4)
c   ileak=0  infinity leakance (NO seepage through confining layer)
c   ileak=1  transient with finite leakance (Hantush 1956 inflection point method)
c   ileak=2  trasient with finite leakaknce (Walton, 1962 Type curve method)
c
c   ileak=4  transient with finite leakance based on the Double Inflection Point Method
c
     dimension h(nobs,nstep),s(nobs,nstep),radius(nobs)
     dimension time(nstep),tao(nstep)
     dimension vL_eff(nsim,nobs),T_eff(nsim,nobs),S_eff(nsim,nobs),
    &        vKB_eff(nsim,nobs)
     dimension vKB_true(ngroup)

c  parameters needed for the inflection point method (ileak=1)
     dimension s_p(nobs),tao_p(nobs),t_p(nobs),delta_sp(nobs)

c  parameters needed for the curve fitting approach (ileak=2)
     dimension u(11*90),RoverL(194),wellfunc(11*90,194)
     dimension trans(100),stor(100),utest(nstep),stest(nstep)

c  parameters needed for the double inflection point method (ileak=4)
          dimension dsdt(nobs,nstep),ds2dt2(nobs,nstep),ds3dt3(nobs,nstep),
    &        tao1(nstep),tao2(nstep),tao3(nstep),
    &        t1(nobs),t2(nobs),t3(nobs)
          dimension dsdtmax1(nobs),dsdtmax2(nobs),dsdtmax3(nobs)

c  parameters needed CDF and pdf computations
```

```
      dimension xcum1(nsim,nobs),xcum2(nsim,nobs),xcum3(nsim,nobs),
     &         xcum4(nsim,nobs)
      dimension xpdf1(nbin*ngroup,nobs),xpdf2(nbin*ngroup,nobs),
     &         xpdf3(nbin,nobs),xpdf4(nbin,nobs)
      dimension bin1(nbin+1),bin2(nbin+1),bin3(nbin+1),bin4(nbin+1)
c   xmin1: lower limit of the vL_eff
c   xmax1: upper limit of the vL_eff
c   xmin2: lower limit of the T_eff
c   xmax2: upper limit of the T_eff
c   xmin3: lower limit of the S_eff
c   xmax3: upper limit of the S_eff
c   xmin4: lower limit of the vKB_eff
c   xmax4: upper limit of the vKB_eff

      character filein*10,  casenum*2, runnum(nreal)*8
c input/output file names:
      open(4,file='dummy',status='old')
      open(14,file='file.nam',status='old')
      open(5,file='time.txt',status='old')
      open(6,file='temp.out',status='unknown')
      open(7,file='parameters1.out',status='unknown')
      open(8,file='parameters2.out',status='unknown')
      open(9,file='parameters3.out',status='unknown')
      open(10,file='parameters4.out',status='unknown')
      open(12,file='t1.out',status='unknown')
      open(13,file='t2.out',status='unknown')
      open(18,file='t3.out',status='unknown')
      open(16,file='cdf.out',status='unknown')
      open(17,file='pdf.out',status='unknown')
      open(11,file='wellfunc.out',status='unknown')
      open(19,file='sss.out',status='unknown')

c     calculate the effective parameters usings
c     Cooper-Jacob Equation (ileak=0),
c     inflection Point method (ileak=1),
c     Walton Type method (ileak=2)
c     DIPM, Double ,nflection point method (ileak=4)
c if ileak=1 estimate the effective parameters using the inflection method
      if(ileak.eq.1)then
c     drawdown at the inflection point
      do 70 i=1,nobs
           s_p(i)=0.5*s(i,nstep)
      do 80 j=1,nstep
           if(s(i,j).le.s_p(i).and.s(i,j+1).gt.s_p(i))
     &then
c     calculate t_p (time at inflection point)
      slope=(tao(j+1)-tao(j))/(s(i,j+1)-s(i,j))
      tao_p(i)=tao(j)+slope*(s_p(i)-s(i,j))
      t_p(i)=10**(tao_p(i))
```

```
c     calculate drawdown rate: ds_p/dtao
      delta_sp(i)=(s(i,j+1)-s(i,j))/(tao(j+1)-tao(j))
      goto 81
      endif
80    continue
c     calculate L using Bessel function of the second kind of order 0
81    do 90 j1=-5,2
      do 95 j2=100,999
      w=2.3*s_p(i)/delta_sp(i)
      rL1=float(j2)/100.*10**(float(j1))
      rL2=float(j2+1)/100.*10**(float(j1))
      w1=exp(rL1)*dbsk0(rL1)
      w2=exp(rL2)*dbsk0(rL2)
          if(w.gt.w2.and.w.le.w1)then
      slope=(rL2-rL1)/(w2-w1)
      rL=rL1+slope*(w-w1)
      write(6,91) k1,k2,j1,j2,rL
91    format(4i5,f12.5)
          goto 99
      endif
95    continue
90    continue
c     write a warning statement that j1/j2 are not sufficient for
c     estimation of r/L (by trial and error
          write(6,92)k1,k2,i,rL
92    format('WARNING j1/j2 range insufficient for calculation of r/L',
     &   3i5,f12.5)
99    vL_eff((k1-1)*nreal+k2,i)=radius(i)/rL
c     calculate transmissvity
      T_eff((k1-1)*nreal+k2,i)= 2.3*q*exp(-rL)/4/3.14159/delta_sp(i)
c     calculate storativity
      S_eff((k1-1)*nreal+k2,i)= 2.*T_eff((k1-1)*nreal+k2,i)
          &*t_p(i)/(vL_eff((k1-1)*nreal+k2,i)*radius(i))
c     calculate Kv/B = aquitard vertical conductivity divided by aquitard thickness
          vKB_eff((k1-1)*nreal+k2,i)=T_eff((k1-1)*nreal+k2,i)
          &                     /vL_eff((k1-1)*nreal+k2,i)**2
70    continue
      endif

c     estimate the effective transmissivity, T_eff, and storativity
c     using the Cooper-Jacob method: T=2Q/4pi/Delta_S*log(t2/t1)          if(ileak.eq.0)then
c     with there is no leakance vKB=C=0.
          if(ileak.eq.0) then
      do 60 i=1,nobs
      T_eff((k1-1)*nreal+k2,i)=0.183*2.*log10(0.993636/0.878235)/
     &     (s(i,203)-s(i,200))
          S_eff((k1-1)*nreal+k2,i)=2.25*t_eff((k1-1)*nreal+k2,i)*0.993636
          &  /radius(i)**2*10.**(-t_eff((k1-1)*nreal+k2,i)*s(i,203)/0.183/2.)
          vKB_eff((k1-1)*nreal+k2,i)=0.
```

```
60    continue
          endif

c if ileak=2 estimate the effective parameters using the Walotn (1962) Type Curve method
c calculacte the Walton Family of type curves
          if(ileak.eq.2) then
          write(*,*)k1,k2
c     calculate the leaky well function (once only)
      if(k1.eq.1.and.k2.eq.1)then
          call walton(u,wellfunc,RoverL)
      do 310 kw=1,194
          do 320 iw=1,11
          do 330 jw=1,90
          write(11,301) iw,jw,kw,RoverL(kw),u(jw+(iw-1)*90),
     /          wellfunc(jw+(iw-1)*90,kw)
301   format(3i5,3d13.6)
330   continue
320   continue
310   continue
      endif

c     define range of transmissivity values: 0.1 to 10
c     define range of storativity values: 0.00001 to 0.001
          do 340 iw=1,100
          trans(iw)=0.1+float(iw-1)*0.1
          stor(iw)=0.00001+float(iw-1)*0.00001
340   continue

      do 345 i=1,nobs
          diffmin=999999.
          do 350 iw=1,100
          do 360 jw=1,100
          do 370 kw=1,194
          diff=0.
          lwmin=1
          do 380 nt=nstep,1,-1
c     calculate u_test value and corresponding  s_test value
          utest(nt)=radius(i)**2*stor(jw)/4./time(nt)/trans(iw)
c     interpolate
          do 390 lw=lwmin,11*90-1
          if(utest(nt).ge.u(lw).and.utest(nt).lt.u(lw+1))then
          stest(nt)=wellfunc(lw,kw)+(wellfunc(lw+1,kw)-wellfunc(lw,kw))*
     &(utest(nt)-u(lw))/(u(lw+1)-u(lw))
      stest(nt)=stest(nt)*q/4./3.14159/trans(iw)
          lwmin=lw
c     calculate the sum of squared differences
      diff=diff+(stest(nt)-s(i,nt))**2
c     if diff is already greater than diffmin, go to next test value
          if(diff.gt.diffmin)then
```

```
          goto 370
          else
          goto 380
          endif
          endif
390   continue
c     write WARNING statement if utest(nt) is greater than u range
      write(6,302) k1,k2,nt,iw,jw,kw,radius(i),utest(nt)
302   format('WARNING u range insufficient',6i5,2d12.5)
380   continue
c     find minimum difference
          diffmin=diff
          iwmin=iw
          jwmin=jw
          kwmin=kw
      write(6,371)iw,jw,kw,RoverL(kw),u(jw+(iw-1)*90),diff,diffmin
371   format(3i5,4d12.5)
370   continue
360   continue
350   continue
c     copy solution to effective parameters arrays
      vL_eff((k1-1)*nreal+k2,i)=radius(i)/RoverL(kwmin)
       T_eff((k1-1)*nreal+k2,i)=trans(iwmin)
      vKB_eff((k1-1)*nreal+k2,i)=T_eff((k1-1)*nreal+k2,i)
          &                  /vL_eff((k1-1)*nreal+k2,i)**2
       S_eff((k1-1)*nreal+k2,i)=stor(jwmin)
345   continue
          endif
c     calculate the effective parameters using the Double Inflection point method
          if(ileak.eq.4) then
      do 150 i=1,nobs
          dsdtmax1(i)=0.
          dsdtmax2(i)=0.
          dsdtmax3(i)=0.
          do 160 j=1,nstep-1
c         calculate the first derivative of the drawdown
          dsdt(i,j)=(s(i,j+1)-s(i,j))/(tao(j+1)-tao(j))
          tao1(j)=(tao(j+1)+tao(j))/2.
c     find maximum value of first derivative of the drawdown
      if(dsdt(i,j).ge.dsdtmax1(i))then
          dsdtmax1(i)=dsdt(i,j)
          t1(i)=10**(tao1(j))
          endif
160   continue
      do 165 j=1,nstep-5
c         calculate the second derivative of the drawdown
          ds2dt2(i,j)=(dsdt(i,j+4)-dsdt(i,j))/(tao1(j+4)-tao1(j))
          tao2(j)=(tao1(j+4)+tao1(j))/2.
c     find maximum (positive) value of second derivative of the drawdown
```

```
      if(ds2dt2(i,j).ge.dsdtmax2(i))then
         dsdtmax2(i)=ds2dt2(i,j)
         jpos=j
         t2(i)=10**(tao2(j))
         endif
c     find maximum (negative) value of second derivative of the drawdown
c        write(7,*)i,j,ds2dt2(i,j),ds3dt3(i,j)
      if(-ds2dt2(i,j).ge.dsdtmax3(i))then
         dsdtmax3(i)=-ds2dt2(i,j)
         jneg=j
         t3(i)=10**(tao2(j))
         endif
165   continue
      do 166 j=1,nstep-9
c        calculate the third derivative of the drawdown
         ds3dt3(i,j)=(ds2dt2(i,j+4)-ds2dt2(i,j))/(tao2(j+4)-tao2(j))
         tao3(j)=(tao2(j+4)+tao2(j))/2.
166   continue
         if(i.eq.29)write(6,*)k1,k2,i,log10(t2(i)),k1
c     refine calculation of t2
      do 167, j=jpos-4,jpos+4
         if(ds3dt3(i,j)*ds3dt3(i,j+1).le.0) then
         slope=(tao3(j+1)-tao3(j))/(ds3dt3(i,j+1)-ds3dt3(i,j))
c        t2(i)=10**(tao3(j)+slope*(0.-ds3dt3(i,j)))
         if(i.eq.29)write(6,*)k1,k2,i,log10(t2(i))
         endif
167   continue
c     refine calculation of t3
      do 168, j=jneg-3,jneg+3
         if(ds3dt3(i,j)*ds3dt3(i,j+1).le.0) then
         slope=(tao3(j+1)-tao3(j))/(ds3dt3(i,j+1)-ds3dt3(i,j))
         endif
168   continue

c     calculate the effective leakance
         rrr=t3(i)/t1(i)/2.
         write(*,*)i,t1(i),t2(i),t3(i)
         vL_eff((k1-1)*nreal+k2,i)=
         &    (rrr**2-0.25)**2/rrr/(rrr**2+0.25)*radius(i)
c     calculate the effective transmissivity
         T_eff((k1-1)*nreal+k2,i)=q/2./3.14159/s(i,220)*
         &   dbsk0(radius(i)/vL_eff((k1-1)*nreal+k2,i))
c     calculate the effective storativity
         S_eff((k1-1)*nreal+k2,i)=2.*t1(i)*T_eff((k1-1)*nreal+k2,i)/
     &   radius(i)*vL_eff((k1-1)*nreal+k2,i)
c     calculate the effective capacitance
         vKB_eff((k1-1)*nreal+k2,i)=T_eff((k1-1)*nreal+k2,i)/
     &   vL_eff((k1-1)*nreal+k2,i)**2
150   continue
```

```
      write(12,11)k1,k2,(t1(ii),ii=1,nobs)
      write(13,11)k1,k2,(t2(ii),ii=1,nobs)
      write(18,11)k1,k2,(t3(ii),ii=1,nobs)
      endif

      write(19,11)k1,k2,(s(ii,220),ii=1,nobs)
      write(7,11)k1,k2,(vL_eff((k1-1)*nreal+k2,i),i=1,nobs)
      write(8,11)k1,k2,(T_eff((k1-1)*nreal+k2,i),i=1,nobs)
      write(9,11)k1,k2,(S_eff((k1-1)*nreal+k2,i),i=1,nobs)
      write(10,11)k1,k2,(vKB_eff((k1-1)*nreal+k2,i),i=1,nobs)
11    format(2i5,29f16.9)
22    continue
       write(7,*)
20    continue

       goto 999

c     calculate the CDF of the parameters
c     for each run, the effective parameters (vL_eff, T_eff, S_eff,vKB_eff) are
c     ranked in increasing order
      do 100 k1=1,ngroup
      do 110 k2=1,nreal
      do 120 i=1,nobs
      xcum1((k1-1)*nreal+k2,i)=9.99e+09
      xcum2((k1-1)*nreal+k2,i)=9.99e+09
      xcum3((k1-1)*nreal+k2,i)=9.99e+09
      xcum4((k1-1)*nreal+k2,i)=9.99e+09
      do 130 kk=1,nreal
      if(xcum1((k1-1)*nreal+k2,i).ge.vL_eff(kk+(k1-1)*nreal,i))then
      xcum1((k1-1)*nreal+k2,i)=vL_eff(kk+(k1-1)*nreal,i)
      min1=kk
      endif
      if(xcum2((k1-1)*nreal+k2,i).ge.T_eff(kk+(k1-1)*nreal,i))then
      xcum2((k1-1)*nreal+k2,i)=T_eff(kk+(k1-1)*nreal,i)
      min2=kk
      endif
      if(xcum3((k1-1)*nreal+k2,i).ge.S_eff(kk+(k1-1)*nreal,i))then
      xcum3((k1-1)*nreal+k2,i)=S_eff(kk+(k1-1)*nreal,i)
      min3=kk
      endif
      if(xcum4((k1-1)*nreal+k2,i).ge.vKB_eff(kk+(k1-1)*nreal,i))then
      xcum4((k1-1)*nreal+k2,i)=vKB_eff(kk+(k1-1)*nreal,i)
      min4=kk
      endif
130   continue
      vL_eff(min1+(k1-1)*nreal,i)=9.99e+09
      T_eff(min2+(k1-1)*nreal,i)=9.99e+09
      S_eff(min3+(k1-1)*nreal,i)=9.99e+09
      vKB_eff(min4+(k1-1)*nreal,i)=9.99e+09
```

```
120   continue
110   continue
100   continue
c     calculate the pdf function of time
c     define the bin ranges
      do 200 i=1,nbin+1
         bin1(i)=xmin1+float(i-1)*(xmax1-xmin1)/float(nbin)
         bin2(i)=xmin2+float(i-1)*(xmax2-xmin2)/float(nbin)
         bin3(i)=xmin3+float(i-1)*(xmax3-xmin3)/float(nbin)
         bin4(i)=xmin4+float(i-1)*(xmax4-xmin4)/float(nbin)
200   continue
         do 210 k1=1,ngroup
      do 220 k2=1,nreal
         do 230 i=1,nobs
         do 240 m=1,nbin
         if(xcum1(k2+(k1-1)*nreal,i).ge.bin1(m).and.
     &   xcum1(k2+(k1-1)*nreal,i).lt.bin1(m+1))then
         xpdf1(m+(k1-1)*nbin,i)=xpdf1(m+(k1-1)*nbin,i)+1./float(nreal)
         &/((xmax1-xmin1)/float(nbin))
         endif
         if(xcum2(k2+(k1-1)*nreal,i).ge.bin2(m).and.
     &   xcum2(k2+(k1-1)*nreal,i).lt.bin2(m+1))then
         xpdf2(m+(k1-1)*nbin,i)=xpdf2(m+(k1-1)*nbin,i)+1./float(nreal)
         &/((xmax2-xmin2)/float(nbin))
         endif
         if(xcum3(k2+(k1-1)*nreal,i).ge.bin3(m).and.
     &   xcum3(k2+(k1-1)*nreal,i).lt.bin3(m+1))then
         xpdf3(m+(k1-1)*nbin,i)=xpdf3(m+(k1-1)*nbin,i)+1./float(nreal)
         &/((xmax3-xmin3)/float(nbin))
         endif
         if(xcum4(k2+(k1-1)*nreal,i).ge.bin4(m).and.
     &   xcum4(k2+(k1-1)*nreal,i).lt.bin4(m+1))then
         xpdf4(m+(k1-1)*nbin,i)=xpdf4(m+(k1-1)*nbin,i)+1./float(nreal)
         &/((xmax4-xmin4)/float(nbin))
         endif
240   continue
c     check whether any values are greater than the max of the bin ranges
         if(xcum1(k2+(k1-1)*nreal,i).ge.bin1(nbin+1))then
         xpdf1(nbin+(k1-1)*nbin,i)=xpdf1(nbin+(k1-1)*nbin,i)+
         &  1./float(nreal)/((xmax1-xmin1)/float(nbin))
         endif
         if(xcum2(k2+(k1-1)*nreal,i).ge.bin2(nbin+1))then
         xpdf2(nbin+(k1-1)*nbin,i)=xpdf2(nbin+(k1-1)*nbin,i)+
         &  1./float(nreal)/((xmax2-xmin2)/float(nbin))
         endif
         if(xcum3(k2+(k1-1)*nreal,i).ge.bin3(nbin+1))then
         xpdf3(nbin+(k1-1)*nbin,i)=xpdf3(nbin+(k1-1)*nbin,i)+
         &  1./float(nreal)/((xmax3-xmin3)/float(nbin))
         endif
```

```
          if(xcum4(k2+(k1-1)*nreal,i).ge.bin4(nbin+1))then
          xpdf4(nbin+(k1-1)*nbin,i)=xpdf4(nbin+(k1-1)*nbin,i)+
          &  1./float(nreal)/((xmax4-xmin4)/float(nbin))
          endif
230   continue
220   continue
210   continue
c     write the cdf
      do 280 k1=1,ngroup
          do 285 k2=1,nreal
          write(16,8)k1,k2,(xcum2(k2+(k1-1)*nreal,i),i=1,nobs)
8     format(2i5,29f12.6)
285   continue
c     write the pdf
      do 290 m=1,nbin
          write(17,9)k1,(bin2(m)+bin2(m+1))/2.,
          &         (xpdf2(m+(k1-1)*nbin,i),i=1,nobs)
9     format(i5,30f12.6)
290   continue
280   continue
999   stop
      end

          subroutine walton(u,wellfunc,RoverL)
c     calculates the  leaky well function
          implicit double precision (a-g,o-z)
      dimension u(11*90),RoverL(194),func(11*90,194),wellfunc(11*90,194)
          open(3,file='sub.out',status='unknown')

c     define the r/L values from 0.001 to 14.9
          do 10 k=1,194
          if (k.le.18) RoverL(k)=0.001+0.0005*float(k-1)
          if (k.ge.19.and.k.le.36) RoverL(k)=0.01+0.005*float(k-19)
          if (k.ge.37.and.k.le.54) RoverL(k)=0.1+0.05*float(k-37)
          if (k.ge.55) RoverL(k)=1.+0.1*float(k-55)
          write(3,*)k,RoverL(k)
10    continue

c     define the u=r^2S/4tT values from 1e-8 to 1e+3
          do 20 i=1,11
          do 30 j=1,90
          u(j+(i-1)*90)=(0.9+0.1*float(j))*10**(float(i-9))
          write(3,*)i,j,j+(i-1)*90,u(j+(i-1)*90)
30    continue
20    continue
c     calculate the function (appearing in the integration) for u values from 1e-3 to 1e+11
          do 40 k=1,194
          do 50 i=1,11
          do 60 j=1,90
```

```
           y=u(j+(i-1)*90)
           func(j+(i-1)*90,k)=1./y*exp(-y-RoverL(k)**2/4./y)
c          write(3,*)k,i,j,j+(i-1)*90,u(j+(i-1)*90),func(j+(i-1)*90,k)
60   continue
50   continue
c    calculate the well function for u values from 1e-8 to 1e+03
c    or 1/u 1e-03 to 1e+8
      do 70 i=11,1,-1
           do 80 j=90,1,-1
      if(i.eq.11.and.j.eq.90) goto 80
c    calculate integral using Trapezoid Rule
           u_ave=0.5*(u(j+(i-1)*90+1)+u(j+(i-1)*90))
           func_ave=1./u_ave*exp(-u_ave-RoverL(k)**2/4./u_ave)
           wellfunc(j+(i-1)*90,k)=wellfunc(j+(i-1)*90+1,k)+
           &  (func(j+(i-1)*90,k)+4.*func_ave+func(j+(i-1)*90+1,k))*
     &  (u(j+(i-1)*90+1)-u(j+(i-1)*90))/6.
           if(k.eq.37.or.k.eq.55)write(3,1)k,u(j+(i-1)*90),
     &    func(j+(i-1)*90,k),wellfunc(j+(i-1)*90,k)
1    format(i5,3d12.5)
80   continue
70   continue
40   continue
           return
           end
```

APPENDIX F: PROGRAM FOR THE APPLICATION OF CD-CONFINED METHOD ANALYSIS TO THE SYNTHETIC DATA

```
c      Calculates the apparent transmissivity and storativity as a function of time
c      using the method of derivatives (CD-confined Method) for:
c      CONFINED aquifers (iaquifer=1)
c ********************************
          implicit double precision (a-h,o-z)
      parameter(nreal=7,ngroup=1,nobs=2,nsim=nreal*ngroup,nstep=300,
     &  q=2.,h0=20.,iaquifer=1,nwellf=17*1000)
c   iaquifer=1  Confined Aquifers
      dimension h(nobs,nstep),s(nobs,nstep),radius(nobs)
      dimension time(nstep),tao(nstep),t_ave(nstep)
      dimension u(nwellf),wellfunc(nwellf)
      dimension trans(nobs,nstep),stor(nobs,nstep),diffus(nobs,nstep)
      dimension t(481,481),tweight(nreal,240),tlweight(nreal,240)
      dimension tmean1(240),tmean2(240),torder(nreal,240)
      dimension t_cj(nobs),t_cj2(nobs),s_cj(nobs),s_cj2(nobs)
      dimension dist0(4),t_scat(4)

      character filein*10,  casenum*2, runnum(nreal)*8
      character filein2*10, runsim(nreal)*8
c input/output file names:
      open(4,file='dummy',status='old')
      open(14,file='file.nam',status='old')
      open(5,file='time.txt',status='old')
      open(6,file='temp.out',status='unknown')
      open(7,file='parameters1.out',status='unknown')
      open(8,file='parameters2.out',status='unknown')
      open(9,file='parameters3.out',status='unknown')
      open(11,file='wellfunc.out',status='unknown')
      open(17,file='scatter.out',status='unknown')
      open(18,file='cj.out',status='unknown')
      open(19,file='sss.out',status='unknown')
      open(3,file='dummy2',status='old')
      open(12,file='effect.out',status='unknown')
      open(13,file='quartiles.out',status='unknown')

c      Define the distance from observation point to pumping well
       do 12 i=1,nobs
          if(i.eq.1)radius(i)=0.2
          if(i.eq.2)radius(i)=1.
          if(i.ge.3.and.i.le.33)radius(i)=radius(i-1)+1.
          if(i.ge.34.and.i.le.49)radius(i)=radius(i-1)+2.
          if(i.ge.50.and.i.le.65)radius(i)=radius(i-1)+4.
12     continue
```

```
c read head data
      do 15 j=1,nstep
      read(5,*)time(j)
      tao(j)=log10(time(j))
15    continue
      do 20 k1=1,ngroup
      read(14,'(a2)') casenum
      do 22 k2=1,nreal
      if(k1.eq.1) read(4,'(a8)') runnum(k2)
      filein(1:2)=casenum
      filein(3:10)=runnum(k2)
      write(*,3)filein
3     format(1x,a10)
c     i=k2+nreal*(k1-1)
      open(15,file=filein,status='old')
      do 30 j=1,nstep
      read(15,4)nt,(h(i,j),i=1,nobs)

4     format(i5,65f12.7)
      do 31, i=1,nobs
         s(i,j)=h0-h(i,j)
31    continue
30    continue

      if(k1.eq.1) read(3,'(a8)') runsim(k2)
      filein2(1:2)=casenum
      filein2(3:10)=runsim(k2)
      write(*,3)filein2
      open(16,file=filein2,status='old')
      do 32 i=1,481
      read(16,5)(t(i,j),j=1,481)
5   format(10f10.6)
32 continue

c    calculate the effective transmissivity weighted average of the point transmissivity
values
      do 33 ii=1,240
         tweight(k2,ii)=0.
         weight=0.0
         sumweigh=0.0
      do 34 i=241-ii,241+ii
      do 35 j=241-ii,241+ii
         dist=sqrt((float(i-241))**2+(float(j-241))**2)
         if(dist.le.0.01)dist=0.25
         if(dist.gt.0.01.and.dist.le.float(ii)) then
c        weight=1./dist**2
         weight=1
         tlweight(k2,ii)=tlweight(k2,ii)+log(t(i,j))*weight
         tweight(k2,ii)=tweight(k2,ii)+t(i,j)*weight
```

```
           sumweigh=sumweigh+weight
           endif
35    continue
34    continue
           tlweight(k2,ii)=tlweight(k2,ii)/sumweigh
           tweight(k2,ii)=tweight(k2,ii)/sumweigh
           write(12,6)float(ii),t(241,241+ii),tweight(k2,ii),
     &          exp(tlweight(k2,ii)),sumweigh
6     format(20f12.4)
33    continue

c ***************************************
c     calculate the flow parameters using
c     CD-confined method for Confined aquifers (iaquifer=1),

789        if(iaquifer.eq.1)then

c     calculate the  well function (once only)
      if(k1.eq.1.and.k2.eq.1)then
           call Well(u,wellfunc)
           do 320 iw=1,nwellf
           write(11,301) iw,u(iw),wellfunc(iw),wellfunc(iw)*exp(u(iw))
320   continue
301   format(i5,3d15.8)
      endif
           write(*,*)"wellfunction computed"
      do 70 i=1,nobs
c     calculate T_cj(i) and S_cj(i) using the Cooper-Jacob  method
      slope=(s(i,186)-s(i,130))/(tao(186)-tao(130))
           t_cj(i)=2.302*2./(4.*3.14159*slope)
           abc=s(i,186)*4*3.14159*t_cj(i)/2.302/2.
           s_cj(i)=2.25*t_cj(i)*time(186)/radius(i)**2/10**(abc)
      slope=(s(i,201)-s(i,198))/(tao(201)-tao(198))
           t_cj2(i)=2.302*2./(4.*3.14159*slope)
           abc=s(i,201)*4*3.14159*t_cj2(i)/2.302/2.
           s_cj2(i)=2.25*t_cj2(i)*time(201)/radius(i)**2/10**(abc)
      do 75 j=1,nstep-1
c     initialize solution arrays
      diffus(i,j)=-9.
      trans(i,j)=-9.
      stor(i,j)=-9.
           www=0.
c     calculate drawdown rate
      ds=(s(i,j+1)-s(i,j))/(tao(j+1)-tao(j))
c     calculate time and drawdown at the center of the time interval
           t_ave(j)=0.5*(tao(j+1)+tao(j))
           s_ave=0.5*(s(i,j+1)+s(i,j))
           u_ave=radius(i)**2*0.0001/4/10**(t_ave(j))
```

```
c     the method is not applicable to very small t because the numerical and Theis solutions
are not identical
      if(u_ave.gt.100) goto 75
      if(ds.ge.0.0000001)then
          www=log(10.)*s_ave/ds
          if(i.eq.2)write(19,*)j,www
          do 81 k=1,nwellf
c         do 81 k=1,nwellf-1000
          x1=wellfunc(k)*exp(u(k))
          x2=wellfunc(k+1)*exp(u(k+1))
          if(www.le.x1.and.www.gt.x2)          then
c     interpolate
          slope=(u(k+1)-u(k))/(x2-x1)
          u0=u(k)+slope*(www-x1)
          slope=(wellfunc(k+1)-wellfunc(k))/(x2-x1)
          well0=wellfunc(k)+slope*(www-x1)
c     calculate diffusivity
      diffus(i,j)=radius(i)**2/4./10**(t_ave(j))/u0
c     calculate transmissivity
      trans(i,j)=q*well0/4/3.14159/s_ave
c     calculate storativity
      stor(i,j)=trans(i,j)/diffus(i,j)
          goto 80
      endif

81    continue
          endif
80        continue
75    continue
70    continue

          do 84, i=1,nobs
           write(18,11)k1,k2,radius(i),t_cj(i),t_cj2(i),s_cj(i),s_cj2(i)
84    continue
      do 85 j=1,nstep-1
            write(7,11)k1,k2,10**(T_ave(j)),
     &    radius(1),Trans(1,j),
     &    radius(2),Trans(2,j)
            write(8,11)k1,k2,10**(T_ave(j)),
     &    radius(1),stor(1,j),
     &    radius(2),stor(2,j)
            write(9,21)k1,k2,10**(T_ave(j)),
     &    radius(1),diffus(1,j),
     &    radius(2),diffus(2,j)
          if(trans(2,j).le.0.or.trans(2,j+1).le.0) goto 85
          dist1=sqrt(4.*0.6*10**(T_ave(j))*Trans(2,j)/0.0001)
          dist2=sqrt(4.*0.6*10**(T_ave(j+1))*Trans(2,j+1)/0.0001)
c define location (r/I) for scatter plots of t_est and t_geom
          dist0(1)=8.
```

```
          dist0(2)=16.
          dist0(3)=32.
          dist0(4)=64.
          do 86 nn=1,4
          if(dist0(nn).ge.dist1.and.dist0(nn).le.dist2)then
          slope=(trans(2,j+1)-trans(2,j))/(dist2-dist1)
          t_scat(nn)=trans(2,j)+slope*(dist0(nn)-dist1)
          endif
86    continue

85    continue
          write(17,11)k1,k2,t_scat(1),exp(tlweight(k2,8)),
     &t_scat(2),exp(tlweight(k2,16)),
     &t_scat(3),exp(tlweight(k2,32)),
     &t_scat(4),exp(tlweight(k2,64))

11    format(2i5,66f16.9)
21    format(2i5,66e16.9)
           endif
22    continue
      write(7,*)
20    continue

c     order the transmissivity estimates to compute mean and upper/lower quartiles

          do 169 m1=1,nreal
          write(13,170)(tlweight(m1,ii),ii=1,240)
169   continue

c     order the weighted transmissivity data
          do 166 ii=1,240
      do 167 m1=1,nreal
      torder(m1,ii)=+999.
          do 168 m2=1,nreal
          if(m1.eq.1)then
          tmean1(ii)=tmean1(ii)+exp(tlweight(m2,ii))/float(nreal)
          tmean2(ii)=tmean2(ii)+tlweight(m2,ii)/float(nreal)
          endif
      if(torder(m1,ii).gt.tlweight(m2,ii)) then
      torder(m1,ii)=tlweight(m2,ii)
          imin=m2
      endif
168   continue
          tlweight(imin,ii)=+9999.
167   continue
166   continue

          write(13,170)(torder(100,ii),ii=1,240)
          write(13,170)(torder(250,ii),ii=1,240)
```

```
      write(13,170)(tmean1(ii),ii=1,240)
      write(13,170)(tmean2(ii),ii=1,240)
      write(13,170)(torder(500,ii),ii=1,240)
      write(13,170)(torder(750,ii),ii=1,240)
      write(13,170)(torder(900,ii),ii=1,240)
170   format(240f10.4)

999   stop
      end

       subroutine Well(u,wellfunc)
c     calculates the  well function
      implicit double precision (a-g,o-z)
      parameter (nwellf=17*1000)
      dimension u(nwellf),ulog(nwellf),func(nwellf),wellfunc(nwellf)


c     define the u=r^2S/4tT values from 1e-15 to 1e+2
      ulog(1)=-15
      u(1)=10**(ulog(1))
      do 20 i=2,nwellf
      ulog(i)=ulog(i-1)+0.001
      u(i)=10**(ulog(i))
20    continue
c     calculate the function (appearing in the integration) for u values from 1e-15 to 1e+2
      do 50 i=1,nwellf
      func(i)=exp(-u(i))/u(i)
50    continue
c     calculate the well function for u values from 1e-15 to 1e+2
c     or 1/u 1e-02 to 1e+15
      do 70 i=nwellf,1,-1
      if(i.eq.nwellf) goto 70
c     calculate integral using Trapezoid Rule
      wellfunc(i)=wellfunc(i+1)+0.5*(func(i)+func(i+1))*(u(i+1)-u(i))
70    continue
      return
      end
```

APPENDIX G: PROGRAM FOR THE APPLICATION OF CD-CONFINED METHOD AND COOPER-JACOB METHOD ANALYSIS TO THE FIELD DATA

```
c     Calculates the apparent transmissivity and storativity as a function of time
c     using the method of derivatives (CD-Confined Method) for:
c     CONFINED aquifers (iaquifer=1)
c ********************************
          implicit double precision (a-h,o-z)
      parameter(nreal=1,nstep0=1000,iaquifer=1,nwellf=17*1000,nm0=10)
c   iaquifer=1  Confined Aquifers
      dimension s(nm0,nstep0),dsdt(nm0,nstep0)
      dimension time(nstep0),tao(nstep0)
      dimension u(nwellf),wellfunc(nwellf)
      dimension trans(nm0,nstep0),stor(nm0,nstep0),diffus(nm0,nstep0),
          &         dist(nm0,nstep0)
       dimension t_cj(nm0),s_cj(nm0)
        character title*60

c input/output file names:
      open(4,file='drawdown.dat',status='old')
      open(7,file='parameters.out',status='unknown')
      open(11,file='wellfunc.out',status='unknown')
      open(18,file='cj.out',status='unknown')

c read drawdown data
      do 10 i=1,nreal
      read(4,'(a60)')title
      read(4,*) nm1,nm2,nstep,q,radius
          do 15 j=1,nstep
      read(4,*)time(j),(s(i,j),i=1,nm1),(dsdt(i,j),i=1,nm2)
        tao(j)=log10(time(j))
15    continue
10    continue

c ****************************************
c    calculate the flow parameters using
c    CD-Confined for Confined aquifers (iaquifer=1),

789      if(iaquifer.eq.1)then
c    calculate the  well function (once only)
          call Well(u,wellfunc)
          do 320 iw=1,nwellf
          write(11,301) iw,u(iw),wellfunc(iw),wellfunc(iw)*exp(u(iw))
320   continue
301   format(i5,3d15.8)
```

```
          write(*,*)"wellfunction computed"
c    calculate T_cj(i) and S_cj(i) using the Cooper-Jacob  method
       do 70 i=1,nm1
          slope=(s(i,200)-s(i,30))/(tao(200)-tao(30))
          t_cj(i)=2.302*q/(4.*3.14159*slope)
          abc=s(i,200)*4*3.14159*t_cj(i)/2.302/q
          s_cj(i)=2.25*t_cj(i)*time(200)/radius**2/10**(abc)
           write(18,11)i,radius,t_cj(i),s_cj(i)
70    continue

        do 75 j=1,nstep
        write(*,*)j
c    initialize solution arrays
       do 76 i=1,nm1
       diffus(i,j)=-9.
       trans(i,j)=-9.
       stor(i,j)=-9.
          www=0.

          k=1
          www=log(10.)*s(i,j)/dsdt(k,j)
          do 81 k=1,nwellf
          x1=wellfunc(k)*exp(u(k))
          x2=wellfunc(k+1)*exp(u(k+1))
          if(www.le.x1.and.www.gt.x2)           then
c    interpolate
          slope=(u(k+1)-u(k))/(x2-x1)
          u0=u(k)+slope*(www-x1)
          slope=(wellfunc(k+1)-wellfunc(k))/(x2-x1)
          well0=wellfunc(k)+slope*(www-x1)
c    calculate diffusivity
       diffus(i,j)=radius**2/4./10**(time(j))/u0
c    calculate transmissivity
       trans(i,j)=q*well0/4/3.14159/s(i,j)
c    calculate storativity
       stor(i,j)=trans(i,j)/diffus(i,j)
       write(7,11)j,radius,time(j),dist(i,j),Trans(i,j),stor(i,j),
     &          diffus(i,j)
          goto 76
          endif

81    continue
76        continue
75        continue

          do 84, i=1,nm1
           write(18,11)i,radius,t_cj(i),s_cj(i)
       do 85 j=1,nstep
          if(trans(i,j).le.0) goto 85
```

```
      dist(i,j)=sqrt(4.*time(j)*Trans(i,j)/1.65/stor(i,j))
   write(7,11)j,radius,time(j),dist(i,j),Trans(i,j),stor(i,j),
  &        diffus(i,j)
85  continue
84  continue

11  format(i5,66f16.9)
      endif

999  stop
   end

       subroutine Well(u,wellfunc)
c   calculates the  well function
   implicit double precision (a-g,o-z)
   parameter (nwellf=17*1000)
      dimension u(nwellf),ulog(nwellf),func(nwellf),wellfunc(nwellf)

c   define the u=r^2S/4tT values from 1e-15 to 1e+2
   ulog(1)=-15
   u(1)=10**(ulog(1))
    do 20 i=2,nwellf
   ulog(i)=ulog(i-1)+0.001
   u(i)=10**(ulog(i))
20  continue
c   calculate the function (appearing in the integration) for u values from 1e-15 to 1e+2
      do 50 i=1,nwellf
      func(i)=exp(-u(i))/u(i)
50  continue
c   calculate the well function for u values from 1e-15 to 1e+2
c   or 1/u 1e-02 to 1e+15
   do 70 i=nwellf,1,-1
   if(i.eq.nwellf) goto 70
c   calculate integral using Trapezoid Rule
      wellfunc(i)=wellfunc(i+1)+0.5*(func(i)+func(i+1))*(u(i+1)-u(i))
70  continue
      return
      end
```

APPENDIX H: PROGRAM FOR THE APPLICATION OF DIP METHOD ANALYSIS TO THE FIELD DATA

```
c     Calculates the apparent transmissivity and storativity as a function of time using:
c     the method of derivatives (CD method) for CONFINED aquifers (iaquifer=1)
c     the DIP method for LEAKY aquifers (iaquifer=2)
c ******************************
        implicit double precision (a-h,o-z)
      parameter(nstep0=1000,iaquifer=2,nwellf=17*1000,nm0=10)
c   iaquifer=1  Confined Aquifers
c   iaquifer=2  Leaky Aquifers DIP method
      dimension s(nm0,nstep0),dsdt(nm0,nstep0),ds2dt2(nm0,nstep0)
      dimension time(nstep0),tao(nstep0)
      dimension u(nwellf),wellfunc(nwellf)
      dimension trans(nm0,nstep0),stor(nm0,nstep0),diffus(nm0,nstep0),
        &         dist(nm0,nstep0),nstep(nm0)
      dimension t_cj(nm0),s_cj(nm0)
        character title*60

c input/output file names:
      open(4,file='drawdown.dat',status='old')
      open(7,file='parameters.out',status='unknown')
      open(11,file='wellfunc.out',status='unknown')
      open(16,file='dipm.out',status='unknown')
      open(18,file='cj.out',status='unknown')

c read drawdown data
      read(4,*) nm
        do 13 ii=1,nm
        if(iaquifer.eq.1) then
      read(4,'(a60)')title
      read(4,*) nm1,nstep(ii),q,radius
        radius=radius*0.3048
        q=q*0.3048**3
        do 15 j=1,nstep(ii)
      read(4,*)tao(j),(s(i,j),i=1,nm1),(dsdt(i,j),i=1,nm1)
        do 16 i=1,nm1
        s(i,j)=  s(i,j)*0.3048
        dsdt(i,j)=dsdt(i,j)*0.3048
16    continue
      time(j)=10**(tao(j))
15    continue
        Endif

        if(iaquifer.eq.2) then
      read(4,'(a60)')title
```

```
      read(4,*) nm1,nstep(ii),q,radius
          radius=radius*0.3048
          q=q*0.3048**3
          do 25 j=1,nstep(ii)
      read(4,*)tao(j),(s(i,j),i=1,nm1),(dsdt(i,j),i=1,nm1),
     & (ds2dt2(i,j),i=1,nm1)
          do 26 i=1,nm1
          s(i,j)=s(i,j)*0.3048
          dsdt(i,j)=dsdt(i,j)*0.3048
          ds2dt2(i,j)=ds2dt2(i,j)*0.3048
26    continue
      time(j)=10**(tao(j))

25    continue
          endif
c ***************************************
c     calculate the flow parameters using
c     CD-Confined method (iaquifer=1),

789      if(iaquifer.eq.1)then
c     calculate the  well function (once only)
          call Well(u,wellfunc)
          do 320 iw=1,nwellf
          write(11,301) iw,u(iw),wellfunc(iw),wellfunc(iw)*exp(u(iw))
320   continue
301   format(i5,3d15.8)

          write(*,*)"wellfunction computed"

c     calculate T_cj(i) and S_cj(i) using the Cooper-Jacob  method
      do 70 i=1,nm1
          slope=(s(i,500)-s(i,150))/(tao(500)-tao(150))
          t_cj(i)=2.302*q/(4.*3.14159*slope)
          abc=s(i,500)*4*3.14159*t_cj(i)/2.302/q
          s_cj(i)=2.25*t_cj(i)*time(500)/radius**2/10**(abc)
           write(18,11)i,radius,t_cj(i),s_cj(i)
70    continue

          do 75 j=1,nstep(ii)
          write(*,*)j
c     initialize solution arrays
      do 76 i=1,nm1
      diffus(i,j)=-9.
      trans(i,j)=-9.
      stor(i,j)=-9.
          www=0.

          k=1
          www=log(10.)*s(i,j)/dsdt(k,j)
```

```
        do 81 k=1,nwellf
c       do 81 k=1,nwellf-1000
        x1=wellfunc(k)*exp(u(k))
        x2=wellfunc(k+1)*exp(u(k+1))

        if(www.le.x1.and.www.gt.x2)         then
c    interpolate
        slope=(u(k+1)-u(k))/(x2-x1)
        u0=u(k)+slope*(www-x1)
        slope=(wellfunc(k+1)-wellfunc(k))/(x2-x1)
        well0=wellfunc(k)+slope*(www-x1)
c   calculate diffusivity
    diffus(i,j)=radius**2/4./time(j)/u0
c    calculate transmissivity
    trans(i,j)=q*well0/4/3.14159/s(i,j)
c    calculate storativity
    stor(i,j)=trans(i,j)/diffus(i,j)
        goto 76
        endif

81      continue
76      continue
75      continue

        do 84, i=1,nm1
         write(18,11)i,radius,t_cj(i),s_cj(i)
    do 85 j=1,nstep(ii)
        if(trans(i,j).le.0) goto 85
        dist(i,j)=sqrt(4.*time(j)*Trans(i,j)/1.65/stor(i,j))
    write(7,11)j,radius,time(j),dist(i,j),
   &  Trans(i,j),stor(i,j),diffus(i,j)
85   continue
84   continue

11      format(i5,66e18.7)
        endif

c    calculate the flow parameters using the DIP method (iaquifer=2),

    if(iaquifer.eq.2) then

        do 210 i=1,nm1
        dsdtmax1=0.
        dsdtmax2=0.
        dsdtmax3=0.
        do 220 j=1,nstep(ii)

c    find maximum value of first derivative of the drawdown
    if(dsdt(i,j).ge.dsdtmax1)then
```

```
          dsdtmax1=dsdt(i,j)
          t1=time(j)
          endif
c     find maximum (positive) value of second derivative of the drawdown
      if(ds2dt2(i,j).ge.dsdtmax2)then
          dsdtmax2=ds2dt2(i,j)
          jpos=j
          t2=time(j)
          endif
c     find maximum (negative) value of second derivative of the drawdown
      if(-ds2dt2(i,j).ge.dsdtmax3)then
          dsdtmax3=-ds2dt2(i,j)
          jneg=j
          t3=time(j)
          endif

 220  continue

c     calculate the effective leakance using ts2
      rrr2=t2/t1/2.
          vL_eff2=(rrr2**2-0.25)**2/rrr2/(rrr2**2+0.25)*radius
c     calculate the effective transmissivity
          T_eff2=q/2./3.14159/s(i,502)*dbsk0(radius/vL_eff2)
c     calculate the effective storativity
          S_eff2=2.*t1*T_eff2/radius/vL_eff2
c     calculate the effective vertical conductance
          vKB_eff2=T_eff2/vL_eff2**2

c     calculate the effective leakance using ts3
      rrr3=t3/t1/2.
          vL_eff3=(rrr3**2-0.25)**2/rrr3/(rrr3**2+0.25)*radius
c     calculate the effective transmissivity
          T_eff3=q/2./3.14159/s(i,502)*dbsk0(radius/vL_eff3)
c     calculate the effective storativity
          S_eff3=2.*t1*T_eff3/radius/vL_eff3
c     calculate the effective vertical conductance
          vKB_eff3=T_eff3/vL_eff3**2

c     write the results obtained using ts2 and ts3
      write(16,230)ii,i,vL_eff2,T_eff2,S_eff2,vKB_eff2,
     &    vL_eff3,T_eff3,S_eff3,vKB_eff3
 230  format(2i5,10e14.7)

 210  continue

          Endif

 13   continue
999   stop
```

```
      end

       subroutine Well(u,wellfunc)
c     calculates the  well function
      implicit double precision (a-g,o-z)
      parameter (nwellf=17*1000)
      dimension u(nwellf),ulog(nwellf),func(nwellf),wellfunc(nwellf)

c     define the u=r^2S/4tT values from 1e-15 to 1e+2
      ulog(1)=-15
          u(1)=10**(ulog(1))
          do 20 i=2,nwellf
          ulog(i)=ulog(i-1)+0.001
          u(i)=10**(ulog(i))
20     continue
c     calculate the function (appearing in the integration) for u values from 1e-15 to 1e+2
          do 50 i=1,nwellf
          func(i)=exp(-u(i))/u(i)
50     continue
c     calculate the well function for u values from 1e-15 to 1e+2
c     or 1/u 1e-02 to 1e+15
      do 70 i=nwellf,1,-1
      if(i.eq.nwellf) goto 70
          u_ave=0.5*(u(i+1)+u(i))
          func_ave=1./u_ave*exp(-u_ave)
          wellfunc(i)=wellfunc(i+1)+(func(i)+4.*func_ave+func(i+1))*
          *   (u(i+1)-u(i))/6.
70     continue
          return
          end
```